

**CATALYTIC CRACKING OF VGO TO PRODUCE LIGHT OLEFINS:**

**EFFECTS OF ADDITIVES AND KINETIC STUDY**

BY

**OMAR RATIB MUHAMMAD AWAYSSA**

A Thesis Presented to the  
DEANSHIP OF GRADUATE STUDIES

**KING FAHD UNIVERSITY OF PETROLEUM & MINERALS**

DHAHRAN, SAUDI ARABIA

In Partial Fulfillment of the  
Requirements for the Degree of

**MASTER OF SCIENCE**

In

**CHEMICAL ENGINEERING**

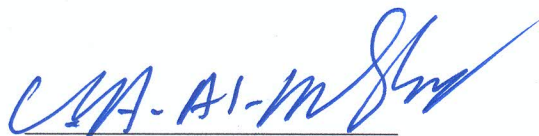
May 2013

KING FAHD UNIVERSITY OF PETROLEUM & MINERALS

DHAHRAN- 31261, SAUDI ARABIA

DEANSHIP OF GRADUATE STUDIES

This thesis, written by **OMAR R. AWAYSSA** under the direction his thesis advisor and approved by his thesis committee, has been presented and accepted by the Dean of Graduate Studies, in partial fulfillment of the requirements for the degree of **MASTER OF SCIENCE IN CHEMICAL ENGINEERING**.



Dr. Usamah A. Al-Mubaiyedh  
Department Chairman



Dr. Salam A. Zummo  
Dean of Graduate Studies



23/6/13  
Date



Dr. Mohammad Mozahar  
Hossain  
(Advisor)



Dr. Suliman Al-Khattaf  
(Co-Advisor)



Dr. Nadhir Al-Baghli  
(Member)



Dr. Abdallah Al-Shammari  
(Member)

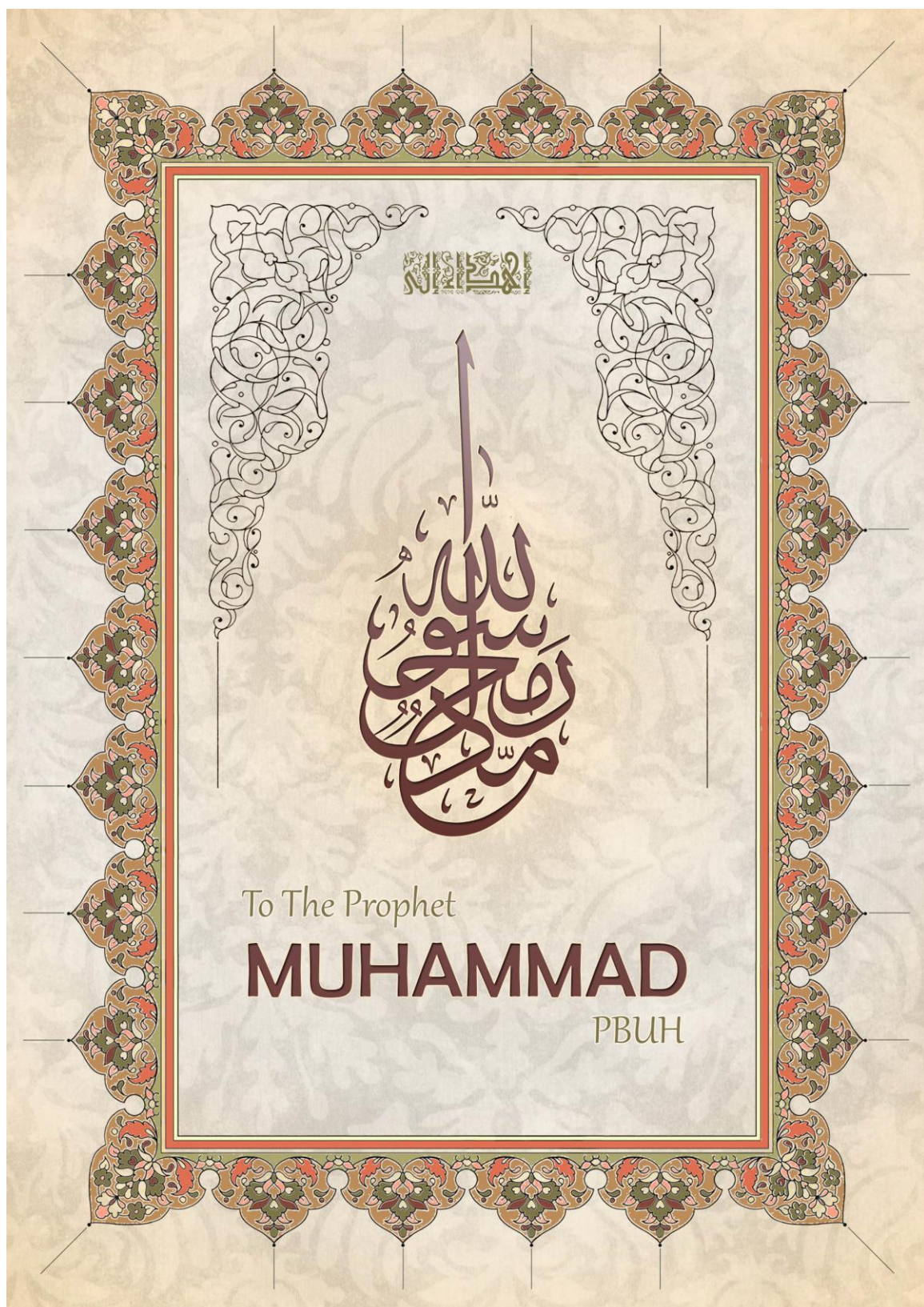


Dr. Shaikh Abdur Razzak  
(Member)

© Omar R. Awayssa

2013





## ACKNOWLEDGMENTS

All praise due to Almighty Allah, Most Gracious and Most Merciful, for his immense beneficence and blessings. He bestowed upon me health, knowledge and patience to complete this work. May peace and blessings be upon prophet Muhammad (PBUH), His Family, His Companions, and those who follow Him.

Thereafter, acknowledgement is due to KFUPM for the support extended towards my research through its remarkable facilities and for granting me the opportunity to pursue graduate studies.

I acknowledge, with deep gratitude and appreciation, the inspiration, encouragement, valuable time and continuous guidance given to me by my thesis advisor, Dr. Mohammad Mozahar Hossain. I am highly grateful and thankful to my thesis co-advisor Dr. Suliman Al-Khattaf for his valuable guidance, suggestions and motivations, pushing me to the front, and teaching me life skills. His strong support and co-operation towards this research during experiments was a boon to me. I extend my deep gratitude to Dr. Nabil Al-Yassir for his endless assistance in preparing the materials, training me on different equipment and for the deep chemistry discussions related to this work. I am also grateful to my Committee members: Dr. Nadhir Al-Baghli, Dr. Abdallah Al-Shammari, and Dr. Sheikh Abdur Razzak for thier constructive guidance and support.

My heartfelt thanks are due to my parents and brothers for their prayers, guidance, and moral support throughout my academic life. My parents' advice, to strive for excellence has made all this work possible.

I am deeply indebted and grateful to Mr. Mian Rahat Saeed for training me on ACE reactor in the FCC Laboratory and for the great scientific discussions and also thanks are due to Mr. Ramzi Al-Shuqaih for training me on the MAT reactor. Thanks for all professors of Chemical Engineering Department and whoever's contributed in this work by any means.

# TABLE OF CONTENTS

ACKNOWLEDGMENTS .....	V
TABLE OF CONTENTS .....	VI
LIST OF TABLES .....	IX
LIST OF FIGURES .....	X
LIST OF ABBREVIATIONS .....	XII
ABSTRACT .....	XIII
CHAPTER 1 INTRODUCTION .....	1
1.1 Background and Statistics .....	2
1.2 Olefins Production Routes .....	5
1.2.1 On-Purpose Processes .....	6
1.2.2 Main Processes .....	7
1.3 Objectives of this work .....	10
CHAPTER 2 LITERATURE REVIEW .....	11
2.1 Catalysts .....	11
2.1.1 Catalyst Material .....	11
2.1.2 Catalyst Modification .....	13
2.1.3 Additives .....	14
2.1.4 Chemistry .....	15
2.1.5 Reaction Mechanism .....	16
2.2 Conclusion of Literature .....	18

<b>CHAPTER 3 EXPERIMENTAL DESCRIPTION .....</b>	<b>20</b>
3.1 Materials and Reagents .....	20
3.2 Preparation of Fluid Catalytic Cracking Additives .....	20
3.2.1 Preparation of Mn-containing HZSM-5 .....	20
3.2.2 Synthesis of Mesoporous HZSM-5 by alkaline treatment (Desilication) .....	21
3.3 Catalyst Preparation (FCC catalyst containing additives) .....	22
3.4 Characterization.....	23
3.5 Catalytic Experiments .....	26
<b>CHAPTER 4 RESULTS AND DISCUSSION.....</b>	<b>29</b>
4.1 Results of Characterization .....	29
4.1.1 Chemical composition .....	29
4.1.2 N <sub>2</sub> adsorption studies .....	30
4.1.3 Structural and Morphological Properties.....	32
4.1.4 Distribution of Mn species by H <sub>2</sub> - and CO- Temperature Programmed Reduction (H <sub>2</sub> -TPR and CO-TPR) 36	
4.1.5 Acidic Properties .....	42
4.1.5.1 FTIR of Pyridine Sorption .....	42
4.2 Description of Catalytic Evaluation Results .....	43
4.2.1 Effect of Silica to Alumina ratio .....	44
4.2.2 Effect of Metal Addition .....	50
4.2.3 Effect of Alkali Treatment (Desilication) .....	57
4.2.4 Kinetic Study .....	59
4.3 Discussion of Results in light of Characterizations.....	65
4.3.1 The enhancement in olefins due to the alkaline treatment .....	65
4.3.2 The enhancement in olefins due to the metal modification .....	66

<b>CHAPTER 5 OTHER METALS AND OTHER ZEOLITES .....</b>	<b>67</b>
5.1 Other Metals.....	67
5.2 Other Zeolites .....	69
<b>CHAPTER 6 CONCLUSIONS AND RECOMMENDATIONS .....</b>	<b>75</b>
6.1 CONCLUSIONS.....	75
6.2 Recommendations .....	76
<b>APPENDIX .....</b>	<b>77</b>
<b>REFERENCES.....</b>	<b>87</b>
<b>VITAE.....</b>	<b>92</b>



## LIST OF TABLES

Table 1 Properties of Arabian Light hydrotreated vacuum gas oil feed .....	27
Table 2 Physic-chemical properties of parent and post-modified HZSM-5 .....	40
Table 3 TPR data for Mn-containing microporous and mesoporous HZSM-5 of different Si/Al .....	41
Table 4 Meso-HZSM-5(30) FCC data .....	57
Table 5 Meso-HZSM-5(80) FCC data .....	59
Table 6 Combined kinetic-deactivation rate constant for Ecat, OM, KFUMP-MAX at T=773 K .....	62
Table 7 Combined kinetic-deactivation rate constant for Ecat, OM, KFUMP-MAX at T=823 K .....	63
Table 8 Combined kinetic-deactivation rate constant for Ecat, OM, KFUMP-MAX at T=873 K .....	64
Table 9 Apparent calculated and literature activation energies .....	64
Table 10 Catalytic data of different metals .....	67
Table 11 A: Catalytic data of different zeolites .....	69
Table 12 B: Catalytic data of different zeolites .....	72
Table 13 Comparative MAT data at constant conversion (70%) over ZSM-5(30)/E-Cat and desilicated ZSM-5/Ecat with different Mn content at 550 C .....	77
Table 14 Comparative MAT data at constant conversion (70%) over ZSM-5(80)/E-Cat and desilicated ZSM-5/Ecat with different Mn content at 550 C .....	78
Table 15 Comparative MAT data at constant conversion (70%) over ZSM-5(280)/E-Cat and desilicated ZSM-5/Ecat with different Mn content at 550 C .....	79
Table 16 Catalytic data of Ecat at different C/O ratios .....	80
Table 17 Catalytic data of Ecat/ZSM-5(30) at different C/O ratios .....	80
Table 18 Catalytic data of Ecat/ZSM-5(80) at different C/O ratios .....	81
Table 19 Catalytic data of Ecat/ZSM-5(280) at different C/O ratios .....	81
Table 20 Catalytic data of Ecat/D-ZSM-5(30) 1C(0.05) at different C/O ratios .....	82
Table 21 Catalytic data of Ecat/D-ZSM-5(80) 1C(0.05) at different C/O ratios .....	82
Table 22 Catalytic data of Ecat/D-ZSM-5(280) 1C(0.05) at different C/O ratios .....	83
Table 23 Catalytic data of Ecat/2wt.% Mn ZSM-5(30) at different C/O ratios .....	83
Table 24 Catalytic data of Ecat/4wt.% Mn ZSM-5(30) at different C/O ratios .....	84
Table 25 Catalytic data of Ecat/2wt.% Mn ZSM-5(80) at different C/O ratios .....	84
Table 26 Catalytic data of Ecat/4wt.% Mn ZSM-5(80) at different C/O ratios .....	85
Table 27 Catalytic data of Ecat/2wt.% Mn ZSM-5(280) at different C/O ratios .....	85
Table 28 Catalytic data of Ecat/4wt.% Mn ZSM-5(280) at different C/O ratios .....	86

## LIST OF FIGURES

Figure 1 Global Propylene and Ethylene Annual Demand Growth [4].....	3
Figure 2 Propylene Demand Forecast Over Two Decade [6].....	4
Figure 3 Global Propylene Consumption Trends by Region [5] .....	5
Figure 4 Flow diagram of catalytic dehydrogenation of propane to propylene [2] .....	6
Figure 5 Typical flow diagram of olefin metathesis process[2] .....	6
Figure 6 Propylene Sources by Region and Process [4] .....	9
Figure 7 Olefin yield versus unit cell size [21] .....	12
Figure 8 Main reactions observed during the cracking of hydrocarbons molecules [42].	15
Figure 9 Simplified reaction network for FCC [42] .....	16
Figure 10 Summary of preparation of FCC additives.....	23
Figure 11 MicroActivity Test (MAT) Unit.....	28
Figure 12 N <sub>2</sub> -adsorption-desorption isotherms and derived BJH mesopore size distribution of parent HZSM-5, Mn-containing HZSM-5, and alkaline treated HZSM-5 (SiO <sub>2</sub> /Al <sub>2</sub> O <sub>3</sub> = 80). Inset: BJH derived Pore size distribution (PSD). The isotherms of 4Mn/HZ80, HZ80DSZ0.05-2C, HZ80DSZ0.10-1C were offset by 45, 75, and 100 cm <sup>3</sup> g- 1 STP, respectively. The corresponding PSD were offset by 0.15, 0.10, and 0.05 cm <sup>3</sup> g- 1 nm <sup>-1</sup> , respectively.....	31
Figure 13 SEM micrographs of (a) parent HZSM-5, and (b,c) alkaline treated HZSM-5 using NaOH of 0.05 M-2cycles and 0.10 M-1 cycle, respectively.....	34
Figure 14 XRD patterns of pure and post-modified HZSM-5 with different Si/Al ratio; (A) 15, (B) 40, and (C) 140. (a) Pure HZSM-5 (Si/Al = 15, 40 or 140), (b,c) 2.0 and 4.0 wt % Mn containing HZSM-5, respectively, (d-f) alkaline treated HZSM-5 using NaOH solution.....	35
Figure 15 CO-TPR Mn-containing microporous and mesoporous HZSM-5 with SiO <sub>2</sub> /Al <sub>2</sub> O <sub>3</sub> = 80; (a,b) 2.0, 4.0 wt % Mn/HZSM-5; (c,d) 2.0 wt % Mn supported onto alkaline treated HZSM-5 using 0.05 M (c) and 0.10 M (d) NaOH (1 cycle); and (e) bulk MnO <sub>2</sub> . .....	38
Figure 16 H <sub>2</sub> -TPR Mn-containing microporous and mesoporous HZSM-5 of different Si/Al ratio; (a,b) 2.0, 4.0 wt % Mn/HZSM-5 (Si/Al = 15); (c,d) 2.0, 4.0 wt % Mn/HZSM- 5 (Si/Al = 40); (e,f) 2.0, 4.0 wt % Mn/HZSM-5 (Si/Al = 140); (g,h) 2.0 wt % Mn supported onto alkali.....	39
Figure 17 CO-TPR Mn-containing microporous and mesoporous HZSM-5 with Si/Al = 40; (a,b) 2.0, 4.0 wt % Mn/HZSM-5; (c,d) 2.0 wt % Mn supported onto alkaline treated HZSM-5 using 0.05 M (c) and 0.10 M (d) NaOH (1 cycle); and (e) bulk MnO <sub>2</sub> .....	39
Figure 18 FTIR of adsorbed pyridine for parent N <sub>2</sub> -adsorption-desorption isotherms and derived BJH mesopore size distribution of parent HZSM-5, Mn-containing HZSM-5, and alkaline treated HZSM-5 (SiO <sub>2</sub> /Al <sub>2</sub> O <sub>3</sub> = 80). (a) Parent HZSM-5, (b) 4Mn/HZ80, and (c) HZ80DSZ0.1 .....	42

Figure 19 IR spectra in the -OH region for parent HZSM-5 ( $\text{SiO}_2/\text{Al}_2\text{O}_3 = 80$ ) (a), Mn/HZ80 of 2.0 wt % (b) and 4.0 wt % (c) Mn loading, alkaline treated HZ80 using NaOH solution of 0.05 M (1cycle) (d), 0.05 M (2 cycle) (e), and 0.10 M (1 cycle) (f), and 2.0 wt % Mn supported onto alkaline treated HZ80 using 0.105 M (1 cycle) (g).....	43
Figure 20 Histogram of conversion and C3= yield % of Ecat, ZSM-5(30), ZSM-5(80), ZSM-5(280), and OM. ....	44
Figure 21 C3= yield % of Ecat, ZSM-5(30), ZSM-5(80), ZSM-5(280), OM .....	46
Figure 22 C3=yield % at 70% conv. of Ecat, ZSM-5(30), ZSM-5(80), ZSM-5(280), OM .....	46
Figure 23 C2=yield % at 70% conv. of Ecat, ZSM-5(30), ZSM-5(80), ZSM-5(280), OM .....	48
Figure 24 C2= - C4= yield % at 70% conv. of Ecat, ZSM-5(30), ZSM-5(80), ZSM-5(280), OM .....	49
Figure 25 Gasoline yield % at 70% conv. of Ecat, ZSM-5(30), ZSM-5(80), ZSM-5(280), OM .....	50
Figure 26 C3= Yield % of Ecat, ZSM-5 additives with Mn, and OM.....	51
Figure 27 C3= Yield % of Ecat, Mn- Containing ZSM-5, and OM .....	52
Figure 28 C3= Yield % @ 70% conv. of Ecat, Mn- Containing ZSM-5, and OM .....	53
Figure 29 C2= Yield % @ 70% conv. of Ecat, Mn- Containing ZSM-5, and OM .....	54
Figure 30 C2= - C4= Yield % @ 70% conv. of Ecat, Mn- Containing ZSM-5, and OM .....	55
Figure 31 Gasoline Yield % @ 70% conv. of Ecat, Mn- Containing ZSM-5, and OM ..	56
Figure 32 C/O ratio v.s. kinetic conversion K at 500 C.....	62
Figure 33 C/O ratio v.s. kinetic conversion K at 550 C.....	63
Figure 34 Figure 28 C/O ratio v.s. kinetic conversion K at 600 C .....	63
Figure 35 Reciprocal of T ( 1/K ) v.s. lnk.....	64

## LIST OF ABBREVIATIONS

<b>FCC</b>	:	Fluid Catalytic Cracking
<b>MAT</b>	:	Micro Activity Testing
<b>Ecat</b>	:	Equilibrium Catalyst
<b>VGO</b>	:	Vacuum Gas Oil
<b>MTO</b>	:	Methanol To Olefins
<b>MTP</b>	:	Methanol To Propylene
<b>USY</b>	:	UltraStable Y zeolite
<b>Y</b>	:	VGO weigh fraction
<b>X</b>	:	Conversion of feed
<b>Ferr</b>	:	Ferrite
<b>MOR</b>	:	Mordenite

## ABSTRACT

Full Name : Omar Ratib Mohammed Awayssa  
Thesis Title : Cracking of VGO to Produce Olefins: Effect of Additives  
Major Field : Chemical Engineering  
Date of Degree : May 2013

Fluid Catalytic Cracking (FCC) is still the major process that deals with converting the heavy portion of the crude oil into high value hydrocarbons. A considerable amount of the global production of light olefins (Ethylene and Propylene) is produced through this process. In this study, the effect of modifying the formulation of catalyst used in FCC will be investigated at fixed temperature and different catalyst to oil ratios. Different additives will be used from different families namely; MOR, Beta, ZSM-11, Ferrierite, MCM, ZSM-5. Samples with different Silica/Alumina ratios will be tested as well as desilicated versions. Different metals will be impregnated on different samples and composites of different zeolites will be prepared and investigated.

The base catalyst of study will be a commercialized equilibrium catalyst (Ecat) obtained from Japan and the gasoil feed will be PR-VGO retrieved from industry. Bench scale reactor will be used in this study, fixed-bed reactor (MAT). Different techniques will be used to characterize the catalysts. Activation Energies will be calculated for the best olefins producing catalysts.

**Keywords:** FCC, Ethylene, Propylene, VGO, MAT, MOR, Beta, ZSM-11, Ferrite, MCM, ZSM-5, and Desilication.



## ملخص الرسالة

الاسم الكامل: عمر راتب محمد عوايصه

عنوان الرسالة: التكسير الحفزي للزيت المفرغ : تأثير الإضافات و التأثير الكيناتيكي

التخصص: الهندسة الكيميائية

تاريخ الدرجة العلمية: أيار 2013

لا يزال التكسير الحفزي المائع العملية الرئيسة التي يتم فيها تحويل الجزء الثقيل من الزيت الخام إلى مركبات هيدروكربونية أعلى قيمة . يتم إنتاج كمية معتبرة من الإنتاج العالمي من الأوليفات الخفيفة ( الإيثيلين و البروبلين ) من خلال عملية التكسير الحفزي المائع هذه . في هذه الدراسة ، سيتم بحث تأثير تعديل تركيبة الحفازات المستخدمة في هذه العملية بحيث يتم تثبيت درجة الحرارة و تغيير نسبة الزيت إلى الحفاز . سيتم دراسة حفازات مختلفة من عائلات مختلفة من مثل : MOR, Beta, ZSM-11, Ferrite, MCM, ZSM-5 . كما سيتم اختبار عينات ذات نسب سيلكا / ألومينا مختلفة بالإضافة إلى العينات منزوعة السيلكا . كما سيتم حقن معادن مختلفة لعينات مختلفة كما سيتم تحضير مركبات مختلفة من زيولائيات مختلفة و سيتم اختبارها . سيكون الحفاز الأساس الذي سيستخدم في هذه الدراسة هو حفاز توازني تجاري تم جلبه من اليابان و سيكون الزيت المستخدم في عملية التكسير هو الزيت المفرغ الذي تم جلبه من أرامكو . سيتم استخدام مفاعل مختبري يسمى الوحدة المصغرة لاختبار نشاط الحفاز MAT . سيتم فحص خصائص الحفازات بطرق مختلفة كما سيتم حساب طاقة التنشيط لأكثر الحفازات إنتاجاً للأوليفينات.

# **CHAPTER 1**

## **INTRODUCTION**

. In today's world, demand on the light olefins (ethylene, propylene, and butylenes) has incrementally increased for the ever increasing production of certain petrochemicals. For that reason, a lot of research has launched looking for possible methods and processes which may play a role in bridging the gap between the production of those light olefins and the rapidly increasing demand on them. Statistics will be provided to show the great need to further explore this area.

In this study, one of the major processes of olefins production has been investigated for further possible improvements in certain dimensions to end up having more efficient process in terms of light olefins production which will be explained thoroughly. Different routes and processes used to produce light olefins will be presented as well. The previous work in this domain will be shown and analyzed in order to identify the drawbacks which in need of improvements and enhancements. A pretty big portion of this work is experimental which will be presented in a specified chapter. The results and discussions will be allocated in independent chapter as well.

## 1.1 Background and Statistics

Light olefins, ethylene, propylene, and butylenes are important feedstocks for the production of useful materials, such as polyethylene and polypropylene, vinyl chloride, ethylene oxide, ethylbenzene, explosives, medicinals, fumigants, resins, synthetic rubber, and many other products [1]. Polyolefins remain the largest sector of light olefins demand showing the highest overall growth rate compared with other derivatives [2].

Ethylene is the largest volume petrochemical industry feedstock, and almost all of the ethylene supply comes from thermal cracking of hydrocarbon feedstocks such as ethane, propane, naphthas, and gas oils [1]. Polypropylene, second in importance to ethylene, accounts for about half of the world propylene consumption, which consequently drives the demand. Other uses of propylene within a refinery include alkylation, catalytic polymerization, and dimerization for the production of high-octane gasoline blends [2].

Ethylene plants charging liquid feedstocks typically produce about 15 wt% propylene and provide almost 70 percent of the propylene consumed by the petrochemical industry [1]. Annual projected growth rate for ethylene and propylene demand is estimated at 4.5 and 5.4%, respectively [3]. Figure 1 shows the annual demand of propylene and ethylene globally.

# Global Propylene and Ethylene Annual Demand

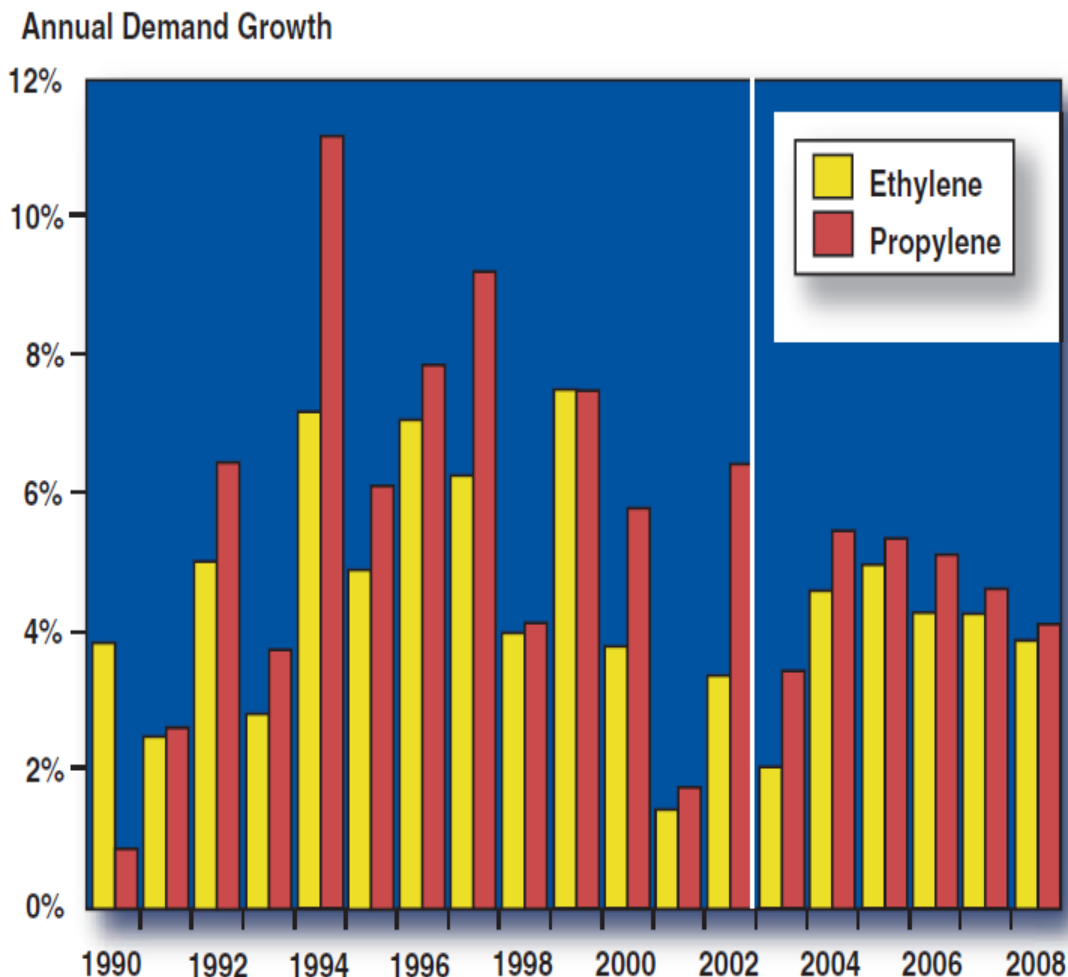


Figure 1 Global Propylene and Ethylene Annual Demand Growth [4]

Global demand for propylene jumped from 37.2 million in 1995 to about 52 million five years later which implies an average growth rate of 5.5 percent annually. In 2006, demand has grown up to approximately 67 million tons with an average annual growth rate of 4.6 percent. Demand is expected to reach more than 100 million tons by 2015 [5]. The forecast of propylene demand over the past decade and the upcoming one is published by the Chemical Market Associates, Inc (CMAI) as presented in figure 2. As

shown in figure 3, the global consumption of propylene is shooting up especially in Asia Pacific, Europe, and MEA region.

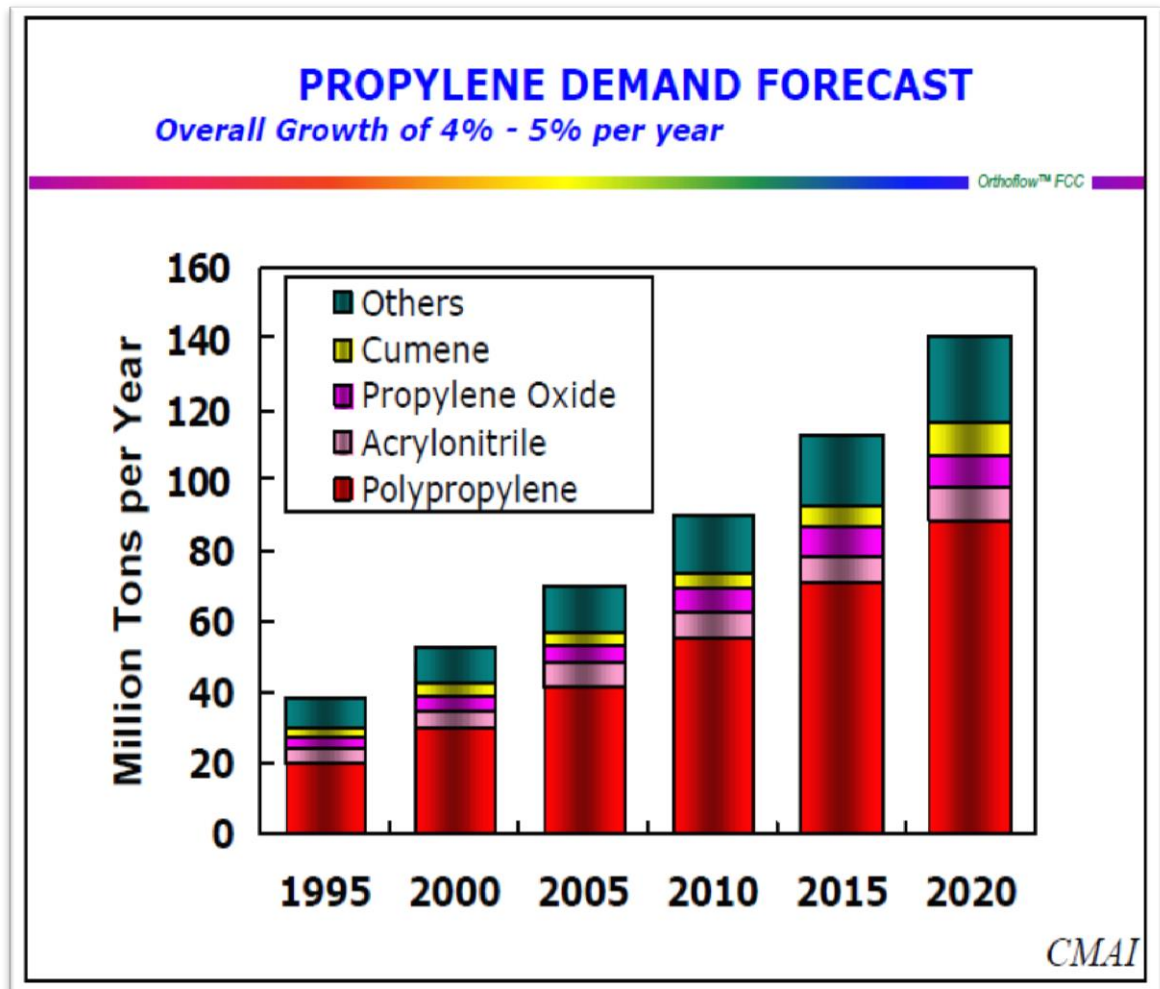


Figure 2 Propylene Demand Forecast Over Two Decade [6]



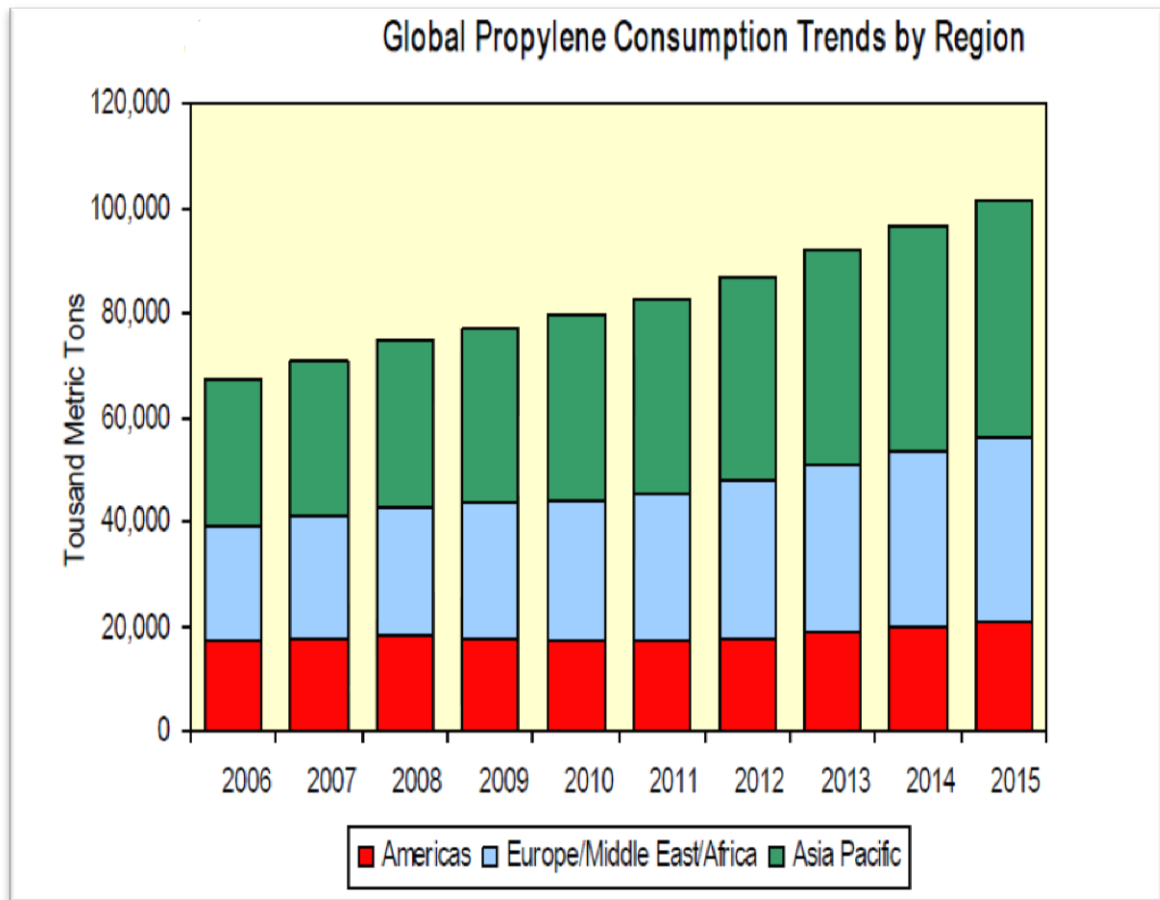


Figure 3 Global Propylene Consumption Trends by Region [5]

## 1.2 Olefins Production Routes

Different routes are used to produce light olefins (mainly ethylene and propylene) in order to meet the ever increasing demand. There are two major categories of producing olefins: Main processes which include steam cracking and catalytic cracking, and On-Purpose processes which include Propane Dehydrogenation, Metathesis, and Methanol to Olefins. Some of the earlier mentioned processes are commercialized here in the Kingdom and some are not yet.

## 1.2.1 On-Purpose Processes

### 1.2.1.1 Propane Dehydrogenation

The main feedstock of this process is propane from which propylene is commercially on purpose produced by dehydrogenation such that the single bond will be omitted and a double bond will be formed and finally giving propylene and hydrogen as shown in figure 4. The reaction is highly endothermic and high reaction temperatures are necessary to achieve high propane conversion [7]. However, this process is expensive in most cases and usually needs relatively low prices of feedstocks. Moreover, the amount of propylene gained from this process is still small compared to the traditional routes [5] [2].

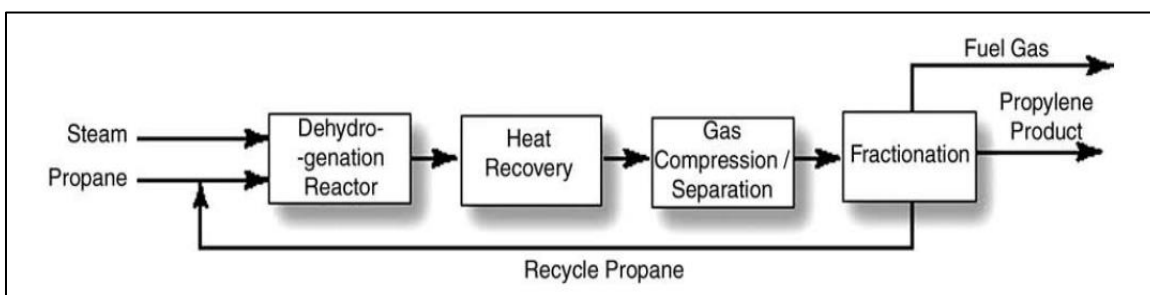


Figure 4 Flow diagram of catalytic dehydrogenation of propane to propylene [2]

### 1.2.1.2 Metathesis

As shown in figure 5, propylene is produced from the conversion of ethylene and butenes such that ethylene is used as a feedstock. This process involves rearrangement of carbon-carbon double bonds of olefins at room temperature [8].

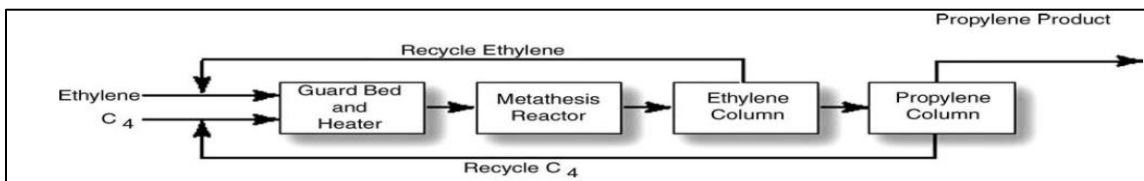


Figure 5 Typical flow diagram of olefin metathesis process[2]

### **1.2.1.3 Methanol To Olefins (MTO)/Methanol To Propylene (MTP)**

As the low cost of methanol is available and the demand on propylene is rising, MTO and MTP processes are viable. Such process more likely exist in regions where gas is much and cheap where ethane cracking is favorable on heavy liquids cracking. As a result, ethylene production is ample whereas propylene supply is insufficient. Such processes need much investment [ 9].

## **1.2.2 Main Processes**

### **1.2.2.1 Steam Cracking**

The major route that is applied to produce light olefins especially ethylene and propylene is steam cracking. It was commercialized in the fifties of last century [2]. This process is endothermic in which the main feedstocks (LPG, naphtha, and ethane) are cracked in the presence of superheated steam (Operation conditions: 700-800 C, 1- 2 atm) which exists as a diluent [10]. Fractionation columns aided with further treatment steps are used to retrieve ethylene and propylene. Globally, 25 percent of cracking units, which were established in 2003-2007 timeframe, were based on ethane as a feedstock. Hence, a minimum amount of propylene is produced. Moreover, steam cracking units would not be able to keep in pace with the rapid increasing demand of propylene [5]. Steam cracking is considered to be the most energy-consuming process in the entire industry of petrochemicals as it consumes around 40 percent of its annual energy which implies high emissions of CO<sub>2</sub>. Additionally, this process does not give full control over the Propylene to Ethylene ratios (P/E) because of its full dependence on the feed itself [11].

### **1.2.2.2 Fluid Catalytic Cracking (FCC)**

Fluid Catalytic Cracking (FCC) is still the major process that deals with converting the heavy portion of the crude oil which represents one third of the total refinery capacity into high value streams (C3-C10). Such hydrocarbons are considered to be the major constituents of the motor gasoline fuel produced as well as the feedstocks for wide variety of petrochemical industry and “other high grade fuel production processes such as alkylation and MTBE synthesis” [12] .

This process (FCC) process works with a distillation range above 623K in the existence of a solid acid catalyst consisting of Y-zeolite as main active constituent [13]. The amount of the high value streams i.e. gasoline, liquefied petroleum gas (LPG), light olefins, and diesel is determined by considering different factors: (i) feed composition (ii) operation conditions (iii) catalyst formulation. In spite the fact that feed composition is said to be the limiting factor in determining the product yields as well as qualities, a crucial role is played by the catalyst selection itself in tuning the distribution of the product in the FCC unit [14].

FCC process is endothermic working at temperatures of 530°C to 650°C which means around 200°C lower than that of steam cracking and thus less energy consumption and lower CO<sub>2</sub> emissions. Also, type of feed used in the process is not of a prominent role as that of steam cracking which results in having the ability to control the Propylene to Ethylene( P/E) ratios coming from the light olefins produced by manipulating the catalyst characteristics such as: acid types, acid strength, and acid distribution. All advantages mentioned earlier are sort of driving force for the researchers to investigate more in this area [11].

The global capacity of gasoline produced from fluid catalytic cracking is about more than 14.2 million barrel per day or 715 million ton per day. About 50% of this capacity is drawn from North America alone as shown in figure 6 below [15].

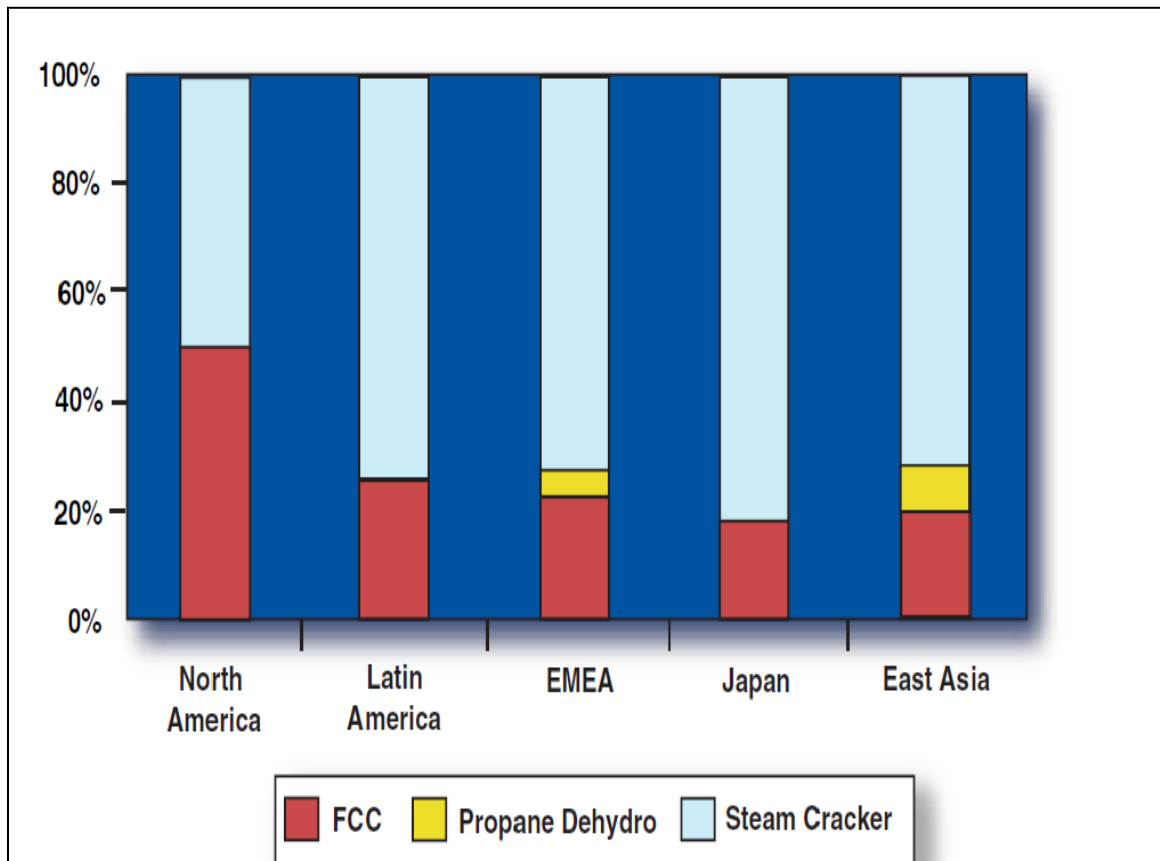


**Figure 6 Propylene Sources by Region and Process [4]**

The great impact of the catalyst on the global performance of the FCC process and its profits justifies the continuous effort put to make sure that the best available formulation is used and proper methodologies of catalyst testing are created [13]. This research has been investigating the effect of manipulating the formulation of the catalyst in boosting the production of the light olefins especially propylene and ethylene using FCC reactors in order to outpace the increasing demand in the olefins global market and that will be presented in chapter two.



### **1.3 Objectives of this work**

Main objective is to study the effects of catalyst modification and additive on the enhancement of olefins from VGO feedstocks. This has been done basically by two main paths: i) introducing mesoporosity in the additives used and observing the effects on the olefins' production ii) introducing metal impregnated on the surface of the additive and testing its contribution in the enhancement of olefins' production.

#### **Specific objectives:**

- i. Catalyst modifications by alkali treatment (desilication).
- ii. Catalyst modification by metal impregnation.
- iii. Catalyst characterization:
  - a. XRD analysis
  - b. Acidity analysis
  - c. Specific surface area
- iv. Catalyst evaluations using MAT unit
- v. Study the effects of additives in MAT unit
- vi. Kinetics study

## CHAPTER 2

### LITERATURE REVIEW

#### 2.1 Catalysts

In the past decade, the production of propylene from FCC units has grown up significantly and is now approaching 20 to 30 percent of the global propylene production. To enhance the propylene yield from FCC units, crucial improvements have been made in the catalyst formulation. This strategy will help meet approximately 5 percent of the global annual demand rate of propylene [16].

##### 2.1.1 Catalyst Material

Since the sixties of the past century, various X and Y zeolites have been used as the major cracking catalysts in FCC. For the higher stability and better selectivity, Y zeolites exclusively become the leading catalysts used in FCC [17] [18]. For enhancing the production of olefins, Y zeolites focused on the Ultrastable Y (USY) which was achieved through the reduction of both the zeolite unit cell size and framework Aluminum content [19] [20]. At constant conversion, the yield of both C3-C4 olefins and octane gasoline is higher and is less in both gasoline and coke when USY is used. Figure 7 shows the olefin yield versus unit cell size such that the olefin yield reached a maximum value at a unit cell size of 24.15-24.20 Å [21]. Unluckily, USY is less active and less stable than its REY counterpart. The latter can accomplish similar benefits of USY but with 35 percent additional activity [22].

For the relatively low cost and versatility of zeolite Y and its variants USY and REY, it is unlikely that they will be displaced in the near future. In the past decade, structures have been synthesized along with complex and costly directing agents at unsuitable conditions. Rather, it is more likely that more research and development will take place in FCC additives where a financial balance is applied in such a way that expensive materials will be tolerated against high yield and property shifts [23].

Research has found that non-Y zeolites could contribute in the production of light olefins (ethylene and propylene) at the expense of gasoline by the seventies of the past century.

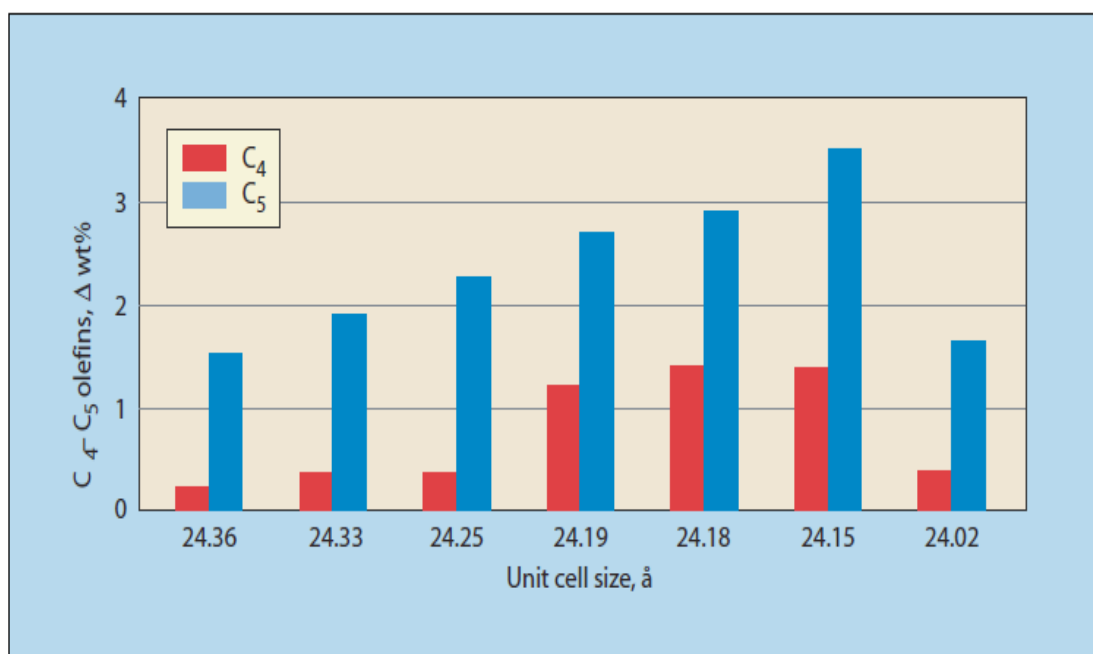


**Figure 7 Olefin yield versus unit cell size [21]**

Various kinds of zeolites have been studied for FCC olefin production (ethylene and propylene) such as: ZSM-5 zeolites, zeolites A, zeolites ZK-4, zeolites ZK-5, synthetic mordenite, dealuminated mordenite, and others [24]. The selectivity to light olefins is determined by the reaction path and residence time, which depend on the zeolite acidity,

pore structure, and crystal size [25]. In other words, weak acidity (lower conversion), small crystal size (shorter residence time), and mesoporosity will enhance the usage of zeolitic volume by the inlet feed molecules and as a result selectivity to olefins is enhanced. Tuning the previously mentioned factors can be done by modifying the catalyst itself and that will be presented in next section.

### **2.1.2 Catalyst Modification**

ZSM-5 is the catalyst of choice in FCC processes as it yields light olefins excellently but on the other hand it suffers from low conversion activity. Modification of ZSM-5 is crucial when olefins are to be produced under more severe operating conditions than those employed for conventional FCC. A long term program has been applied in the Research Institute of Petroleum Processing (RIPP) of SINOPEC, aiming at enhancing the hydrothermal stability and selectivity of ZSM-5. Different methods have been suggested to improve the active sites' accessibility in ZSM-5, for instance, nanocrystals [26], composite materials low level of acid concentration provided by high Si/Al molar ratio, and incorporation of intra-crystalline mesoporosity [27].

Additionally, there are two methodologies which have proven to be simple, versatile and highly effective in achieving combined micro/ mesoporous zeolites: hard templating and desilication. Hard templating routes, where mostly a secondary carbon source is included in the hydrothermal synthesis, have been successfully applied to fabricate hierarchically structured MFI [28], LTA [29], MEL [30], FAU [31], and BEA [32] zeolites. Moreover, Dealumination approaches have been applied on Y zeolite for the sake of achieving the balance in activity, stability, and gasoline yield and octane.

Desilication, framework silicon extraction by the treatment in basic solution, was firstly applied to zeolites with MFI and FAU framework topologies in the late eighties from the formal century for the sake of investigating the dissolution phenomena and structural changes [33] [34]. However, distinguished achievement related to the creation of hierarchical zeolite structures by controlled intra-crystalline mesoporosity development was accomplished recently through in-depth studies over commercial and synthesized MFI zeolites [35] [36]. Such attempts disclosed vital role of the framework Si/Al ratio in a sense that lattice aluminum controls silicon extraction of the zeolite framework due to a suppressed extraction of neighboring silicon species. As a result, an optimal range of Si/Al ratios of 25–50 was identified [37]. Similar to the work done on the ZSM-5, the alkaline treatment route was used on the synthesis of mesoporous ZSM-12 and some other types of zeolites [38]. In this contribution, the effect of desilication will be investigated on different types of zeolites mixed physically with equilibrium catalyst retrieved from the industry of at different operational conditions.

### **2.1.3 Additives**

The addition of ZSM-5 to FCC catalyst is such an efficient approach for enhancing propylene yield for it offers refiners a high degree of flexibility to optimize the production output of their FCC units [39]. There have been many studies on the effect of ZSM-5 additives on FCC products selectivities done by different people around the world such as Degnan et al, and Triantafillidi et al. To overcome the loss in the activity of FCC catalysts, different approaches have been proposed such as incorporating active components such as phosphorus and metals in the additive formulation that aid in the conversion of heavier molecules, optimization of additive formulations with high ZSM-5

levels and use of Y-zeolite in the additive formulation [40] [41]. Other types of zeolites considered to be FCC additives have been utilized such as mordenite, MCM-22, MCM-68, and others. In this work, ZSM-5 based additives have been investigated on commercial FCC equilibrium catalyst along with some other zeolites.

### 2.1.4 Chemistry

For better comprehension of the revolutionary contribution of zeolites, there is a need to examine the various reactions happening during the cracking process. Figure 6 summarizes these reactions by hydrocarbon types: paraffins, olefins, naphthenes and aromatics [42].

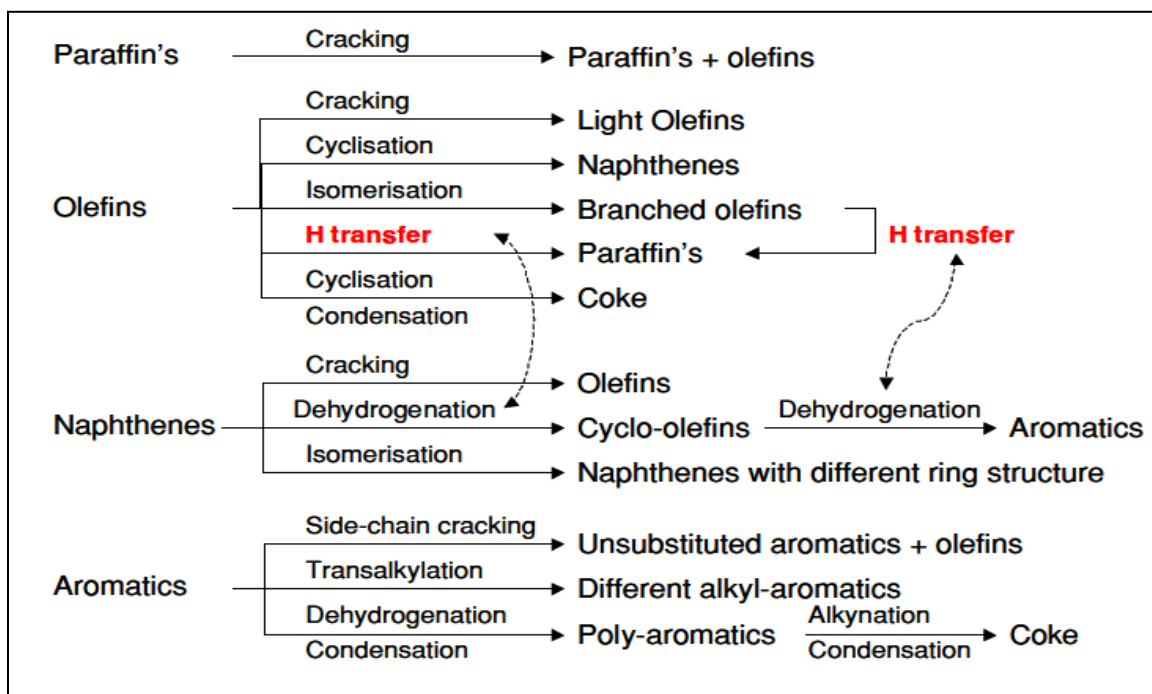


Figure 8 Main reactions observed during the cracking of hydrocarbons molecules [42]

Catalytic Cracking of Vacuum Gas Oil (VGO) goes with the same types of reaction. The main products are Dry gas which incorporates hydrogen, C1-C2 paraffins with a considerable content of C2 olefins. Additionally, LPG is produced which mainly contains

both C3 paraffins and olefins along with C4 olefins. Moreover, gasoline which represents the liquid portion of the products containing mainly light cyclic olefins as shown in figure 7. Coke is produced as well from the process of catalyst regeneration.

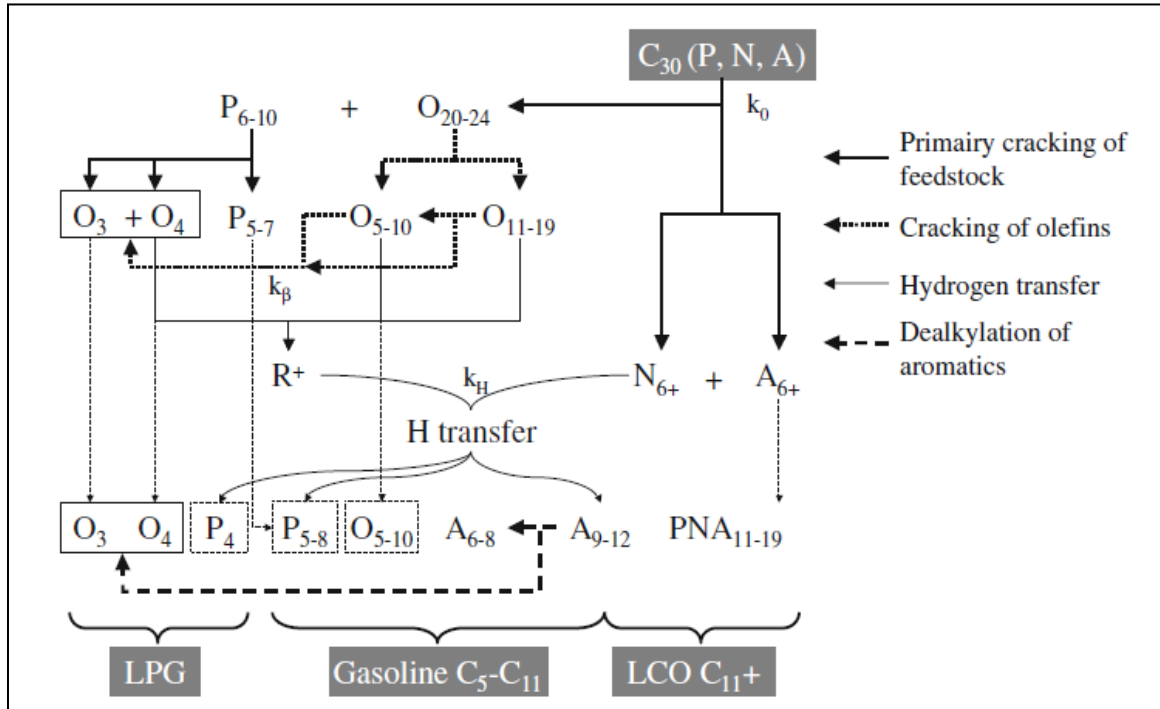


Figure 9 Simplified reaction network for FCC [42]

In order for a catalytic cracking to occur, a mass transport of the reactants should take place between their bulk and the catalyst surface. Consequently, diffusion regardless of its type, adsorption, and desorption along with the reaction itself are of a great importance for the process to happen [43].

### 2.1.5 Reaction Mechanism

There are seven steps through which the cracking on catalyst takes place:

**Step One:** External diffusion of the reactants from their bulk state to the surface of the catalyst.

**Step Two:** Internal diffusion of the reactants from the surface of the reactants into the pores all the way to the active sites.

**Step Three:** Adsorption of the reactants on the active sites.

**Step Four:** Reaction takes place on the active sites producing products along with unreacted feed.

**Step Five:** Desorption of the products and the unreacted feed out of the active sites.

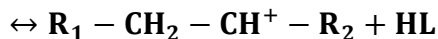
**Step Six:** Internal Counter Diffusion of the products and the unreacted materials out of the cavity of the pore to the surface of the catalyst.

**Step Seven:** External Counter Diffusion of the products and the unreacted materials from the surface of the catalyst back to the bulk state.

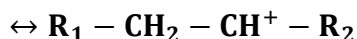
Step four is considered to be the key step through which the cracking of the hydrocarbons over acidic catalysts happens. It is accepted that catalytic cracking occurs by carbocation reaction mechanism. It is believed that the active sites on which the reaction happens are acidic and of two kinds: Bronsted and Lewis acid sites. Carbocation reaction proceeds through three steps: *Initiation* when the carbonium and /or carbenium are formed via the interaction between the adsorbed feed and the active site, *Propagation* of the carbocation ions, and *Termination* which involves desorption of the products and restoring the active sites [44]. *Initiation* step takes place according to different suggested paths:

1. Carbenium ion can be formed through the abstraction of a hydride ion from a paraffinic compound by Lewis sites [45] [46] [47].

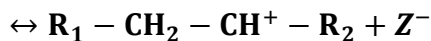




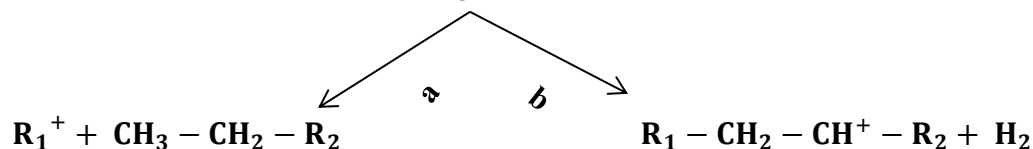
2. Carbenium ion can be formed through the abstraction of a hydride ion from a paraffinic compound by strong Bronsted sites [48] [49] [50] [51].



3. Protonation of olefins exist in the feed via Bronsted acid sites [52].



4. Protonation of paraffins via Bronsted acid sites to produce Carbonium transition state ion –pentacoordinated- which is unstable. Later, it splits into either: a) smaller paraffin and carbenium ion or b) hydrogen gas and carbenium [53].



Subsequently, carbenium ions may desorb as olefins and restore the Bronsted acid sites.

## 2.2 Conclusion of Literature

There is always a need for improving the yield of olefins' production through the catalyst route as it is much easier for the already established industrial FCC units. Investigating

the effect of modifying catalysts and incorporating additives in FCC processes will be of a great value financial wise as well as energy saving wise.

Considering new zeolites and new techniques of preparation will be of a great significance as it affects the performance. Thus, the area of formulating the catalysts will be explored seeking enhancements in the performance of the catalysts.

In depth study is needed to study different routes to enhance the catalytic performance of FCC additives as well as their selectivities to olefins especially propylene. ZSM-5 based additives will be more highlighted using different techniques of modification in order to boost the performance towards the production of propylene.

## CHAPTER 3

### EXPERIMENTAL DESCRIPTION

This chapter will describe the materials used in preparing the catalysts and their recipes.

It also presents the techniques used in characterizing the catalysts.

#### 3.1 Materials and Reagents

The commercial ZSM-5 zeolites used in this study were supplied by Zeolyst; 3024E, Nominal Si/Al = 15, NH<sub>4</sub>-form, CBV8014, Nominal Si/Al = 40, NH<sub>4</sub>-form, and CBV28014, Nominal Si/Al = 140. Prior to post-synthesis treatments, the as-received NH<sub>4</sub>-form zeolites were air-calcined at 550 °C for 5 h (3 °Cmin<sup>-1</sup>), in order to get the H-form. Reagents used for post-synthesis treatments included manganese (II) nitrate hexahydrate, sodium hydroxide and ammonium chloride. All reagents were obtained from ALDRICH, and used without further purification. The base catalyst used in this study was a commercial equilibrium FCC catalyst (E-Cat) obtained from a domestic refinery. It is based on USY zeolite with a surface area of 135 m<sup>2</sup>/g and a pore volume of 0.23 cm<sup>3</sup>/g. This E-Cat was calcined at 500 °C for 3 h before further use.

#### 3.2 Preparation of Fluid Catalytic Cracking Additives

##### 3.2.1 Preparation of Mn-containing HZSM-5

Mn-containing HZSM-5 was prepared via aqueous incipient wetness impregnation method. In a typical preparation, appropriate amount of manganese (II) nitrate hexahydrate corresponding to Mn loading of 2.0 - 4.0 wt. % was dissolved in deionized

water. Subsequently, HZSM-5 powder (Si/Al = 15, 40 or 140) was slowly added. The slurry was mixed at ambient temperature for 2 h, and then water was evaporated by placing the slurry inside an oven set at 60 °C. Finally, the resulting solid was dried at 100 °C and then calcined in standing air at 550 °C (holding time 5 h, ramping 3°Cmin<sup>-1</sup>).

Samples obtained by impregnation are labeled as Mn(x)/HZ(y) where x and y indicate Mn loading in wt. %, and Si/Al, respectively. For example, Mn2/HZ15 corresponds to Mn-containing HZSM-5 with Mn loading of 2.0 wt. % and Si/Al ratio of 15.

### **3.2.2 Synthesis of Mesoporous HZSM-5 by alkaline treatment (Desilication)**

Mesoporous HZSM-5 (desilicated or alkaline treated HZSM-5) was prepared by one or two cycles of desilication with 0.05 or 0.10 M NaOH solutions at 60 °C for 2 h, under atmospheric pressure. Typically, 300 ml of the desired NaOH solution was heated up to 60 °C in a flask connected to a reflux, then 5 g of HZSM-5 (Si/Al ratio of 15, 40 or 140) was added and the mixture was vigorously stirred for 2 h. The zeolite suspension was then cooled down immediately using an ice bath, and subsequently was isolated by suction filtration. The product was washed thoroughly with deionized water until the pH is neutral. It was then dried at ambient temperature, followed by drying at 100 °C overnight. Then, the dried alkaline-treated samples were transformed into ammonium form by twofold ion-exchange with 2.2 M of ammonium chloride at 80 °C for 3 h (1.0 g solid per 20 ml solution) without calcination between ion-exchange procedures. The samples were subjected to typical drying treatments followed by calcination to get the H-form in standing air at 550 °C (holding time 5 h, 3°Cmin<sup>-1</sup>). The samples are hereafter designated as HZ(x)-DS(y), where x, y and DS correspond to Si/Al ratio, concentration of sodium hydroxide in M, and desilication treatment, respectively. For example, HZ15-

DS0.10 corresponds to one cycle of alkaline treatment of HZSM-5 ( $\text{Si}/\text{Al} = 15$ ) using 0.10 M of NaOH solution. While, HZ15-DS010-1C corresponds to 2 cycles of alkaline treatment of HZSM-5 ( $\text{Si}/\text{Al} = 15$ ) using 0.10 M of NaOH solution.

### **3.2.3 Synthesis of Mn-containing mesoporous HZSM-5**

Mn-containing mesoporous HZSM-5 was prepared via aqueous incipient impregnation, following similar procedures as those of Mn-containing HZSM-5. The samples are hereafter designated as Mn(x)/DS(y)-HZ (z) (x, y, z, and DS correspond to Mn content in wt. %, [NaOH] in M, Si/Al, and desilication treatment). For example, Mn2/DS010-HZ15 corresponds to Mn-containing desilicated HZSM-5 (2 wt. % Mn loading,  $\text{Si}/\text{Al} = 15$ , one cycle of desilication treatment using 0.10 M of NaOH solution).

### **3.3 Catalyst Preparation (FCC catalyst containing additives)**

The calcined additives were added at 25 wt. % with E-Cat prior to catalyst catalytic performance evaluation [54]. All catalyst preparations are summarized in figure 10.

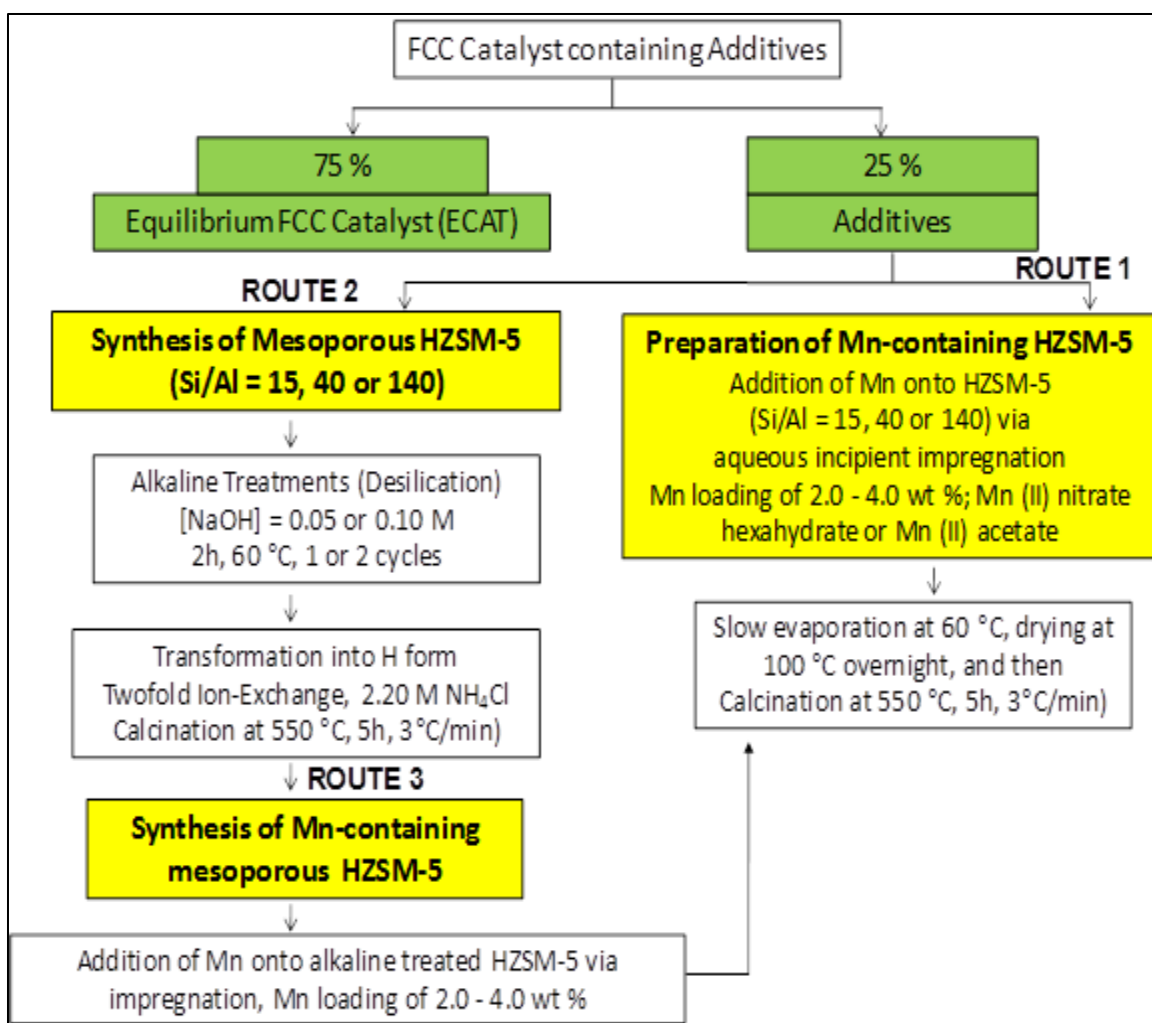


Figure 10 Summary of preparation of FCC additives

### 3.4 Characterization

The amounts of Si, Al, and Mn in the solids and filtrates were determined by inductively coupled plasma spectrometer (ULTIMA 2, ICP-OES) from HORBIA scientific.

Textural properties were characterized by N<sub>2</sub> adsorption-desorption measurements at 77 K, using Quantachrome Autosorb 1-C adsorption analyzer. Samples were outgassed at 220 °C under vacuum ( $10^{-5}$  Torr) for 3 h before N<sub>2</sub> physisorption. The Brunauer-Emmett-Teller (BET) specific surface areas were determined from the desorption data in the relative pressure ( $P/P_0$ ) range from 0.06-0.3, assuming 0.164 nm<sup>2</sup> for the cross-section of

the N<sub>2</sub> molecule. Contribution of micropores and mesopores was derived from the t-plot method according to Lippens and de Boer [55]. Whereas, the mesopore size distribution was calculated using the Barret-Joyner-Halenda (BJH) pore size model applied to the adsorption branch of the isotherm [56].

High- angle X-ray diffraction patterns were recorded on a Rigaku Miniflex II XRD powder diffraction system using CuK $\alpha$  radiation ( $\lambda_{K\alpha1} = 1.54051\text{\AA}$ , 30 Kv and 15 mA). The XRD patterns were recorded in the static scanning mode from 1.2 - 60° (2 $\theta$ ) at a detector angular speed of 2 °/min and step size of 0.02°.

Transmission FTIR spectra of lattice vibration were recorded in the 400 - 1200 cm<sup>-1</sup> range, at 4 cm<sup>-1</sup> resolution, using Nicolet FTIR spectrometer (Magna 500 model).

Scanning Electron Microscopy (SEM) was performed on selected samples to determine the particle size, morphology, and surface elemental compositions. The SEM images, electron diffraction SEM (EDSEM) mappings, and energy-dispersive X-ray spectroscopy were recorded using FESEM/FIB (Tescan Lyra-3). The field Emission Dual Beam (Electron/ Focused Ion Beam) system combines high-end field-emission scanning electron microscope (FESEM) and high-performance focused ion beam (FIB) system in one chamber.

<sup>27</sup>Al and <sup>29</sup>Si Magic Angle Spinning (<sup>27</sup>Al and <sup>29</sup>Si MAS NMR) measurements were performed using Bruker Avance 400 MHz wide-bore spectrometer. <sup>27</sup>Al MAS NMR spectra were obtained by a single pulse length of  $\pi/4$ , and relaxation delay of 0.5 s. The <sup>29</sup>Si MAS NMR spectra were obtained by 20 pulse (B1~55HZ) followed by 13 ms acquisition with 1H decoupling (tppm, B1~55 HZ). All studied samples were spun at

ca. 12 KHz in Air using 4 mm ZrO<sub>2</sub> rotors. The Al and Si chemical shifts were referenced to (NH<sub>4</sub>) Al (SO<sub>4</sub>)<sub>2</sub> and 4, 4-dimethyl-4-silapentane-1-sulfonic acid, respectively.

Temperature-programmed reduction (TPR) measurements were carried out using Micromeritics chemisorb 2750. Typically, about 100 mg of sample was pretreated at 300 °C for 2 h (ramping rate of 10 °Cmin<sup>-1</sup>) under argon flow. After cooling the sample to 50 °C in argon flow, the reduction was performed in a mixture of 5% H<sub>2</sub>/Ar flowing at flow of 20 mlmin<sup>-1</sup> and heating rate of 10 °Cmin<sup>-1</sup>, up to 1100 °C. Hydrogen consumed during TPR run was monitored by a thermal conductivity detector.

NH<sub>3</sub>-Temperature-Programmed Desorption (NH<sub>3</sub>-TPD) was carried out using Micromeritics chemisorb 2750 equipped with a mass spectrometry detector (Cirrus 2, mks, spectra products). Samples (ca. 50 mg) were pretreated at 300 °C in a flow of helium (25 mlmin<sup>-1</sup>) for 2 h. This was followed by the adsorption of 10% NH<sub>3</sub>/He at 100 °C for 30 min. Samples were then purged in a helium stream for 2 h at 100 °C in order to remove loosely bound ammonia (i.e. physisorbed and H-bonded ammonia). Then, the samples were heated again from 100 to 700 °C at a heating rate of 10 °Cmin<sup>-1</sup> in a flow of helium (25 mlmin<sup>-1</sup>) while monitoring the evolved ammonia using TCD.

Infrared spectroscopy of adsorbed pyridine was used to determine the types of available acid sites (i.e. Bronsted and/or Lewis acid sites). The measurements were carried out using a Fourier transform infrared using Nicolet FTIR spectrometer (Magna 500 model). The samples in the form of a self-supporting wafer (ca. 40 mg in weight and 20 mm in diameter) were obtained by compressing a uniform layer of powder. The wafer was then placed in an infrared vacuum cell equipped with KBr windows (Makuhari Rikagaku



Garasu Inc., JAPAN), and pretreated under vacuum ( $P = \text{ca. } 2 \times 10^{-5} \text{ Torr}$ ) at  $300\text{ }^{\circ}\text{C}$  for 2 h. The pretreated wafer was then contacted with pyridine vapor at ambient temperature for 5 min, followed by evacuation at  $150\text{ }^{\circ}\text{C}$  for 1 h. The IR cell was then cooled down to ambient temperature and placed in an IR beam compartment while under vacuum and transmission spectra were recorded. Desorption of pyridine was also carried out at  $350$  and  $450\text{ }^{\circ}\text{C}$  in order to evaluate the strength of Bronsted and Lewis sites. For a quantitative characterization of acid sites, the extinction coefficient ratio ( $R_{\epsilon} = \epsilon_{1450}/\epsilon_{1550}$ ) ( $1450$  and  $1550\text{ cm}^{-1}$  bands correspond to Lewis and Bronsted sites) was calculated experimentally.

### **3.5 Catalytic Experiments**

The feed used in all MAT runs was an Arabian Light hydrotreated vacuum gas oil (VGO) procured from a Saudi Aramco domestic refinery. The properties of VGO are listed in Table 1. Laboratory scale studies are the most commonly used methods in order to characterize the performance of FCC catalysts because of lower costs of investments, operation, and analysis [41]. The catalytic cracking of VGO was carried out in a fixed-bed microactivity test (MAT) unit (Figure 11), manufactured by Sakuragi Rikagaku, Japan according to ASTM D-3907 and D-5154 test methods. Prior to MAT test, the system will be purged with  $\text{N}_2$  flow. For each MAT run, a full mass balance was obtained. If the material balance was less than 96% or greater than 102%, the test was repeated. All MAT runs were performed at a cracking temperature of  $550\text{ }^{\circ}\text{C}$  and a time-on-stream of 30 s. Conversion was varied by changing catalyst/oil (C/O) ratio in the range of 1.0 to 4.0 g/g. This variable was changed by keeping constant the amount of VGO (1.0 g) and changing the amount of catalyst.

A thorough gas chromatographic analysis of the gaseous products was conducted to provide detailed yield patterns and information on the selectivity of the catalyst/additives being tested. Gaseous products (dry gas and LPG) were analyzed using two Varian gas chromatographs equipped with 50 m (0.32 mm diameter) Alumina Plot capillary column and FID/TCD detectors. Coke on catalyst was determined by a Horiba carbon analyzer. For liquid products, three different cuts were considered: gasoline (C5, 221°C), LCO (light cycle oil, 221-343 °C), and HCO (heavy cycle oil, + 343 °C). The weight percentage of liquid products was determined by a simulated distillation GC equipped with 10 m (0.53 mm diameter) RTX-2887 capillary column and FID detector according to ASTM D-2887. Gasoline composition was determined using a Shimadzu GC system that was configured to give paraffins, olefins, naphthenes and aromatics (POINA) distribution. The GC was equipped with 50 m (0.15 mm diameter) BP-1 PONA capillary column and FID detector. Conversion was defined as the sum of yields for dry gas (H<sub>2</sub> and C1-C2), LPG (C3-C4), gasoline, and coke.

**Table 1 Properties of Arabian Light hydrotreated vacuum gas oil feed**

Property	Value
Density (g/cm <sup>3</sup> ) (15 °C)	0.896
Sulfur (ppm)	300
Nitrogen (ppm)	170
Saturates (wt. %)	59
Aromatics (wt. %)	40
Residue (wt. %)	0.8
Simulated Distillation (°C)	
Initial boiling point	308
5%	348
25%	376
50%	420
90%	507
Final boiling point	568

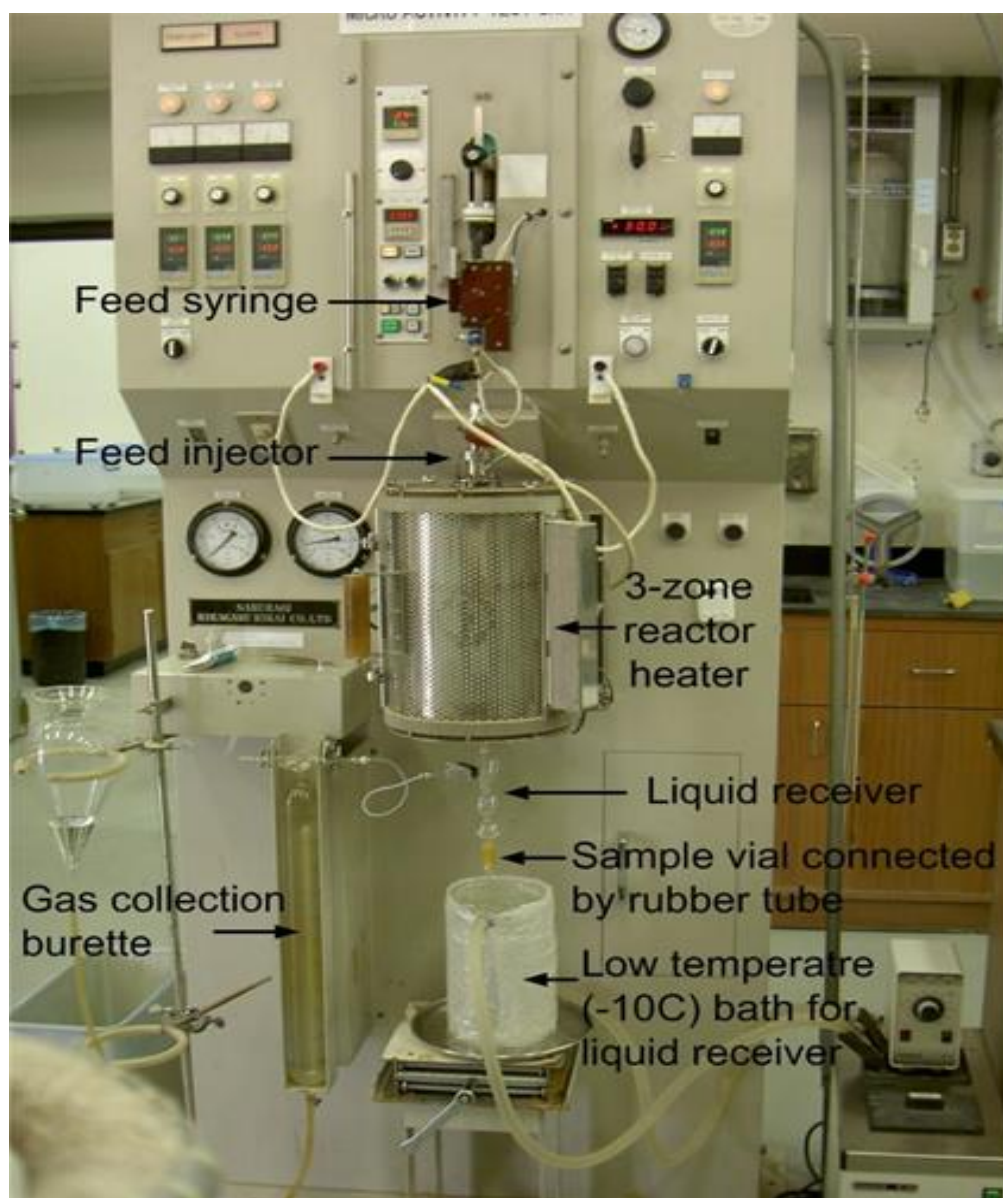


Figure 11 MicroActivity Test (MAT) Unit

## CHAPTER 4

### RESULTS AND DISCUSSION

This chapter reveals the results of characterization of both different modified and unmodified additives as well as the catalytic evaluation. Additionally, it will discuss those results and connect the dots in order to have a fine picture of what happened.

#### 4.1 Results of Characterization

##### 4.1.1 Chemical composition

Table 2 shows the molar  $\text{SiO}_2/\text{Al}_2\text{O}_3$  ratio and Mn content for parent HZSM-5, Mn-containing HZSM-5, and alkaline treated HZSM-5, obtained by ICP analysis. It can be seen from Table 1 that there is a negligible change in the  $\text{SiO}_2/\text{Al}_2\text{O}_3$  upon alkaline treatment of HZSM-5 with  $\text{SiO}_2/\text{Al}_2\text{O}_3 = 30$ . This was observed regardless of alkaline treatment conditions (i.e. sodium hydroxide concentration or number of alkaline treatments). On the contrast, the  $\text{SiO}_2/\text{Al}_2\text{O}_3$  of HZSM-5 ( $\text{SiO}_2/\text{Al}_2\text{O}_3 = 80$ ) was affected significantly upon alkaline treatment. The ratio decreased from 80.0 in the parent HZSM-5 to 57.8 (27.8% decrease) and 58.4 (27% decrease) in those treated with 0.05 M of NaOH using 1 and 2 cycles of treatment, respectively. Upon alkaline treatment using 0.10 M NaOH solution, the ratio of parent HZSM-5 decreased to 50.4 (37%). Similar findings were observed upon alkaline treatment of HZSM-5 containing quite high  $\text{SiO}_2/\text{Al}_2\text{O}_3$  (280). Table 2 revealed that the  $\text{SiO}_2/\text{Al}_2\text{O}_3$  ratio of parent HZSM-5 decreased from 280 to 206, 136, and 128 upon alkaline treatment using 0.05 M NaOH (1 cycle), 0.05 M NaOH (2cycles), and 0.10 M NaOH (1 cycle), respectively. This corresponds to 26%,

51% and 54% decrease in  $\text{SiO}_2/\text{Al}_2\text{O}_3$  ratio. This suggests that the extent of Si extraction for HZSM-5 of  $\text{SiO}_2/\text{Al}_2\text{O}_3 = 280$  is comparable to that of HZSM-5 of lower ratio (80.0). It is also worth mentioning that the extent of Si extraction via more concentrated NaOH solution (0.10 M-1cycle) appears to be comparable to that of lower concentration (0.05M-2cycles), as suggested by ICP analysis of the solid samples (Table 1). This was observed for alkaline treated HZSM-5 of  $\text{SiO}_2/\text{Al}_2\text{O}_3 = 80$ -280.

It can be also seen from Table 2 that the experimental loading of Mn (ICP analysis) was quite comparable to the nominal ones, regardless of zeolite silica/alumina ratios.

#### **4.1.2 N<sub>2</sub> adsorption studies**

Figure 12 shows the N<sub>2</sub> adsorption-desorption isotherms and the derived BJH mesopores size distribution for parent HZSM-5, Mn-containing HZSM-5, and alkaline treated HZSM-5. The textural parameters calculated from the nitrogen sorption isotherms are compiled in Table 2. The parent microporous HZSM-5 and Mn-containing HZSM-5 exhibit type I isotherm (BDDT classifications with a plateau at higher relative pressure in agreement with the microporous nature of limited mesoporosity of the samples. Upon alkaline treatment, samples exhibit isotherms representing type I behavior, with enhanced N<sub>2</sub> uptake at higher relative pressures. The increased adsorption in the relative pressure ( $p/p_0$ ) range  $> 0.30$  and the appearance of hysteresis loops in the desorption branch at  $p/p_0 \sim 0.40 - 0.50$  of the treated samples indicate the development of mesopores. The samples also exhibited remarkable enhance N<sub>2</sub> uptake at  $p/p_0 > 0.8$  due to textural mesoporosity arising from interparticle (voids) mesopores. In addition, the position of capillary condensation step slightly shifted to higher relative pressure with increasing the

concentration of NaOH solutions, indicating a slight increase in the size of mesopores (Table 2).

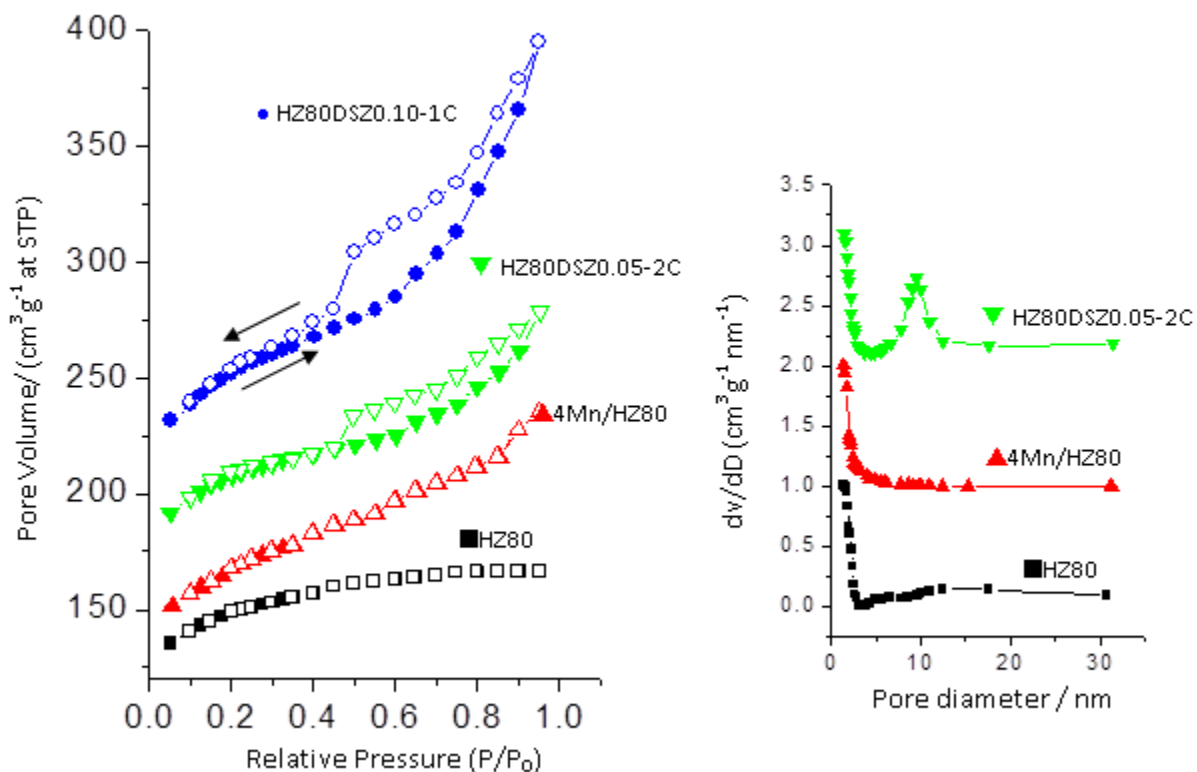


**Figure 12** N<sub>2</sub>-adsorption-desorption isotherms and derived BJH mesopore size distribution of parent HZSM-5, Mn-containing HZSM-5, and alkaline treated HZSM-5 (SiO<sub>2</sub>/Al<sub>2</sub>O<sub>3</sub> = 80). Inset: BJH derived Pore size distribution (PSD). The isotherms of 4Mn/HZ80, HZ80DSZ0.05-2C, HZ80DSZ0.10-1C were offset by 45, 75, and 100 cm<sup>3</sup>g<sup>-1</sup> STP, respectively. The corresponding PSD were offset by 0.15, 0.10, and 0.05 cm<sup>3</sup>g<sup>-1</sup>nm<sup>-1</sup>, respectively.

BJH pore size distributions derived from the adsorption branch of the isotherm (inset of Figure 12) further confirm the presence of mesoporosity in the alkaline treated samples, showing a well-defined distribution of mesopores in the range of 9.0 - 10.0 nm. Alkaline treated HZSM-5 samples showed a noticeable development of a broad band centered around 9.00, which increased slightly with increasing the concentration of sodium hydroxide solutions. Groen et al. reported the presence of relatively narrow distribution

of pores centered around 10.0 nm, upon alkaline treatment of HZSM-5 (Si/Al = 40, 0.20 M NaOH, 65 °C, 30 min).

#### **4.1.3 Structural and Morphological Properties**

The XRD patterns of parent and post-synthesis treated HZSM-5 with different Si/Al ratio (15, 40 and 140) are shown in Figure 12A-C. The relative crystallinity (RC) of all samples is summarized in Table 2.

The XRD patterns of parent and modified HZSM-5 exhibit XRD reflections that are characteristic of MFI structure with a certain decrease of the characteristic reflections. Figure 14A-C revealed that long-range ordering and relative crystallinity were influenced by post-synthesis methods. The effects of the post-synthesis modifications appear to depend on the treatment conditions and more importantly zeolite Si/Al ratio. Upon alkaline treatment, for example, there was no change in the position of the XRD peaks, suggesting the preservation of long-range ordering. This was observed regardless of zeolite Si/Al ratio. However, the degree of crystallinity of HZSM-5 (Si/Al = 15) evaluated by the ratio between the areas of the diffraction peaks ( $2\theta = 20 - 25^\circ$ ) of the NaOH-treated samples and parent sample, was higher than 95 % (Table 2). This was observed regardless of the concentration of NaOH solution and number of desilication cycle. However, the relative crystallinity of HZSM-5 of higher Si/Al ratio (i.e. 40) decreased with increasing the concentration of NaOH solution and number of desilication cycle, all of which are much lower than that for parent HZSM-5 (Si/Al = 40). The RC of HZSM-5 (Si/Al = 40) decreased to 90, 84, and 78 upon alkaline treatment using 0.05 M (1 cycle), 0.05 M (2 cycles)) and 0.10 M (1 cycle) NaOH, respectively. The RC of HZSM-5 of quite high Si/Al ratio (140) was not affected by alkaline treatment.

These findings imply that high degree of desilication only occurred for zeolite with Si/Al ratio of 40. The results are in complete agreement with the elemental and N<sub>2</sub> sorption measurements, and further demonstrate the essential role of framework aluminum in controlling the process of silicon extraction and subsequently the formation of intracrystalline mesopores [37] [57] [58] [59]. Extraction of Si species from HZSM-5 of Si/Al of 15 is very difficult, owing to the high concentration of framework aluminum species (negatively charge  $\text{AlO}_4^-$ ) that stabilizes the surrounding silicon atoms against hydrolysis by  $\text{OH}^-$ . On the contrary, the cleavage of Si-O-Si bond is much easier for HZSM-5 (Si/Al = 40), owing to the low concentration of neighboring Al tetrahedra. Nevertheless, alkaline treatment of zeolite with quite high Si/Al results in excessive Si extraction and large mesopores of low degree of interconnectivity.

Upon post-synthesis modification with Mn salt, the relative crystallinity of HZSM-5 decreased with increasing the loading of Mn (up to 4.0 wt %), reaching as low as 64 %. The decrease in relative crystallinity was more pronounced for zeolite with very high  $\text{SiO}_2/\text{Al}_2\text{O}_3$  ratio, most probably due to the presence of few zeolite exchange sites. Thus, post-treatment methods result in crystallinity loss, according to desilication (regardless of concentration of NaOH and number of treatment cycle) < Mn salt (Table 2). Further it is seen from Figure 14A-C that No XRD reflections belonging to bulk  $\text{MnO}_2$  particles (inset of Figure 14A) can be resolved from the XRD patterns. This implies that Mn species exist as highly dispersed extracrystalline (nanosized) oxides at the external zeolite surface, framework species, and/or dispersed extra framework species in the form of mononuclear or binuclear hydroxo-Mn species. However, the presence of framework species is very doubtful since Mn was incorporated by aqueous impregnation.



The SEM images of parent HZSM-5 and alkaline treated HZSM-5 ( $\text{SiO}_2/\text{Al}_2\text{O}_3 = 80$ ) are shown in Figure 13. As can be seen, there is no significant changes in the morphology and particle size of parent HZSM-5 upon alkaline treatment using solution of NaOH with concentration up to 0.10 M.

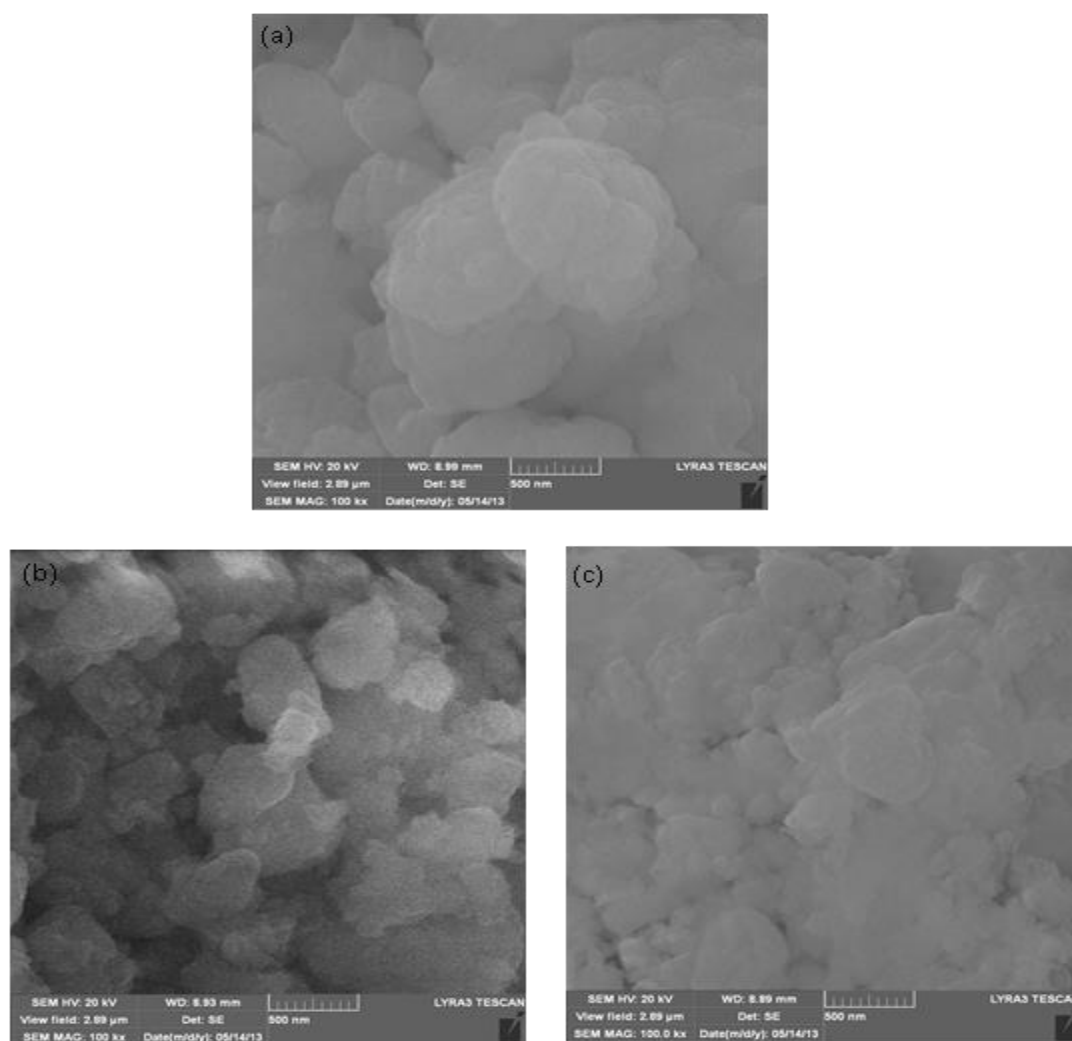


**Figure 13** SEM micrographs of (a) parent HZSM-5, and (b,c) alkaline treated HZSM-5 using NaOH of 0.05 M-2cycles and 0.10 M-1 cycle, respectively.

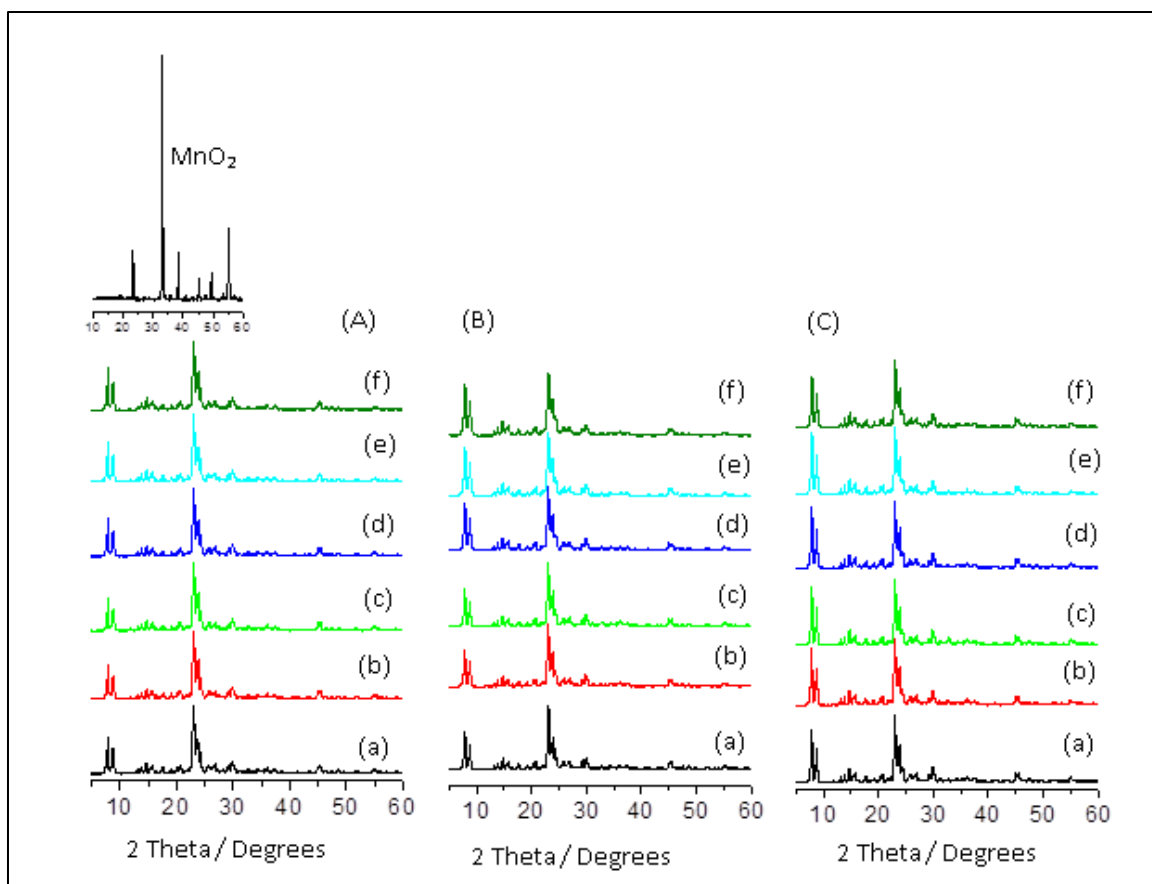


**Figure 14** XRD patterns of pure and post-modified HZSM-5 with different Si/Al ratio; (A) 15, (B) 40, and (C) 140. (a) Pure HZSM-5 (Si/Al = 15, 40 or 140), (b,c) 2.0 and 4.0 wt % Mn containing HZSM-5, respectively, (d-f) alkaline treated HZSM-5 using NaOH solution

Upon post-synthesis modification with Mn salt, the relative crystallinity of HZSM-5 decreased with increasing the loading of Mn (up to 4.0 wt %), reaching as low as 64 %. The decrease in relative crystallinity was more pronounced for zeolite with very high Si/Al ratio, most probably due to the presence of few zeolite exchange sites. Thus, post-treatment methods result in crystallinity loss, according to desilication (regardless of concentration of NaOH and number of treatment cycle) < Mn salt (Table 2). Further it is seen from Figure 14A-C that No XRD reflections belonging to bulk MnO<sub>2</sub> particles (inset of Figure 14A) can be resolved from the XRD patterns. This implies that Mn species exist as highly dispersed extracrystalline (nanosized) oxides at the external zeolite

surface, framework species, and/or dispersed extra framework species in the form of mononuclear or binuclear hydroxo-Mn species. However, the presence of framework species is very doubtful since Mn was incorporated by aqueous impregnation.

#### **4.1.4 Distribution of Mn species by H<sub>2</sub>- and CO- Temperature Programmed Reduction (H<sub>2</sub>-TPR and CO-TPR)**

TPR measurements have been used to gain qualitative information on the reducibility of oxidic species, and thus details on the nature of oxidic species (i.e. metal oxide cluster, framework and extra framework species, as well as naked isolated ions), and the degree of metal-support interactions. The H<sub>2</sub>-TPR profiles of MnO<sub>x</sub>-containing microporous and mesoporous HZSM-5 with different Si/Al ratio are depicted on Figure 16, the numerical results related to the TPR analysis are given in Table 3. H<sub>2</sub>-TPR profile of bulk MnO<sub>2</sub> (shown in the inset of Figure 16) revealed the presence of sharp peak at ~ 545 °C with an ill-defined shoulder peak at ~ 400 °C. According to Kapteijn's proposal [60], assuming that MnO is the final reduction state from various Mn species in the initial MnO<sub>x</sub>, the shoulder peak at ~ 400 °C can be assigned to the reduction of MnO<sub>2</sub>/Mn<sub>2</sub>O<sub>3</sub> to Mn<sub>3</sub>O<sub>4</sub>, while the peak at a high temperature of 545 °C can be assigned to the reduction of Mn<sub>3</sub>O<sub>4</sub> to MnO. Parent microporous HZSM-5 (not shown here) showed no distinct hydrogen consumption except for a small peak at ~ 100 - 200 °C, most probably due to the adsorption of H<sub>2</sub> on zeolite surface. The H<sub>2</sub> uptake profiles of Mn-containing microporous and mesoporous HZSM-5, irrespective of Mn loading and Si/Al ratio, revealed the presence of two well-defined temperature regions of reduction of MnO<sub>x</sub> species with maximums at ~ 291 - 322 °C, and 401 - 438 °C. These peaks correspond to the consecutive reduction of MnO<sub>x</sub> species to MnO. Hence, it can be inferred that most

MnO<sub>x</sub> species exist as highly dispersed nanostructured MnO<sub>2</sub> particles. However, this does not rule out the presence of isolated (naked) Mn ions or hydroxo-Mn species (i.e. HO-Mn-O-Mn-OH), but certainly the concentration of these species is much lower than that of nanosized MnO<sub>2</sub> particles. It was also observed that there was a gradual shift in the reduction temperatures as the zeolite Si/Al ratio increases, slowly approaching those of bulk MnO<sub>2</sub>. For instance, the first and second reduction temperature of 2.0 wt % Mn/HZSM-5 shifted from 291,404 to 322,438 °C upon increasing the zeolite Si/Al ratio from 15 to 140 (Table 3, Figure 16). Higher shift was also observed for Mn-containing alkaline treated HZSM-5 (Figure 16(g,h)). The shift in the reduction temperature may arise from structural differences, as the reduction kinetics of metal oxide is greatly influenced by particle size, morphology, and defect density [61]. The noted shift can be mainly ascribed to the increase in the size of MnO<sub>2</sub> particles owing to the decrease in the zeolite exchange sites.

Reduction by CO has been used to differentiate between isolated (naked) ion and oxo-ions, since only an oxygen-containing species can be reduced with CO [62]. The CO-TPR profiles of MnO<sub>x</sub>-containing HZSM-5 (SiO<sub>2</sub>/Al<sub>2</sub>O<sub>3</sub> = 80) are shown in Figure 15. It can be noted from Figure 15 that the CO-TPR profiles exhibit similar characteristics as those of H<sub>2</sub>-TPR profiles (viz. two well-defined reduction peaks at ~ 331 - 352 °C and 434 - 505 °C. These findings rule out the existence of isolated Mn ions, but further support the existence of large concentration of cluster of nanostructured MnO<sub>2</sub> particles.

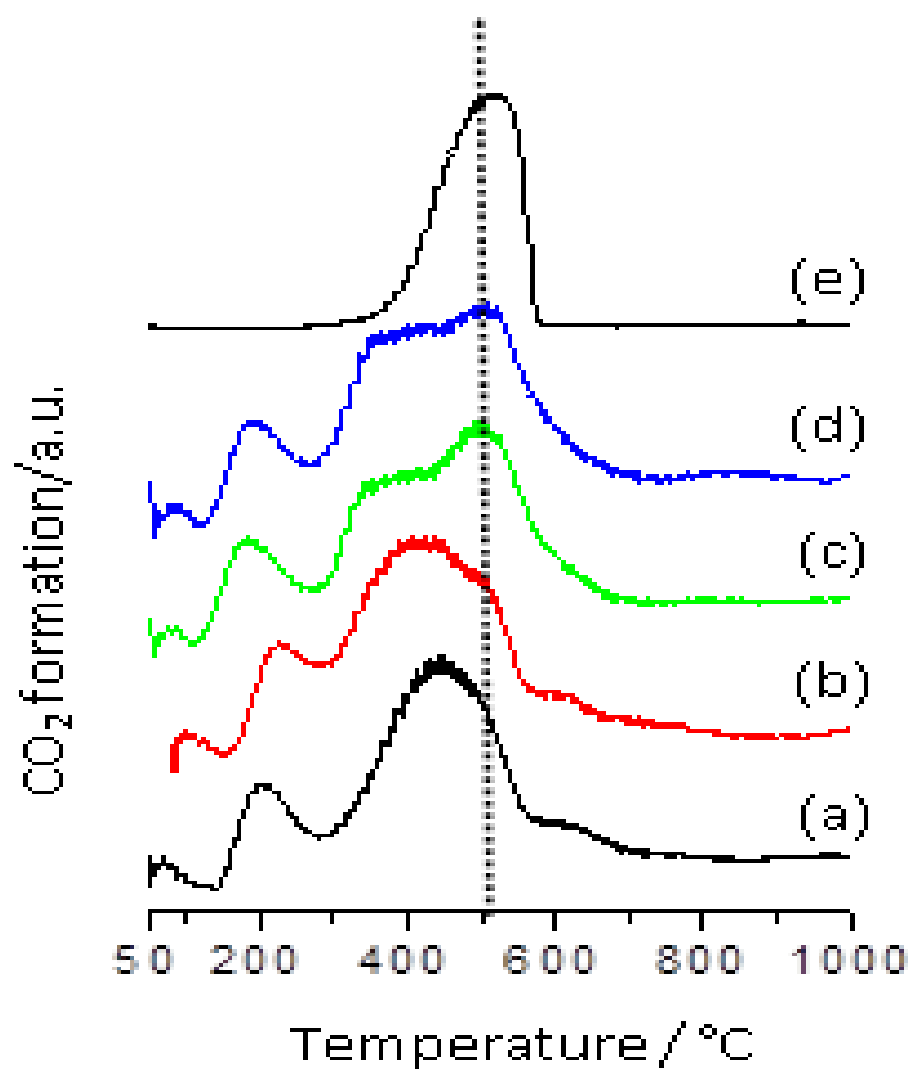


Figure 15 CO-TPR Mn-containing microporous and mesoporous HZSM-5 with  $\text{SiO}_2/\text{Al}_2\text{O}_3 = 80$ ; (a,b) 2.0, 4.0 wt % Mn/HZSM-5; (c,d) 2.0 wt % Mn supported onto alkaline treated HZSM-5 using 0.05 M (c) and 0.10 M (d) NaOH (1 cycle); and (e) bulk  $\text{MnO}_2$ .

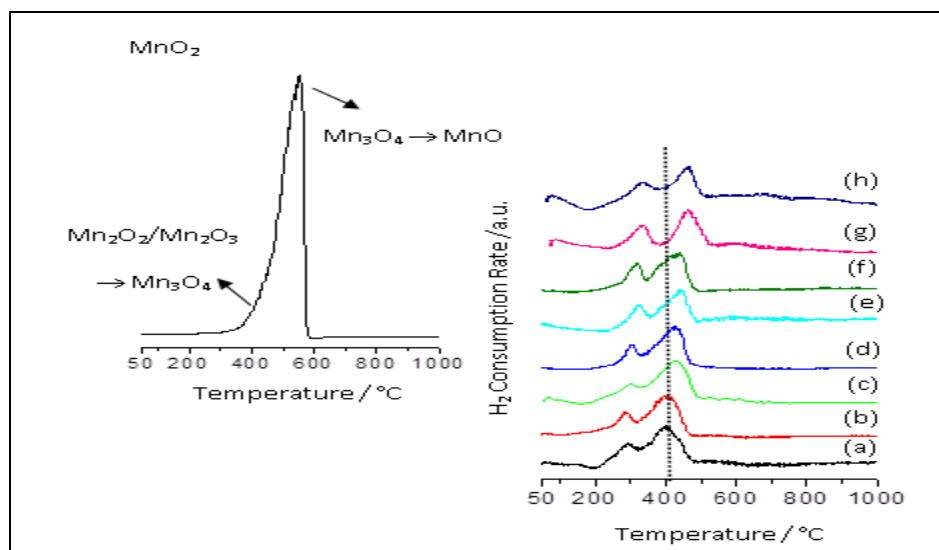


Figure 16  $H_2$ -TPR Mn-containing microporous and mesoporous HZSM-5 of different Si/Al ratio; (a,b) 2.0, 4.0 wt % Mn/HZSM-5 (Si/Al = 15); (c,d) 2.0, 4.0 wt % Mn/HZSM-5 (Si/Al = 40); (e,f) 2.0, 4.0 wt % Mn/HZSM-5 (Si/Al = 140); (g,h) 2.0 wt % Mn supported onto alkali

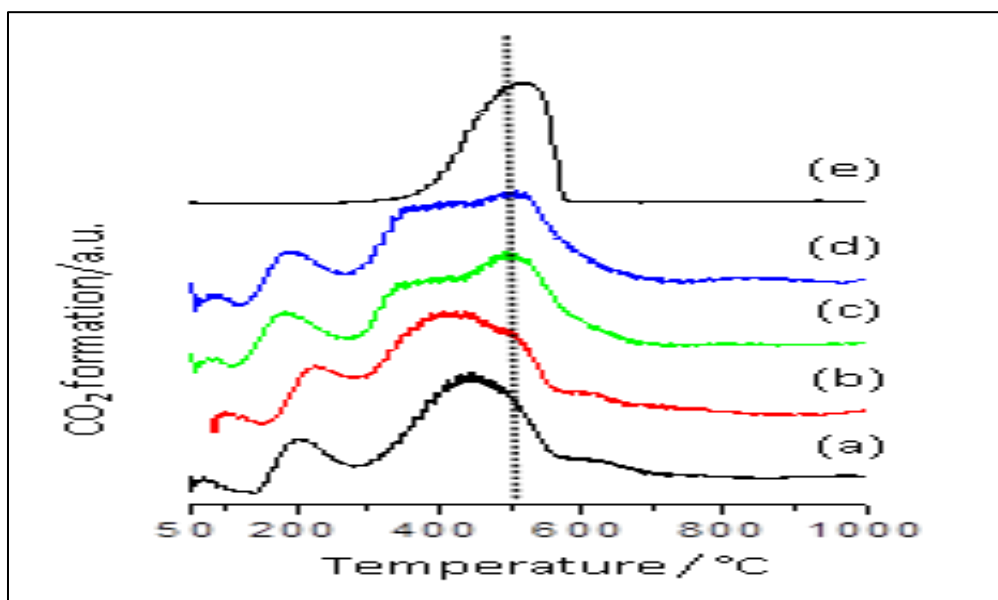


Figure 17  $CO_2$ -TPR Mn-containing microporous and mesoporous HZSM-5 with Si/Al = 40; (a,b) 2.0, 4.0 wt % Mn/HZSM-5; (c,d) 2.0 wt % Mn supported onto alkaline treated HZSM-5 using 0.05 M (c) and 0.10 M (d) NaOH (1 cycle); and (e) bulk  $MnO_2$ .

**Table 2** Physic-chemical properties of parent and post-modified HZSM-5

Catalyst	Treatment Conditions <sup>a</sup>	Chemical Composition <sup>b</sup>			N <sub>2</sub> sorption			XRD
		Molar SiO <sub>2</sub> /Al <sub>2</sub> O <sub>3</sub>	Mn (wt %)	S <sub>BET</sub> (m <sup>2</sup> g <sup>-1</sup> )	V (cm <sup>3</sup> /g) <sup>c,d</sup>	S <sub>meso</sub> (m <sup>2</sup> g <sup>-1</sup> ) <sup>e</sup>	d <sub>meso</sub> (nm) <sup>f</sup>	RC (%) <sup>g</sup>
HZ30	Parent	30.0	-	357	0.25 (0.15)	44	-	100
2Mn/HZ30	Impregnation	30.0	2.0	350	0.26 (0.15)	53	-	95
4Mn/HZ30	Impregnation	30.0	3.9	344	0.26 (0.14)	77	-	81
HZ30DSZ0.05-1C	0.05 M, 1-cycle	30.0	-	364	0.25 (0.15)	55	-	100
HZ30DSZ0.05-2C	0.05 M, 2-cycle	30.0	-	391	0.29 (0.15)	88	-	100
HZ30DSZ0.10-1C	0.10 M, 1-cycle	27.5	-	395	0.31 (0.14)	91	-	100
HZ80	Parent	80.0	-	425	0.28 (0.19)	68	-	100
2Mn/HZ80	Impregnation	80.0	2.0	411	0.30 (0.17)	74	-	84
4Mn/HZ80	Impregnation	80.0	3.7	395	0.35 (0.14)	157	-	75
HZ80DSZ0.05-1C	0.05 M, 1-cycle	57.8	-	450	0.34 (0.17)	125	9.12	90
HZ80DSZ0.05-2C	0.05 M, 2-cycle	58.4	-	477	0.41 (0.16)	164	9.20	84
HZ80DSZ0.10-1C	0.10 M, 1-cycle	50.4	-	485	0.46 (0.17)	171	10.0	78
HZ280	Parent	280	-	443	0.23 (0.21)	33	-	100
2Mn/HZ280	Impregnation	280	2.0	415	0.27 (0.17)	77	-	65
4Mn/HZ280	Impregnation	280	3.9	387	0.33 (0.15)	141	-	64
HZ280DSZ0.05-1C	0.05 M, 1-cycle	206	-	401	0.27 (0.17)	56	-	100
HZ280DSZ0.05-2C	0.05 M, 2-cycle	136	-	431	0.46 (0.06)	230	-	93
HZ280DSZ0.10-1C	0.10 M, 1-cycle	128	-	454	0.51 (0.04)	281	-	91

<sup>a</sup>: alkaline treatment using NaOH; <sup>b</sup>: ICP analysis; <sup>c</sup>: total pore volume; <sup>d</sup>: number in parenthesis corresponds to micropore volume calculated using the t-plot; <sup>e</sup>: S<sub>meso</sub> includes the mesoporous and external surface area <sup>f</sup>: average pore diameter (BJH pore size distributions derived from the adsorption branch of the isotherm), and <sup>g</sup>: relative crystallinity

**Table 3 TPR data for Mn-containing microporous and mesoporous HZSM-5 of different Si/Al**

Catalyst	Treatment Conditions <sup>a</sup>	Chemical Composition		N <sub>2</sub> sorption				XRD
		Molar Si/Al	Mn (wt %)	S <sub>BET</sub> (m <sup>2</sup> g <sup>-1</sup> )	V <sub>meso</sub> (cm <sup>3</sup> /g) <sup>b</sup>	S <sub>meso</sub> (m <sup>2</sup> g <sup>-1</sup> ) <sup>c</sup>	d <sub>meso</sub> (nm) <sup>d</sup>	RC (%) <sup>e</sup>
HZ15	Parent	15	-	425	0.23	68	-	100
2Mn/HZ15	Impregnation	15					-	95
4Mn/HZ15	Impregnation	15					-	81
HZ15DSZ0.05-1C	0.05 M, 1-cycle		-					100
HZ15DSZ0.05-2C	0.05 M, 2-cycle		-					100
HZ15DSZ0.10-1C	0.10 M, 1-cycle		-					100
2Mn/HZ15DSZ0.10	Impregnation							80
HZ40	Parent	40	-				-	100
2Mn/HZ40	Impregnation	40					-	84
4Mn/HZ40	Impregnation	40					-	75
HZ40DSZ0.05-1C	0.05 M, 1-cycle		-	450	0.31	125	9.12	90
HZ40DSZ0.05-2C	0.05 M, 2-cycle	29	-					84
HZ40DSZ0.10-1C	0.10 M, 1-cycle	25	-	485	0.44	171	10.0	78
2Mn/HZ40DSZ0.10	Impregnation							62
HZ140	Parent	140	-				-	100
2Mn/HZ140	Impregnation	140					-	65
4Mn/HZ140	Impregnation	140					-	64
HZ140DSZ0.05-1C	0.05 M, 1-cycle		-					100
HZ140DSZ0.05-2C	0.05 M, 2-cycle		-					93
HZ140DSZ0.10-1C	0.10 M, 1-cycle		-					91



## 4.1.5 Acidic Properties

### 4.1.5.1 FTIR of Pyridine Sorption

The acidic properties of parent HZSM-5, Mn-containing HZSM-5, and alkaline treated HZSM-5 evaluated by pyridine sorption are shown in Figure 18 and the numerical data are summarized in Table 3.

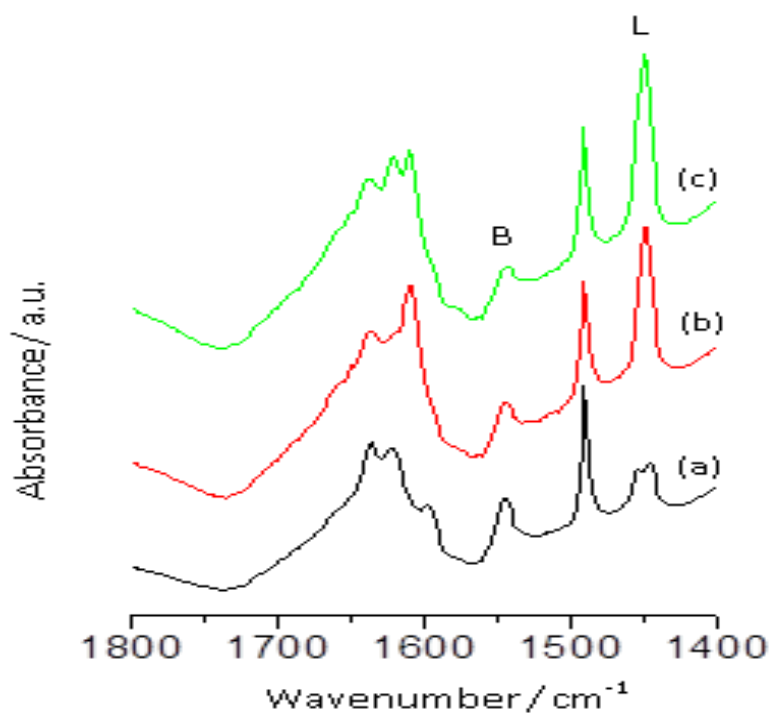


Figure 18 FTIR of adsorbed pyridine for parent N<sub>2</sub>-adsorption-desorption isotherms and derived BJH mesopore size distribution of parent HZSM-5, Mn-containing HZSM-5, and alkaline treated HZSM-5 (SiO<sub>2</sub>/Al<sub>2</sub>O<sub>3</sub> = 80). (a) Parent HZSM-5, (b) 4Mn/HZ80, and (c) HZ80DSZ0.1

The presence of such acidic sites was further confirmed by FTIR of -OH region (Figure 19). It can be seen from Figure 18 that all samples exhibited both Brönsted and Lewis acidic sites. However, there was a marked increase in Lewis acidity upon the addition of Mn and alkaline treatment.

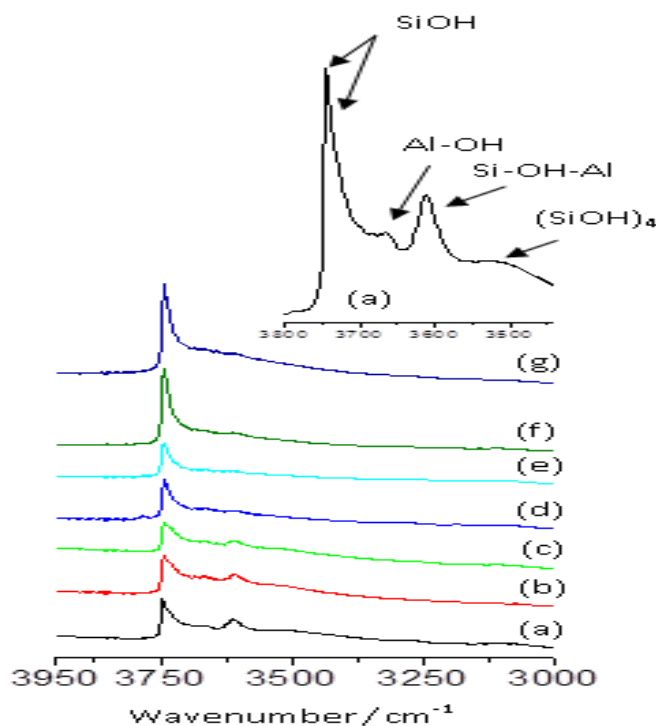


Figure 19 IR spectra in the -OH region for parent HZSM-5 ( $\text{SiO}_2/\text{Al}_2\text{O}_3 = 80$ ) (a), Mn/HZ80 of 2.0 wt % (b) and 4.0 wt % (c) Mn loading, alkaline treated HZ80 using NaOH solution of 0.05 M (1cycle) (d), 0.05 M (2 cycle) (e), and 0.10 M (1 cycle) (f), and 2.0 wt % Mn supported onto alkaline treated HZ80 using 0.105 M (1 cycle) (g).

## 4.2 Description of Catalytic Evaluation Results

In this section, results of ZSM-5 family will be presented based on: i) effect of Silica to Alumina ratio ii) post modification by introducing mesoporosity using alkali solution iii) post modification by metal impregnation.

The baseline for this work is the USY catalyst that is used commercially in refineries as an equilibrium catalyst (Ecat). The topline aimed to be crossed is the commercial additive that is used to enhance the olefins' production (OM).

Three different additives with three different silica to alumina ratios have been evaluated; namely ZSM-5(30), ZSM-5(80), and ZSM-5(280). Furthermore, versions of alkali treated versions of the previously mentioned additives have been tested. Also, metal-containing additives have been catalytically evaluated.

#### 4.2.1 Effect of Silica to Alumina ratio

The following histogram shows the conversion as well as the propylene yield measured at catalyst to oil ratio 3 at 550°C.

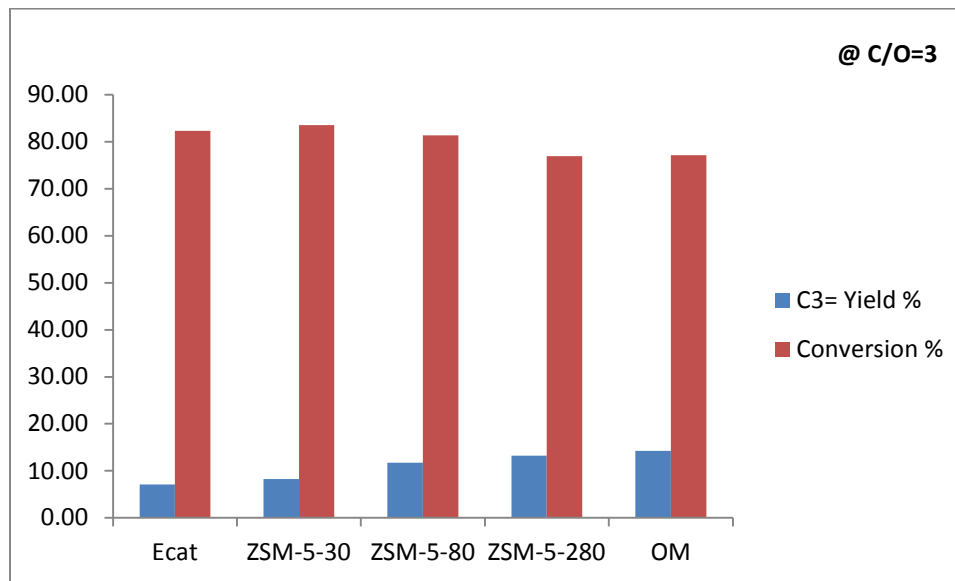


**Figure 20 Histogram of conversion and C3= yield % of Ecat, ZSM-5(30), ZSM-5(80), ZSM-5(280), and OM.**

The baseline catalyst produced 7wt% propylene at conversion of 82.30% whereas the topline (OM) produced double that 14.25wt% at conversion of 77%. Silica to Alumina ratio of 30 produced 16 wt% better of propylene (8.23 wt%) than that of baseline catalyst

(7wt% )at slightly better conversion (83.5%) than that of the latter one (82.3%) but it has been behind the commercial additive (OM) in the yield of propylene with around 42 wt% and 8% better in the conversion. Silicon to Aluminum ratio of 40 has hit the mark of 11.74 wt% propylene with 81.4% conversion which implies that it has exceeded the baseline catalyst with 66 wt% and kept a close enough conversion . At the very same time, it has reduced the difference with the commercial additive to approximately 18wt% propylene whereas it has kept an elevation in the conversion of 5.5%. Silica to Alumina ratio of 280 has lower conversion of that of the baseline catalyst while it happened to have similar one as that of the commercial additive. With respect to the propylene yield, 280 is around 87 wt% better than the baseline catalyst and approximately 8 wt% away from the commercial topline catalyst mark. To wrap up things: as Silica to Alumina ratio increases the propylene yield has increased as expected. For the three silicon to aluminum ratios used, they improved the propylene yield over the equilibrium catalyst (E-cat) and on the other hand they did not work as efficient as the commercial additive. Silica to Alumina ratio 280 has recorded a comparable propylene yield as that of the commercial additive. Information related to propylene yield for the commercial baseline catalyst and the additives is well depicted in figure 20.

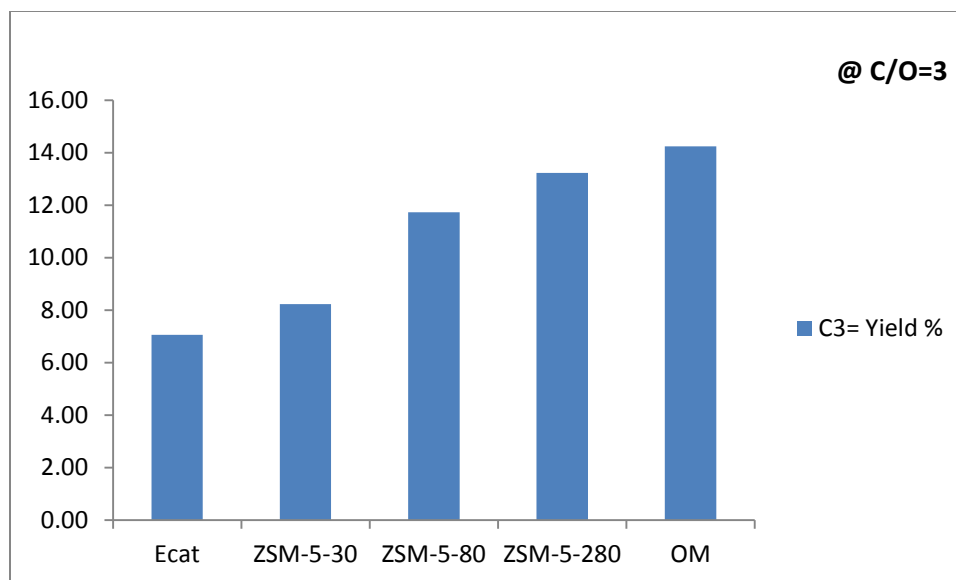


**Figure 21 C3= yield % of Ecat, ZSM-5(30), ZSM-5(80), ZSM-5(280), OM**

The same scenario is repeated when propylene yield was calculated at 70% conversion. The commercial additive (OM) has surpassed the ZSM-5 based additives with at least 10% as shown in the following bar chart.

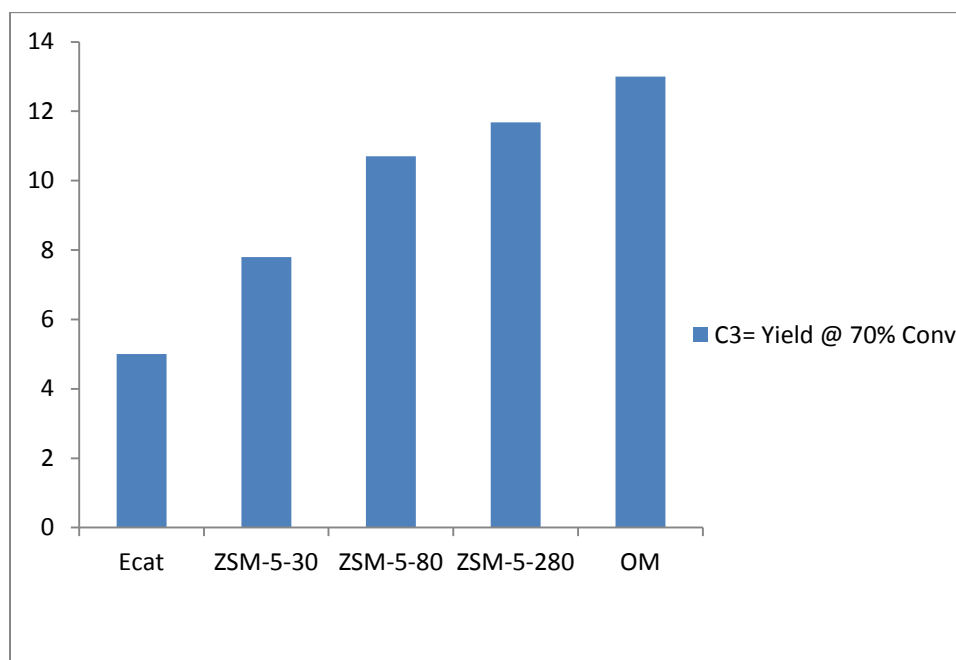


**Figure 22 C3=yield % at 70% conv. of Ecat, ZSM-5(30), ZSM-5(80), ZSM-5(280), OM**

Looking at the ethylene yield percentage which is considered to be an important light olefin as well, it is very obvious that using the ZSM-5 based additives with commercial equilibrium catalyst has boosted the ethylene yield significantly. Addition of ZSM-5(30) to the commercial base catalyst has improved ethylene yield with about 36% whereas the addition of ZSM-5(80) to the commercial base catalyst has enhanced ethylene yield with about 29%. Double the quantity of ethylene has been produced when adding ZSM-5(280) to the commercial base catalyst (Ecat) while the commercial additive (OM) has been 7% better in ethylene yield than ZSM-5(280) as shown in figure 23.

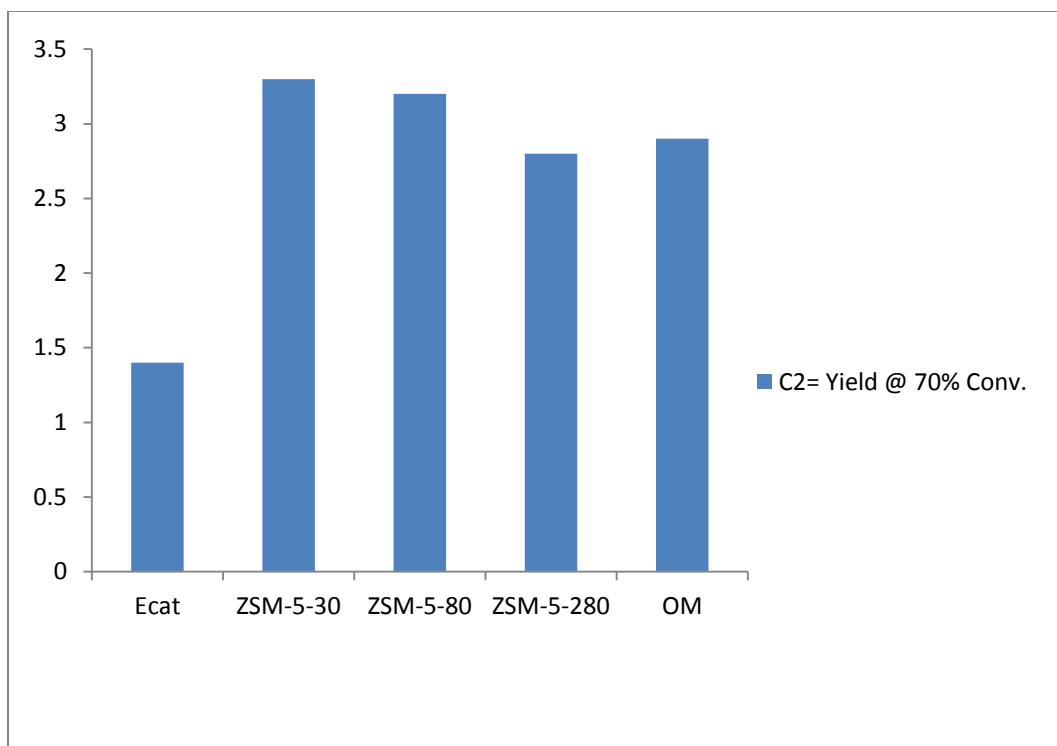


**Figure 23 C2=yield % at 70% conv. of Ecat, ZSM-5(30), ZSM-5(80), ZSM-5(280), OM**

Speaking generally about the sum of the light olefins ( C2= , C3= , C4=) produced, it is clear as shown in figure 24 that the commercial additive (OM) leads the trend of the light olefins' yield with a percentage of 28.4 wt.% whereas the commercial base catalyst produced only 13.8 wt.% light which implies 105.6 % better is the (OM).

ZSM-5(30) additive has hit the mark of 17.3 wt.% of light olefins which means 25% enhancement comparing to the commercial base catalyst but still 39% away from the commercial additive (OM). Increasing the Si/ Al ratio to 40 yield of light olefins has jumped to 24.5 wt.% surpassing the commercial catalyst (Ecat) with 77% and at the very same time it has got closer to the mark of the commercial additive as it is just 13.7% away from the latter recorded value of light olefins. When a higher silica to alumina ratio

of 280 has been tested 25.92 wt.% of light olefins have been obtained implying that it is 88% closer to the value of commercial additive (OM).

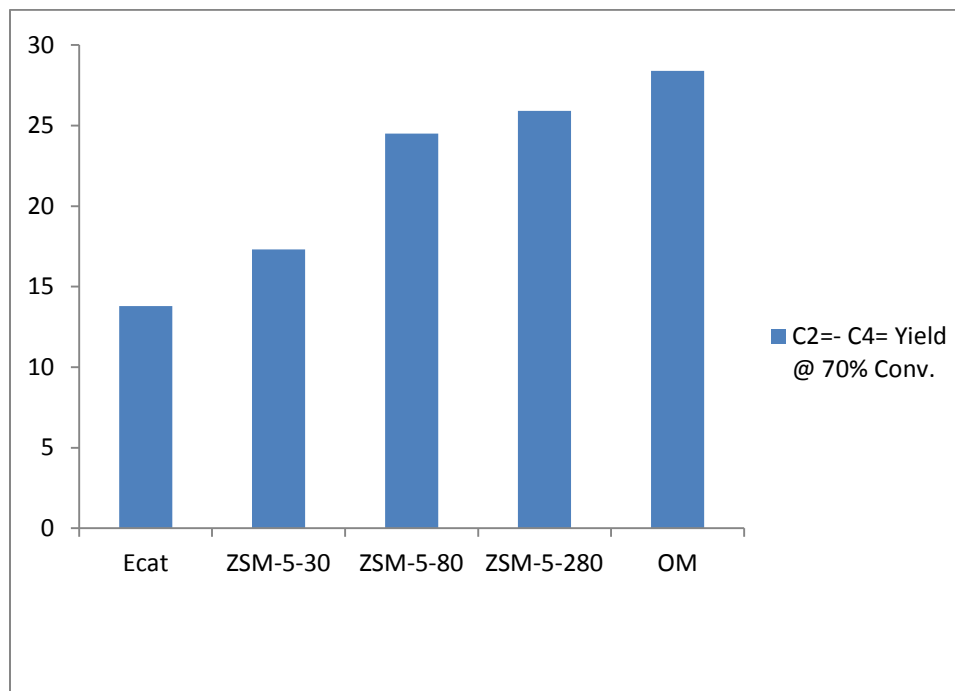


**Figure 24 C2= - C4= yield % at 70% conv. of Ecat, ZSM-5(30), ZSM-5(80), ZSM-5(280), OM**

As known, the FCC process has been made mainly for the production of gasoline so it is of a great value to look the gasoline yield.

As depicted in figure 25, the commercial catalyst produced 50 wt.% of gasoline was 70% conversion while the commercial additive has produced 35% less with a value of only 32.4 wt.%

ZSM-5(30) and ZSM-5(80) have given 33% less gasoline yield than the commercial base catalyst with values of 33.5 wt.% and 33.4 wt.% respectively. They also exceeded the commercial additive with 3%. ZSM-5(280) gave approximately 35 wt% gasoline which implies 8% better than the commercial additive. Comparing 280 silica to alumina ratio



with the commercial base catalyst, its 30% away of the latter gasoline's yield at the same conditions.

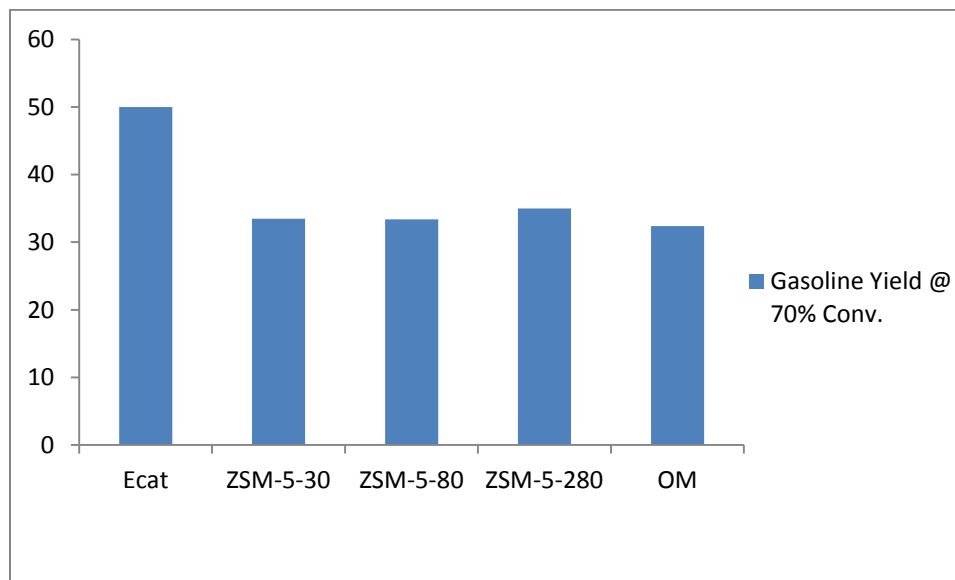


**Figure 25 Gasoline yield % at 70% conv. of Ecat, ZSM-5(30), ZSM-5(80), ZSM-5(280), OM**

#### 4.2.2 Effect of Metal Addition

The following histogram (figure 26) shows the effect of the metal impregnation of the surface of the ZSM-5 based additives on the propylene yield at catalyst to oil ratio of 3. It is observed that modifying ZSM-5(x) with 2 wt.% manganese and 4 wt.% manganese had a great impact on the propylene yield.

ZSM-5(30) has been modified with 2 wt.% manganese such that 2% Mn ZSM-5(30) additive has produced 13.22 wt% propylene with an increase over the parent catalyst ZSM-5(30) of around 61%. When manganese percentage was increased to 4 wt.% propylene yield increased to 14 wt.% which means 70% better than the parent ZSM-5(30).

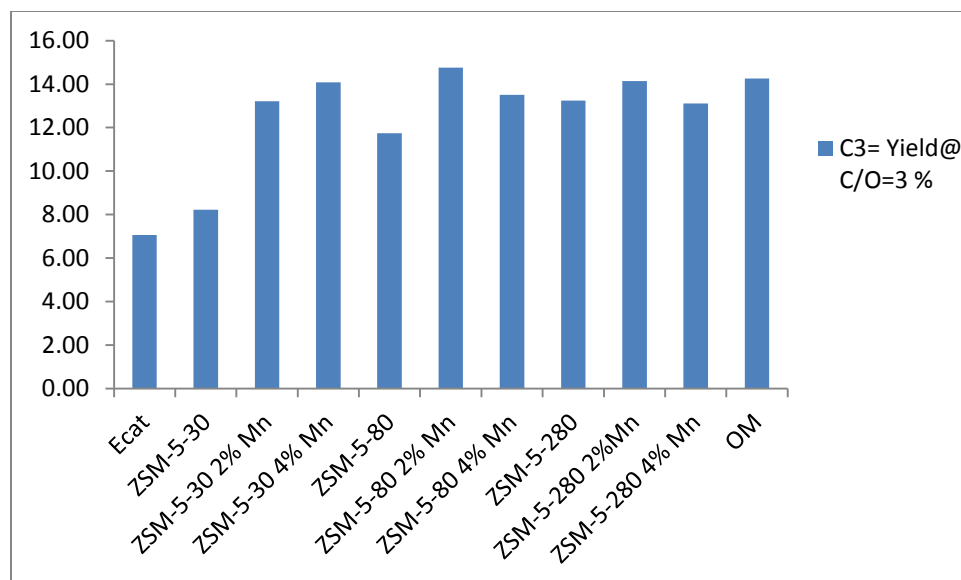


**Figure 26 C3= Yield % of Ecat, ZSM-5 additives with Mn, and OM**

Regarding ZSM-5(80), addition of 2 wt.% Mn has boosted the propylene yield with 25% over the parent additive. Numerically speaking, it has jumped from 11.74 wt.% propylene yield to 14.74 wt.% propylene yield as per the addition of 2 wt.% metal. On the other hand, increasing metal addition to 4 wt.% has elevated propylene yield to 15% over the parent. It has basically jumped from 11.74 wt.% ( ZSM-5(80) ) to 13.51 wt.% (4% Mn ZSM-5(80) ) .

With respect to ZSM-5(280), 2 wt.% of Mn added to it has improved the propylene yield with 6.7% such that the parent additive (ZSM-5(280) ) gave 13.24 wt.% propylene while 2%Mn ZSM-5(280) gave 14.13 wt.% propylene. When coming to impregnating ZSM-5(280) with 4 wt.% Mn, propylene yield has dropped with around 1% comparing to the unmodified parent additive (ZSM-5(280) ).

It is observed that volcano phenomena has appeared in modifying both ZSM-5(80) and ZSM-5(280) with 2 wt.% Mn and 4 wt.% Mn. As shown is figure 27 propylene yield at

C/O 3 of ZSM-5(80) has increased when adding 2 wt.% Mn then decreased when Mn content elevated to 4 wt.% . Same scenario is applicable to ZSM-5(280).

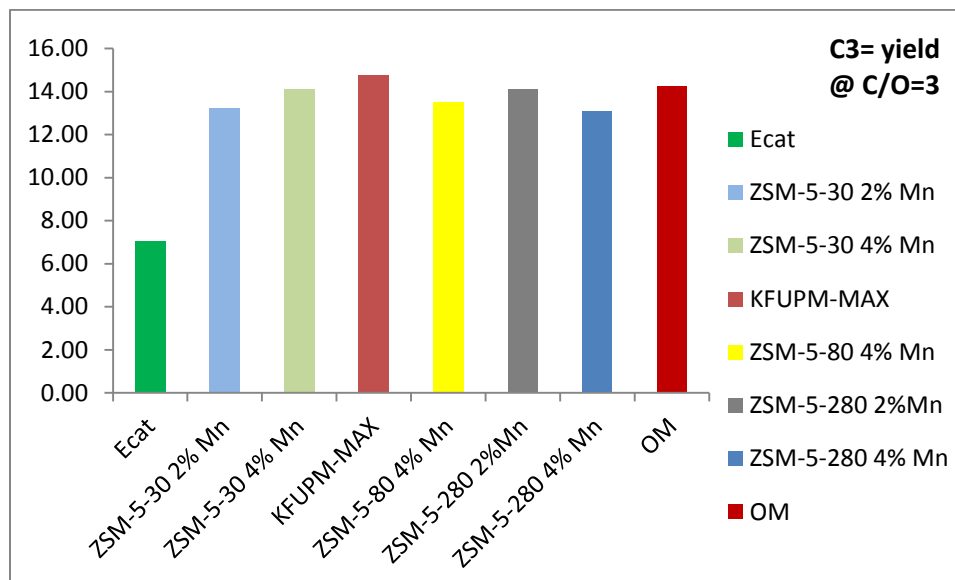


Figure 27 C3= Yield % of Ecat, Mn- Containing ZSM-5, and OM

2%Mn ZSM-5(30) has exceeded the commercial equilibrium catalyst in propylene yield with around 87% such that the former has hit the mark of 13.22 wt% propylene whereas the latter has achieved 7 wt.% propylene only. Comparing this modified version with the commercial additive (OM) which has yielded an average value of propylene of 14.25 wt.% it is obvious that the latter is still have the superiority on 2%Mn ZSM-5(30) with around 7.8% . For the 4%Mn ZSM-5(30), it has gone better than the commercial catalyst in terms of propylene yield with double the quantity, while the commercial additive (OM) has kept its superiority with just 1.2 %.

2%Mn ZSM-5(80) ( KFUPM-MAX) has achieved a landmark propylene yield as it exceeded the mark of the commercial catalyst with 109 % and at the very same time it exceeded the mark of the commercial additive (OM) with 3.5% as the former yielded

14.75 wt.% propylene while the latter yielded 14.25 wt.% propylene. 4%Mn ZSM-5(80) has produced 13.51 wt.% propylene which means 91% better than that of the commercial catalyst and 5.2 % less than that of the commercial additive.

2%Mn ZSM-5(280) has produced 14.13 wt.% propylene which in fact an enhancement of 99.9% over the commercial the catalyst. Comparing this Mn-containing ZSM-5 with the commercial additive (OM) led to the conclusion of having less than 1% optimality for the favor of the commercial additive of course. Doubling the manganese content in the same additive (4%Mn ZSM-5(280)) recorded 85% superiority over the commercial catalyst and 8% inferiority with respect to the commercial additive (OM).

Same scenario is repeated when doing the previous comparison on corresponding data computed at 70% conversion as shown in figure 28.

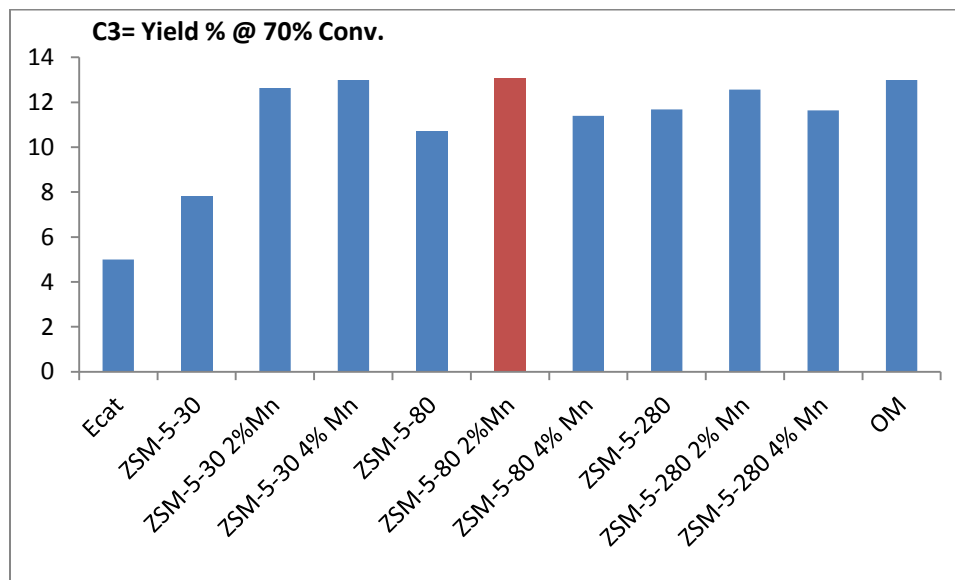


**Figure 28 C3= Yield % @ 70% conv. of Ecat, Mn- Containing ZSM-5, and OM**

Regarding the ethylene yield, figure 29 shows clearly the advancement of 2%Mn ZSM-5(80) over all other additives with a yield of 3.32 wt.%. ZSM-5(30) parent comes in the

second place with ethylene yield of 3.3 wt.% . ZSM-5(80) parent has a competitive yield of ethylene of 3.2 wt.% . 2%Mn ZSM-5(30) returned 3 wt.% ethylene. The commercial additive (OM) has given 2.9 wt.% ethylene and not far from it is 4%Mn ZSM-5(30) with an ethylene yield of 2.85 wt. % as well as ZSM-5(280) parent with 2.8 wt.% ethylene yield.

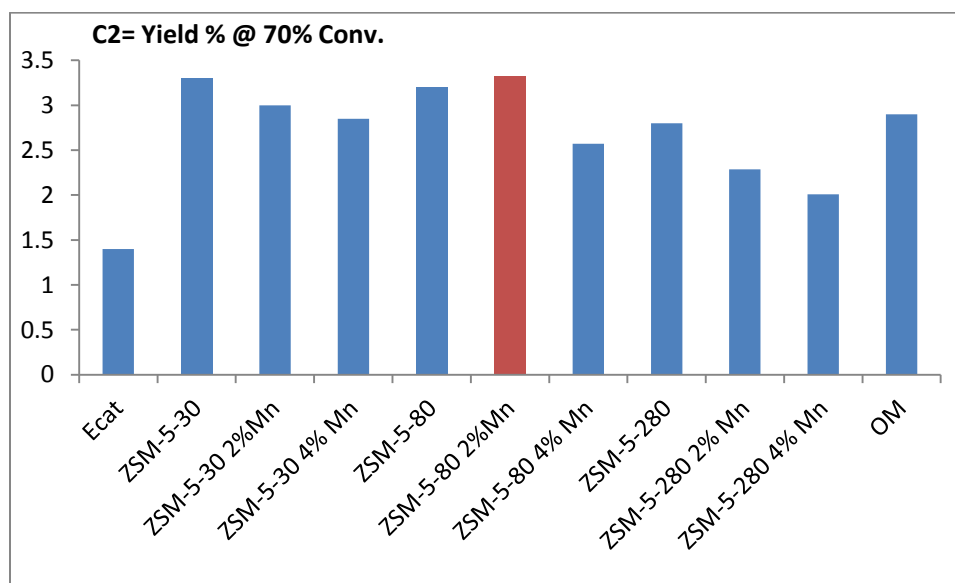


**Figure 29 C2= Yield % @ 70% conv. of Ecat, Mn- Containing ZSM-5, and OM**

Addition of 4 wt.% Mn to ZSM-5(80) has boosted ethylene yield to 2.57 wt.% whereas adding 2 wt.% Mn to ZSM-5(280) returned an ethylene yield of 2.29 wt.% . 4%Mn ZSM-5(280) gave 2 wt.% ethylene. A minimum enhancement of 43.6% has been achieved over the commercial catalyst (yields 1.4 wt.% ethylene) and a maximum enhancement of 137% has been recorded as well.

As shown in figure 30, the total amounts of light olefins at 70% conversion showed a superiority of 2%Mn ZSM-5(80) over the commercial base catalyst as well as all other additives in this study as it has yielded 29wt.% light olefins (C2= - C4=) which is

basically 110% better than the commercial base catalyst and 2% better than the commercial additive OM.

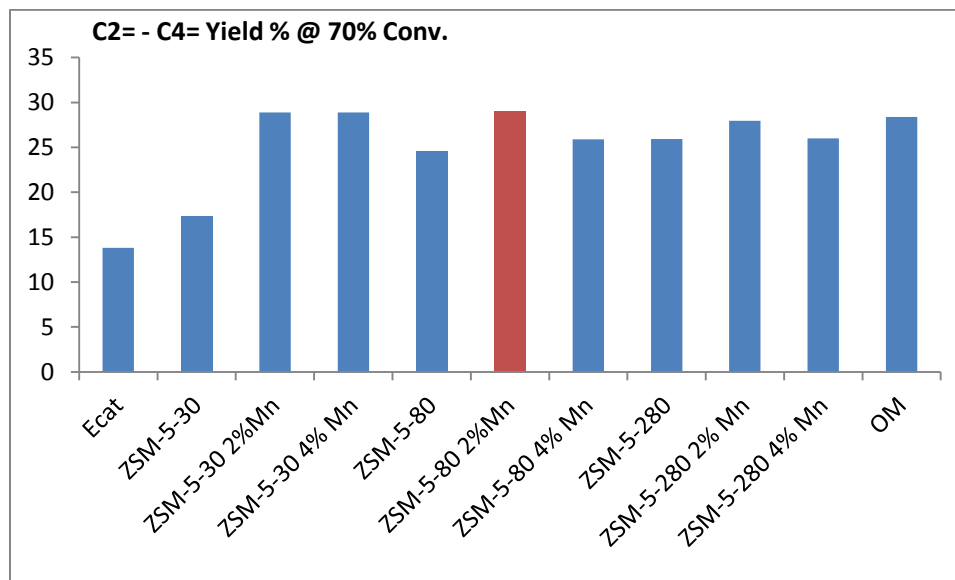


**Figure 30 C2= - C4= Yield % @ 70% conv. of Ecat, Mn- Containing ZSM-5, and OM**

ZSM-5(30) has produced a total amount of light olefins of 17.3 wt.% which is 25% better over the commercial base catalyst. Addition of 2wt.% and 4wt.% of Mn on ZSM-5(30) has resulted in having 28.9 wt.% light olefins of each which means an enhancement of 109% over the base catalyst Ecat. Unmodified ZSM-5(80) had a light olefin yield of 24.5 wt.% implying that 78% enhancement has been achieved over Ecat. An improvement of 87% in the light olefins' yield over the base catalyst has been achieved when ZSM-5(80) has been impregnated with 4wt.% of Mn. ZSM-5(280) has hit the mark of 25.92 wt.% light olefins making it 88% ahead of the commercial base catalyst. Upon the addition of 2wt. % Mn over ZSM-5(280) , the total yield of light olefins has reached a value of 27.97 wt.% which makes it 103% better than that of the commercial catalyst Ecat. Increasing the load of Mn to 4wt. % loaded to the same catalyst ZSM-5(280) had a light olefins' yield value of 26 wt.% which turned to be 88% better than the commercial base catalyst

Ecat. The commercial additive OM has hit the mark of 28.4wt.% light olefins which is 106% better than that of the commercial base catalyst.

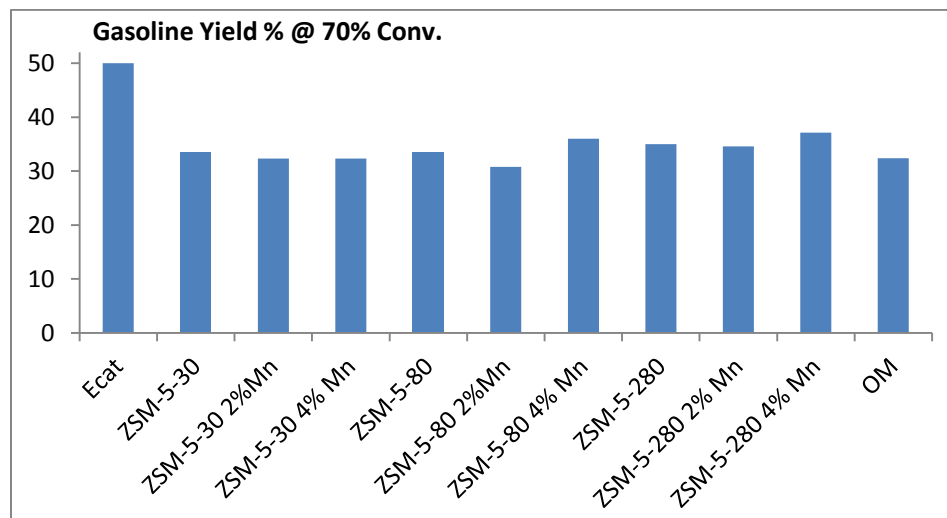


**Figure 31 Gasoline Yield % @ 70% conv. of Ecat, Mn- Containing ZSM-5, and OM**

Figure 31 shows the gasoline yield at 70% conversion. The commercial base catalyst Ecat has produced 50wt.% gasoline at 70% conversion. Upon the addition of ZSM-5(30), a reduction of 33% in the gasoline yield has been record as its gasoline yield is 33.5 wt.%. 2%Mn ZSM-5(30) has yielded 32.3 wt.% gasoline with a reduction of 35% . 4%Mn ZSM-5(30) has produced 32.35 wt.% gasoline. ZSM-5(80) had 33.4wt.% gasoline yield at 70% conversion which is 33.2% less than that of the commercial catalyst whereas 2%Mn ZSM-5(80) has returned 30.8 wt.% gasoline which means 38.4% less than the returned gasoline yield when Ecat has been used alone. A reduction of 28% in the gasoline yield at 70% conversion compared to that of the Ecat has been recorded upon the addition of 4wt.% Mn to ZSM-5(80) as it has yielded 36 wt.% gasoline. 34.97 wt.% gasoline has been produced when ZSM-5(280) has been used as an additive which is 30% less than that of the recorded gasoline yield of Ecat alone. 2wt.% of Mn added to ZSM-5(280) has resulted in a gasoline yield of 34.56 wt% which is 30.88% less than that of the

commercial base catalyst. 4 wt.% Mn ZSM-5(280) has produced 37 wt.% gasoline which is nothing but 25.8% less than that of the Ecat. The commercial additive OM has yielded 32.4 wt.% gasoline which is 35.2 less than that of the commercial base catalyst Ecat.

#### 4.2.3 Effect of Alkali Treatment (Desilication)

Concentration of Alkali solution used in the treatment was investigated for possible impact as well as number of cycles of treatment. Generally speaking, both factors have a great impact on the structure of the catalyst and consequently effect on the performance of the catalyst.

As shown in the table below, the ethylene yield upon the modification by alkali solution with different concentrations (0.05M, 0.10M) and for different cycles of treatment (1 cycle, 2 cycles) has been in the range of 4 wt.% and 5 wt.% with a span of enhancement between 145 % and 207% comparing to the base catalyst .

**Table 4 Meso-HZSM-5(30) FCC data**

C/O=3 , T=550	D-ZSM-5 (30) 1C (0.1)	D-ZSM-5(30) 2C (0.05)	D-ZSM5-(30) 1C (0.05)
Conv.%	76.3	75.8	82.4
C2= %	4.78	4.18	4.81
C3=%	10.92	10.1	11.22
C4=%	8.49	8.22	8.83
Gasoline%	35.02	34.36	37.77

On the other hand, the propylene yield at the same treatment conditions has been in the range of 10 wt.% and 11.22 wt.% with an enhancement range of 41% to 59 % with



respect to the base catalyst . The butylenes were in the range of 8 wt.% to 9 wt.% with a reduction between 6% and 16.5 % in comparison with the Ecat. A reduction range between 32 % and 39 % has been accomplished in the gasoline yield compared to that of the base catalyst such that these modified version of HZSM=5(30) have produced gasoline in the range of 34 wt.% and 38 wt.% depending on the treatment conditions.

Washing the catalyst with 0.10 M NaOH for one cycle has given almost same olefins yield as washing it with 0.05M for one cycle. Conversion was better of 0.05M NaOH. In terms of olefins, it is obviously observed that there is no significant impact of the way of treatment.

With respect to meso-HZSM-5(80), two batches of 1C 0.10M NaOH have been tested. They behaved approximately the same with a slight advantage for the first batch. Comparing the ethylene yield with that of the base catalyst, meso-HSZM-5(80) has yielded ethylene in the range of 4 wt.% and 4.6 wt.% which implies an enhancement range of 146% to 182 %. With respect to the propylene yield, it has been in the range of 13.5 wt.% and 14 wt.% with a range of enhancement comparing to the Ecat 91% to 98 %. The butylenes' yield ranged from 11.5 wt.% and 12.1 wt.% with enhancements ranged from 20% to 26% over the commercial catalyst. Gasoline yield (34 wt.% - 36 wt.% ) has been reduced with values 35 % to 39 % compared to that of the base catalyst. Comparing 1C 0.10M NaOH with 1C 0.05M NaOH gives the impression of similar results of conversion, slight difference in C2= for the favor of 1C 0.05M NaOH, slight difference in C3= for the favor of 1C 0.10M NaOH, difference in C4= for 1C 0.10M NaOH, and slight difference in gasoline yield for the favor of 1C 0.05M NaOH.

As a result, it is observed that there is no significant effect of way of treatment as presented in the table below.

**Table 5 Meso-HZSM-5(80) FCC data**

C/O=3 , T=550	D-ZSM-5 (80) 1C (0.1) Batch #1	D-ZSM-5 (80) 1C (0.1) Batch#2	D-ZSM-5(80) 2C (0.05)	D-ZSM5-(80) 1C (0.05)
Conv. %	<b>80.82</b> ( 80.4 , 81.24)	<b>77.4</b> ( 77.6, 77.2)	75.13	<b>80.44</b> (77.94, 82.94)
C2= %	<b>4.4</b> (4.34, 4.46)	<b>4.09</b> (4.07, 4.11)	4.22	<b>4.55</b> (4.29, 4.81)
C3=%	<b>13.84</b> ( 13.5 , 14.17)	<b>13.54</b> (13.55, 13.52)	11.02	<b>13.51</b> (12.99, 14.02)
C4=%	<b>12.095</b> (12, 12.19)	<b>12.07</b> (12.16, 11.98)	9.56	<b>11.53</b> (11.18, 11.88)
Gasoline%	<b>35.79</b> (35.98, 35.6)	<b>34.08</b> (34.3, 33.86)	32.32	<b>36.01</b> (35.25, 36.77)

**Bold values:** average of what's inside the brackets

#### 4.2.4 Kinetic Study

It's been well established in the literature that the catalytic cracking of heavy feedstocks such as vacuum gas oil is a second order reaction (Weekman and Nace, 1970). This has been justified by the complicity of the feed in a sense that it comprises thousands of compounds from different cuts with respect to properties especially the boiling point.

In order to write the rate equation of the reaction, the wide general picture will be adapted in order to do so.

$$-r_{VGO} = -\frac{dY_{VGO}}{dt_{t.o.s}} = kY_{VGO}^2 \quad (4.1)$$

$$Y = 1 - X \quad (4.2)$$

Where  $Y_{VGO}$  is the weight fraction of VGO,  $t_{t.o.s}$  is the time on stream,  $k$  is the kinetic rate constant, and  $X$  is the VGO conversion.

$$\left(\frac{C}{O}\right) = t_{t.o.s} \quad (4.3)$$

Substituting both (4.3) and (4.2) in (4.1) and doing the mathematics, the following equation is obtained:

$$-r_{VGO} = \frac{dX_{VGO}}{d(C/O)} = k(1 - X)^2 \quad (4.4)$$

Where  $C/O$  is the catalyst to gasoil ratio.

Integrating equation (4.4):

$$\int \frac{dX_{VGO}}{d(C/O)} = \int k(1 - X)^2 \quad (4.5)$$

Computing the integration yields:

$$\frac{1}{1-X} = k(C/O) + c \quad (4.6)$$

Where  $c$  is the integration constant.  $C$  is evaluated at conditions of  $t_{t.o.s}$  equals to zero i.e.  $C/O$  equals to zero which leads of course to a conversion  $X$  of zero. Equation (4.6) falls into:

$$\frac{X}{1-X} = k(C/O) \quad (4.7)$$

The term  $\frac{x}{1-x}$  is defined as the kinetic conversion K. Plotting the kinetic conversion versus the C/O yields a slope of a value of the kinetic rate constant k.

In order to evaluate the activation energy, Arrhenius equation has been used for that sake such that three different temperatures have been used in order to make the plots of kinetic conversion versus catalyst to oil ratio as precise as possible.

$$k = A \exp\left(-\frac{E_a}{RT}\right) \quad (4.8)$$

Where k is the kinetic rate constant (  $\text{mol}^{-1} \text{s}^{-1}$ ), A (  $\text{mol}^{-1} \text{s}^{-1}$ ) is the Arrhenius constant,  $E_a$  (J/mol) is the activation energy, R (J/mol.K) is the gas constant, and T is the temperature in kelvin.

Figures 32, 33, and 34 show the scatter of three catalyst to oil ratios (C/O= 1, 2, 3) versus the kinetic conversion at temperatures 500°C, 550°C, and 600°C respectively. Tables 6, 7, and 8 show the results of combined kinetic-deactivation rate constant at three temperatures 500°C, 550°C, and 600°C respectively.

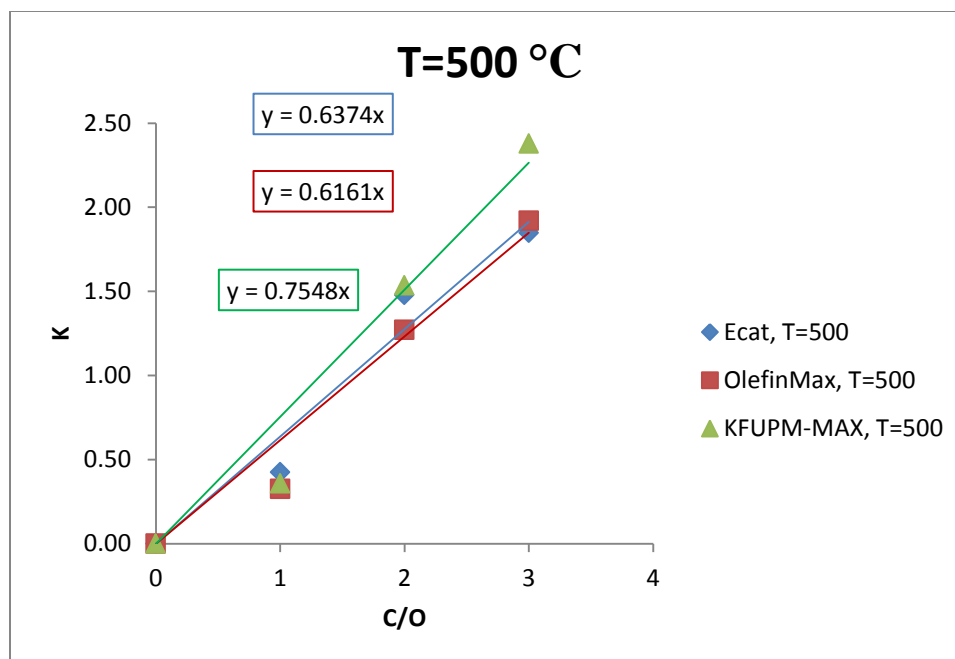


Figure 32 C/O ratio v.s. kinetic conversion K at 500 C

The following table (table 6) shows the results of the slope for the three catalysts as well as the reciprocal of the temperature and the anti-exponential (ln) values of the slope that are going to be used to evaluate the apparent activation energies. Same info is presented in tables 7 and table 8.

Table 6 Combined kinetic-deactivation rate constant for Ecat, OM, KFUMP-MAX at T=773 K

Cat. Name	SLOPE	T (K)	k(Slope)	1/T	lnk
Ecat	0.64	773.00	0.64	1.29E-03	-4.50E-01
Olefin-MAX	0.62	773.00	0.62	1.29E-03	-4.84E-01
KFUPM-MAX	0.75	773.00	0.75	1.29E-03	-2.81E-01

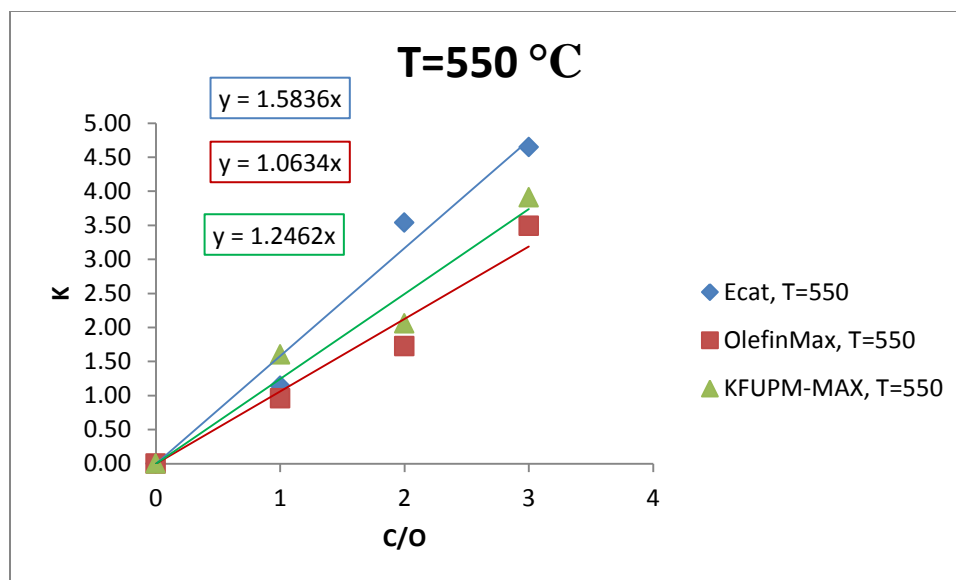


Figure 33 C/O ratio v.s. kinetic conversion K at 550 C

Table 7 Combined kinetic-deactivation rate constant for Ecat, OM, KFUMP-MAX at T=823 K

Cat. Name	SLOPE	T (K)	k(Slope)	1/T	lnk
Ecat	1.58	823.00	1.58	1.22E-03	4.60E-01
Olefin-MAX	1.06	823.00	1.06	1.22E-03	6.15E-01
KFUPM-MAX	1.25	823.00	1.25	1.22E-03	2.20E-01

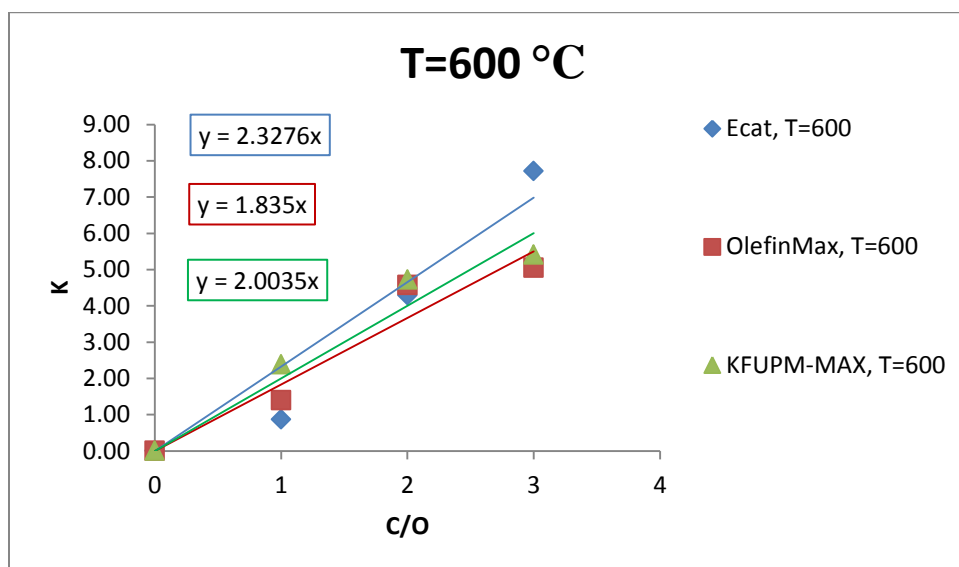


Figure 34 Figure 28 C/O ratio v.s. kinetic conversion K at 600 C

**Table 8 Combined kinetic-deactivation rate constant for Ecat, OM, KFUMP-MAX at T=873 K**

Cat. Name	SLOPE	T (K)	K(Slope)	1/T	lnk
Ecat	2.33	873.00	2.33	1.15E-03	8.45E-01
Olefin-MAX	1.84	873.00	1.84	1.15E-03	6.07E-01
KFUPM-MAX	2.00	873.00	2.00	1.15E-03	6.95E-01

Using the ln form of Arrhenius equation leads to:

$$\ln k = \ln A - \left( \frac{E_a}{RT} \right) \quad (4.9)$$

When 1/T versus lnk has been plotted, the following graph has been produced.

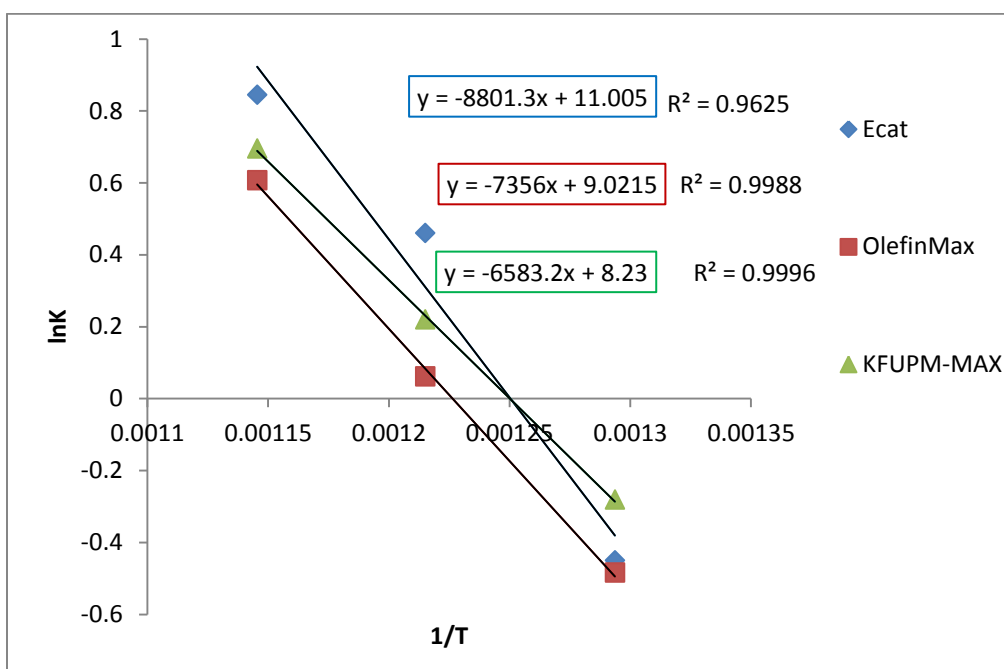


**Figure 35 Reciprocal of T ( 1/K ) v.s. lnk**

**Table 9 Apparent calculated and literature activation energies**

Cat. Name	Ea (kJ/mol)	Ea (Kcal/mol)	Ea* (Kcal/mol) literature
Ecat	73.17	17.85	10-36
OM	54.73	13.35	
KFUPM-MAX	61.16	14.92	

\*: A. Avidan, R. Shinnar, Ind. Eng Chem. Res. 29 (1990) 931 942.

As shown in table 9, the cracking activation energy of Ecat has been calculated to be approximately 18 kcal/mol whereas that of the commercial additive OM has been found to be approximately 13.4 kcal/mol. The KFUPM-MAX has recorded a value of cracking activation energy of approximately 15 kcal/mol. The three activation energies for the three catalysts have been with the values established in the literature [57]. Approximately 17% reduction has been achieved in the activation energy upon the usage of KFUPM-MAX along with Ecat instead of using the latter alone.

### **4.3 Discussion of Results in light of Characterizations**

#### **4.3.1 The enhancement in olefins due to the alkaline treatment**

Based on the activity evaluation data, there has been an enhancement in the propylene production as an example in the range of 90% over that of the commercial catalyst. This enhancement is attributed to two main factors:

- i. The existence of secondary network of intracrystalline mesopores.
- ii. The increase in the acidity due to the extraction of Si species which results in the decrease in the Si/Al ratio in the structure of the active matrix in the zeolite which implies an elevation in the concentration of Al in the matrix.

These two factors played a substantial role in the following:

- i. The suppression or the reduction of secondary hydrogen transfer reactions and that is achieved by lowering the residence time of reaction intermediates inside the pores which basically doesn't give the chance for the intermediates to go back to the paraffinic form but to desorb as olefinic products.



- ii. Offering easier transport and accessibility for the hydrocarbon cuts to the active sites especially those with lower accessibility to zeolite micropores due to their size (Aromatics) or their branching (branched isomers). By this, diffusion limitations are reduced.

#### **4.3.2 The enhancement in olefins due to the metal modification**

Based on the activity evaluation data, there has been an enhancement in the propylene production as an example in the range of 85% - 109% over that of the commercial catalyst. This enhancement is attributed to a main factor:

- i. The presence of cluster of nanostructured MnO<sub>2</sub> particles.

This factor played a substantial role in the following:

- i. The partial reduction in the pore diameter of ZSM-5 micropore, and thus reducing the extent of hydride transfer reactions which are responsible for the consumption of olefins i.e. converting olefins to saturated paraffinic hydrocarbons as well as the formation of coke and hence catalyst deactivation.
- ii. Providing new dehydrogenating sites that are capable of dehydrogenating larger paraffins into C<sub>5</sub><sup>+</sup> olefins that can be cracked into light olefins.

Above factors explain the enhancement in the cracking activation energy calculated for the commercial base catalyst and the KFUPM-MAX which is basically modified by metal. The reduction of the cracking activation energy of the latter may be attributed to the existence of the nanostructured MnO<sub>2</sub> particles.

## CHAPTER 5

### OTHER METALS AND OTHER ZEOLITES

#### 5.1 Other Metals

In this work, different metals have been impregnated on HZSM-5(30) for catalytic testing and comparison with the commercial base catalyst. Zinc, Gallium, Chromium, Iron, and Nickel metals have been loaded on the HZSM-5(30) via wet impregnation, and the load was 2 wt.% . Later on, Manganese has been introduced as the metal of choice for the enhancement of olefins as explained in the previous chapters.

As shown in table 10, 2 wt.% Zn HZSM-5(30) has produced 3.51 wt.% ethylene which is basically 115% better than that of the commercial catalyst . Same modified additive has yielded 10.70 wt.% propylene which is 51% better than that of the Ecato.

Table 10 Catalytic data of different metals

C/O=3	Ecat	Different metals				
		Zn	Ga	Cr	Fe	Ni
Conversion, %	82.30	81.01	78.70	85.35	84.37	82.50
Yield, %						
C2=	1.63	3.51	3.51	4.70	4.66	3.41
C3=	7.07	10.70	10.07	12.40	12.19	8.34
C4=	9.58	9.31	8.52	9.58	9.09	6.29
Light Olefins (C2=-C4=)	18.27	23.51	22.10	26.68	25.94	18.04
Gasoline	55.75	41.20	38.61	36.25	35.21	40.98

The butylenes were almost same as those of the commercial catalyst The gasoline has dropped from 55.75 wt.% ( Ecato) to 41.20 wt.% with a reduction value of 26%.

2wt.% GaHZSM-5(30) has produced 3.51 wt.% ethylene which is 115% better than that of the commercial base catalyst and at the very same time it could produce 10.07 wt.% propylene which is nothing but 42% better than that of the Ecat. On the other hand, it has produced 8.52 wt.% butylenes which is 11% less than that of the commercial base catalyst. 38.61 wt.% gasoline has been obtained with a reduction value of 31 % compared with the commercial base equilibrium catalyst.

2wt.% CrHZSM-5(30) has yielded 4.70 wt.% ethylene which is 188% better than that of the commercial base catalyst. It also produced 12.40 wt.% propylene with an enhancement of 75% over the commercial Ecat. With respect to butylenes, it has produced exactly the same amount of the Ecat (9.58 wt.%). A reduction of 36% in the yield of gasoline has been recorded compared to the Ecat.

2wt.% FeHZSM-5(30) has yielded 4.66 wt.% ethylene which is 188% better than that of the commercial base catalyst. It also produced 12.19 wt.% propylene with an enhancement of 72% over the commercial Ecat. With respect to butylenes, it has produced 9.09 wt% with a reduction value of 5% compared to the commercial catalyst. A reduction of 37% in the yield of gasoline has been recorded compared to the Ecat with a yield of 35.21 wt.% .

2wt.% NiHZSM-5(30) has yielded 3.41 wt.% ethylene which is 186% better than that of the commercial base catalyst. It also produced 8.34 wt.% propylene with an enhancement of 18% over the commercial Ecat. With respect to butylenes, it has produced 6.29 wt% with a reduction value of 34% compared to the commercial catalyst. A reduction of 27%

in the yield of gasoline has been recorded compared to the Ecat with a yield of 40.98 wt.% .

When 2wt.%MnHZSM-5(30) has been catalytically evaluated, it could produce 13.22 wt.% Propylene which happens to be 87% better than that of the commercial so, Mn has been the metal of choice to further study its impacts on the olefins' production. Consequently, it has been loaded to different Si/Al ratio of HZSM-5 with different loads (2wt% - 4wt.%) as clearly presented previously in chapters 3 and 4.

## 5.2 Other Zeolites

Also, other zeolites have been investigated for possible breakthrough in the olefins' production such as: Mordenite and desilicated version of it, ZSM-11 and desilicated version of it, Beta 39 and desilicated version of it, and Beta 24.

**Table 11 A: Catalytic data of different zeolites**

C/O=3	Ecat	Different Zeolites						
		Mor 18.3	D-Mor 18.3	ZSM-11	D-ZSM-11	Beta 39	D-Beta 39	Beta 24
<b>Conversion, %</b>	82.3	80.66	86.74	80.22	80.58	90.86	87.74	80.83
<b>Yield, %</b>								
<b>C2=</b>	<b>1.63</b>	<b>1.98</b>	<b>2.02</b>	<b>4.64</b>	<b>4.01</b>	<b>2.75</b>	<b>2.79</b>	<b>2.23</b>
<b>C3=</b>	<b>7.07</b>	<b>7.08</b>	<b>8.28</b>	<b>10.82</b>	<b>10.55</b>	<b>9.25</b>	<b>9.77</b>	<b>7.87</b>
<b>C4=</b>	9.58	8.89	10.84	8.33	8.73	9.15	9.31	8.53
<b>Light Olefins (C2=-C4=)</b>	18.27	1.95	21.14	23.79	23.28	21.15	21.88	18.64
<b>Gasoline</b>	55.75	40.46	43.99	34.95	39.31	39.65	39.07	36.84

As shown in table 11 A, Mor 18.3 has produced 1.98 wt.% ethylene which is basically 21% better than that of the Ecat whereas it has produced almost the same amount of propylene. 7% less butylenes Mor 18.3 has yielded compared to the base catalyst

butylenes yield. Gasoline has dropped down with a percentage of 27% compared to that of the Ecat.

The desilicated version of Mor 18.3 (D-Mor 18.3) has recorded a 24% enhancement in the ethylene production when compared to that of the base commercial catalyst. D-Mor 18.3 could yield 8.28 wt.% propylene which is nothing but 17% better than that of the Ecat. It has produced 10.84 wt.% butylenes with an enhancement of 13%. In contrast, gasoline has been lowered to a value of 44 wt.% which is 21% less than that initially produced by the commercial Ecat.

A yield of 4.64 wt.% of ethylene has been obtained using ZSM-11 as an FCC additive which is 185% better than using Ecat alone. The propylene yield has been recorded to be 10.82 wt.% which is basically 53% better than that of the commercial base catalyst. With respect to the butylenes, ZSM-11 could produce 8.33 wt.% which is 13% less than that of the commercial base catalyst. A reduction of 37% in the gasoline yield has occurred upon the addition of ZSM-11 to the Ecat as well.

The desilicated ZSM-11 (D-ZSM-11) has behaved quiet close to the parent ZSM-11. It has 146% enhancement over the base catalyst when talking about the ethylene yield and 49% enhancement at the case of propylene. On the other hand, there has been a reduction of 9% in the butylenes and 30% in the gasoline.

Beta 39 has produced 2.75 wt.% ethylene which is 69% better than that of the commercial bas catalyst. 9.25% wt.% of propylene has been yielded with an enhancement of 31% over the Ecat. A reduction of 5% has been recorded in the butylenes yield compared to the commercial Ecat as Beta 39 has yielded 9.15 wt.% butylenes only.

Moreover, 29% reduction has been recorded in the gasoline yield as Beta 39 has produced 39.65 wt.% gasoline compared to 55.75 wt.% in the case of Ecat.

The desilicated version of Beta 39 ( D-Beta 39) had a similar behavior of the parent Beta-39. It could produce 2.75 wt.% ethylene ( 71% enhancement over Ecat), 9.77 wt.% propylene ( 38% enhancement over Ecat), 9.31 wt.% butylenes ( 3% reduction compared to the Ecat), and 39 wt.% gasoline ( 30% reduction in comparison to the Ecat).

The catalytic performance of Beta 24 has shown improvements in the ethylene yield which was 2.23 wt.% which is 37% ahead of that of the commercial catalyst. With respect to the propylene yield, it has yielded 7.87 wt.% giving Beta 24 11% enhancement over the Ecat. A reduction of 11% has been recorded in the butylenes compared to the Ecat as Beta 24 has yielded 8.53 wt.% butylenes. At the same time, 36.84 wt.% gasoline has been produced with a reduction of 34% in comparison with the Ecat.

Furthermore, other zeolites have been tested for possible improved propylene production modified Ferrite with Mn, MCM-22 and its modified version with Mn, MCM-56 and its modified version with Mn, and others. Table 12B shows the results of those zeolites.

MCM-22 could produce 4.18 wt.% ethylene which is 156% better than that of the commercial Ecat. It has recorded an enhancement of 42% in the propylene yield such that the latter was 10.02 wt.% . A yield of 7.15 wt.% of butylenes has been obtained with a reduction of 25% compared to the commercial base catalyst. A reduction of 45% has been recorded in the gasoline yield as MCM-22 has produced only 30.84 wt.% .

Upon the modification using 2wt.%Mn, MCM-22 catalytic performance has been improved in sense that the 12.47 wt.% propylene has been obtained with an enhancement

of 25% over the parent MCM-22 as well as an enhancement of 76% over the base catalyst. With respect to the ethylene, it has produced 2.76 wt.% with a reduction value of 34 % in comparison with parent MCM-22, but it has recorded an enhancement of 69% compared to the Ecat. The butylenes' yield has been recorded to be 10.73 wt.% which is 50% better than the parent MCM-22 and at the very same time it is 12% better than that of the commercial base catalyst Ecat. When talking about the gasoline, there has been a yield of 36.16 wt.% with a reduction value of 34% in comparison with the commercial base catalyst.

**Table 12 B: Catalytic data of different zeolites**

C/O=3	Ecat	Different Zeolites						
		MCM-22	2%Mn MCM-22	MCM-56	2%Mn MCM-56	Ferr	2%Mn Ferr	4%Mn Ferr
<b>Conversion, %</b>	82.3	88.07	83.26	84.99	83.68	74.73	73.52	77.57
<b>Yield, %</b>								
<b>C2=</b>	<b>1.63</b>	<b>4.18</b>	<b>2.76</b>	<b>3.27</b>	<b>2.67</b>	<b>3.87</b>	<b>2.81</b>	<b>2.7</b>
<b>C3=</b>	<b>7.07</b>	<b>10.02</b>	<b>12.47</b>	<b>10.72</b>	<b>13.18</b>	<b>12</b>	<b>9.56</b>	<b>10.02</b>
<b>C4=</b>	9.58	7.15	10.73	8.82	10.67	9.27	8.67	9.34
<b>Light Olefins (C2=-C4=)</b>	18.27	21.35	25.96	22.81	26.53	25.13	21.03	22.07
<b>Gasoline</b>	55.75	30.83	36.61	34.84	37.53	38.19	43.63	46.65

MCM-56 has yielded 3.27 wt.% ethylene with an enhancement value of 100 % over the commercial base catalyst. With respect to the yield of propylene, MCM-56 could produce 10.72 wt.% propylene with an increase value of 51.63 % over the Ecat. A reduction of 8% in comparison with the Ecat in the yield of butylenes has occurred upon the addition of MCM-56 as the latter has produced 8.82 wt.% of C4= only. Also, a reduction of 38 % in the gasoline yield compared to the Ecat has been recorded when adding MCM-56.

Upon the modification by using 2wt.%Mn, MCM-56 catalytic performance has been improved in sense that the 13.18 wt.% propylene has been obtained with an enhancement of 23% over the parent MCM-56 as well as an enhancement of 86% over the base catalyst. With respect to the ethylene, it has produced 2.67 wt.% with a reduction value of 18 % in comparison with parent MCM-56, but it has recorded an enhancement of 64% compared to the Ecat. The butylenes' yield has been recorded to be 10.67 wt.% which is 21% better than the parent MCM-56 and at the very same time it is 11.4% better than that of the commercial base catalyst Ecat. When talking about the gasoline, there has been a yield of 37.53 wt.% with a reduction value of 33% in comparison with the commercial base catalyst.

Ferr has yielded 3.87 wt.% ethylene with an enhancement value of 137 % over the commercial base catalyst. With respect to the yield of propylene, Ferr could produce 12 wt.% propylene with an increase value of 70 % over the Ecat. A reduction of 3% in comparison with the Ecat in the yield of butylenes has occurred upon the addition of Ferr as the latter has produced 9.27 wt.% of C4= only. Also, a reduction of 32 % in the gasoline yield compared to the Ecat has been recorded when adding Ferr.

Upon the modification by using 2wt.%Mn, Ferr catalytic performance has dropped down in sense that the 9.56 wt.% propylene has been obtained with an a reduction of 35% compared to the parent Ferr but with an enhancement of 72% over the base catalyst. With respect to the ethylene, it has produced 2.81 wt.% with a reduction value of 27% in comparison with parent Ferr, but it has recorded an enhancement of 72% compared to the Ecat. The butylenes' yield has been recorded to be 8.67 wt.% which is 6.5% less than that of the parent Ferr and at the very same time it is 9.5% less than that of the commercial



base catalyst Ecat. When talking about the gasoline, there has been a yield of 43.63 wt.% with a reduction value of 22% in comparison with the commercial base catalyst.

Upon the modification by using 4wt.%Mn, Ferr catalytic performance has dropped down in sense that the 10.02 wt.% propylene has been obtained with an a reduction of 16.5% compared to the parent Ferr but with an enhancement of 42% over the base catalyst. With respect to the ethylene, it has produced 2.7 wt.% with a reduction value of 30% in comparison with parent Ferr, but it has recorded an enhancement of 66% compared to the Ecat. The butylenes' yield has been recorded to be 9.34 wt.% which is similar to that of the parent Ferr but it is 2.5% less than that of the commercial base catalyst Ecat. When talking about the gasoline, there has been a yield of 46.65 wt.% with a reduction value of 16% in comparison with the commercial base catalyst

## CHAPTER 6

### CONCLUSIONS AND RECOMMENDATIONS

#### 6.1 CONCLUSIONS

This work has gone in depth of enhancing the olefins' production through using different unmodified zeolites as FCC additives. A later stage has come to the scene in which those zeolites have been post modified via different routes: a) Metal addition using wet impregnation with different loads b) introducing mesoporosity via alkaline treatment using Sodium Hydroxide solution with different treatment conditions.

Using different zeolites as FCC additives led to a conclusion of highlighting the MFI based additives (ZSM-5 family) and seeking the best enhancements from it

Upon the usage of unmodified versions of ZSM-5 based catalysts as FCC additives enhancements of 16% to 87% in the propylene yield compared to that of the commercial base catalyst has been achieved and at the very same time enhancements of 95% to 170% has in the ethylene yield compared to that of the Ecat has been attained.

Upon the metal (manganese) addition to the ZSM-5 based FCC additives, enhancements of 85% all the way to 109% have been recorded. KFUPM-MAX (2wt.% MnZSM-5(80)) has performed the best when talking about the propylene yield.

Upon the alkaline treatment of ZSM-5 based additives using sodium hydroxide solution, the propylene yield has been boosted to values in the range of 90% in comparison with the commercial base catalyst Ecat. The enhancements have been attributed to the increase

in the acidity as well as the presence of secondary network of intracrystalline mesopores which facilitated the transport to/ from the pores.

Upon the addition of Mn metals to ZSM-5 Based additives, a reduction in the activation energy of the cracking reaction has been observed. The activation energy of KFUPM-MAX has been calculated to be 15kcal/mol whereas that of the commercial base catalyst has been found to be 18 kcal/mol. This has been owed to the existence of manganese nano sized particles that enhanced the dehydrogenation of parafiins and increased the acidity as well.

## **6.2 Recommendations**

The recommendations of a great value to this work would be the following:

1. Scaling up the work using KFUPM-MAX as an FCC additive in different reactors such as Advanced Cracking Evaluation (ACE) reactor. Then, scaling it up using a pilot plant in order to check its commerciality.
2. Investigating more different zeolites' structures with different metals as well as manganese to check any possible enhancements.
3. Usage of different methods of preparations other than post modification by wet impregnation such as direct synthesis and chemical vapor deposition as well as using different metal salts as precursors for the metal modification other than the one used in this work.
4. Using different method other than alkaline treatment for creating mesoporsity such as CTAB-mediated assembly.

## APPENDIX

**Table 13 Comparative MAT data at constant conversion (70%) over ZSM-5(30)/E-Cat and desilicated ZSM-5/Ecat with different Mn content at 550 C**

ZSM-5	E-Cat		ZSM-5(30)/E-Cat				D-ZSM-5(30)/E-Cat			
Mn, wt%	0	0	1.0	2.0	4.0	0	0 *	1.0	2.0	4.0
Catalyst/oil ratio, g/g	1.7	2.5	2.0	1.7	1.8	2.0	2.5	2.4	2.0	2.2
Product Yields, %										
Dry Gas	3.2	5.8	6.0	4.6	4.7	5.6	6.7	5.0	4.5	4.4
H <sub>2</sub>	0.05	0.2	0.1	0.05	0.08	0.1	0.16	0.08	0.08	0.09
C <sub>1</sub>	0.7	0.9	0.9	0.7	0.8	0.9	1.2	0.8	0.8	0.9
C <sub>2</sub> =	1.4	3.3	3.9	3.0	2.9	3.4	4.0	3.0	2.9	2.5
C <sub>2</sub>	0.8	1.3	1.1	0.9	0.9	1.1	1.3	1.0	0.9	1.0
LPG	15.9	31.0	32.6	32.8	32.4	30.6	30.3	28.0	30.5	28.8
C <sub>3</sub> =	5.0	7.8	11.4	12.6	13.0	9.8	10.0	10.8	11.6	11.6
C <sub>3</sub>	0.6	8.6	4.2	2.0	1.7	4.8	5.0	2.40	1.9	1.5
C <sub>4</sub> =	7.4	6.5	10.8	13.2	13.1	9.2	8.3	10.4	12.1	11.8
n-C <sub>4</sub>	0.4	2.5	1.7	1.2	0.9	1.9	1.9	1.2	1.1	0.8
i-C <sub>4</sub>	2.1	5.3	4.4	3.7	3.2	4.8	4.6	3.5	3.8	3.0
C <sub>2</sub> = - C <sub>4</sub> =	13.80	17.3	26.1	28.9	28.9	22.5	22.0	24.2	26.5	25.8
Gasoline	50.0	33.5	30.6	32.3	32.4	33.2	32.1	35.0	34.2	35.9
LCO	12.8	8.1	10.5	10.9	11.5	10.0	10.3	11.5	12.5	11.9
HCO	17.2	21.8	19.4	19.1	18.6	19.6	19.5	18.5	17.6	18.2
Coke	0.5	0.8	0.60	0.20	0.56	0.52	0.82	0.50	0.72	0.84

**Table 14 Comparative MAT data at constant conversion (70%) over ZSM-5(80)/E-Cat and desilicated ZSM-5/Ecat with different Mn content at 550 C**

ZSM-5	E-Cat	ZSM-5(80)/E-Cat		D-ZSM-5(80)/E-Cat		
Mn, wt%	0	0	2.0	4.0	0	0 *
Catalyst/oil ratio, g/g	1.7	1.8	2.3	2.0	2.3	1.9
Product Yields, %						
Dry Gas	3.15	5.1	5.4	4.4	5.8	5.30
H <sub>2</sub>	0.05	0.07	0.1	0.08	0.1	0.08
C <sub>1</sub>	0.7	0.8	0.9	0.8	0.9	0.8
C <sub>2</sub> =	1.4	3.2	3.3	2.5	3.8	3.4
C <sub>2</sub>	0.8	1.0	1.0	0.9	1.2	1.0
LPG	15.9	31.4	33.3	29.2	32.2	31.0
C <sub>3</sub> =	5.0	10.7	13.1	11.4	10.7	11.8
C <sub>3</sub>	0.6	3.8	2.35	1.6	4.7	2.4
C <sub>4</sub> =	7.4	10.6	12.6	11.9	9.9	11.6
n-C <sub>4</sub>	0.4	1.7	1.2	0.8	1.9	1.2
i-C <sub>4</sub>	2.1	4.8	4.2	3.4	4.9	3.9
C <sub>2</sub> = - C <sub>4</sub> =	13.8	24.5	29.0	25.9	24.3	26.7
Gasoline	50.0	33.4	30.8	36.0	31.2	33.5
LCO	12.8	11.2	10.8	11.3	10.2	11.6
HCO	17.2	19.0	19.1	18.4	19.8	18.5
Coke	0.5	0.8	0.8	0.7	0.9	0.6

\*: One treatment cycle with 0.05M NaOH.

**Table 15 Comparative MAT data at constant conversion (70%) over ZSM-5(280)/E-Cat and desilicated ZSM-5/Ecat with different Mn content at 550 C**

ZSM-5	E-Cat	ZSM-5(280)/E-Cat			D-ZSM-5(280)/E-Cat
Mn, wt%	0	0	2.0	4.0	0 *
Catalyst/oil ratio, g/g	1.7	2.3	2.0	1.8	1.9
Product Yields, %					
Dry Gas	3.2	4.6	4.0	3.7	4.1
H <sub>2</sub>	0.05	0.06	0.06	0.06	0.06
C <sub>1</sub>	0.7	0.8	0.8	0.7	0.9
C <sub>2</sub> =	1.4	2.8	2.3	2.0	2.6
C <sub>2</sub>	0.8	0.9	0.9	0.8	0.8
LPG	15.9	29.8	31.1	28.9	30.8
C <sub>3</sub> =	5.0	11.7	12.6	11.6	12.1
C <sub>3</sub>	0.6	1.9	1.4	1.2	1.7
C <sub>4</sub> =	7.40	11.5	13.1	12.4	12.5
n-C <sub>4</sub>	0.4	0.9	0.7	0.7	0.9
i-C <sub>4</sub>	2.1	3.9	3.3	3.0	3.6
C <sub>2</sub> = - C <sub>4</sub> =	13.8	25.9	26.0	26.0	27.2
Gasoline	50.0	35.0	37.1	37.1	34.6
LCO	12.8	11.4	12.1	12.1	12.5
HCO	17.2	18.6	17.9	17.9	17.5
Coke	0.5	0.6	0.5	0.5	0.5

\*: One treatment cycle with 0.05M NaOH.

**Table 16 Catalytic data of Ecat at different C/O ratios**

<b>Ecat</b>			
<b>C/O</b>	<b>1</b>	<b>2</b>	<b>3</b>
<b>Conv.%</b>	53.30	77.97	82.30
<b>Dry Gas</b>	2.87	3.21	3.62
<b>H2</b>	0.04	0.06	0.08
<b>C1</b>	0.70	0.79	0.93
<b>C2</b>	0.80	0.88	0.97
<b>C2=</b>	1.33	1.47	1.63
<b>C3</b>	0.51	0.75	0.98
<b>C3=</b>	3.65	5.81	7.07
<b>iC4</b>	1.22	2.68	3.56
<b>nC4</b>	0.27	0.51	0.70
<b>LPG</b>	10.88	18.33	21.88
<b>C4=</b>	5.24	8.59	9.58
<b>C2= - C4=</b>	10.22	15.86	18.27
<b>Gasoline</b>	39.22	55.78	55.75
<b>LCO</b>	13.59	11.59	10.48
<b>HCO</b>	33.11	10.44	7.22
<b>Coke</b>	0.32	0.66	1.05

**Table 17 Catalytic data of Ecat/ZSM-5(30) at different C/O ratios**

<b>Ecat/ZSM-5(30)</b>			
<b>C/O</b>	<b>1</b>	<b>2</b>	<b>3</b>
<b>Conv%</b>	51.87	54.50	83.53
<b>Dry Gas</b>	4.79	5.17	6.35
<b>H2</b>	0.09	0.12	0.19
<b>C1</b>	0.89	1.07	0.99
<b>C2</b>	1.14	1.33	1.32
<b>C2=</b>	2.66	2.65	3.85
<b>C3</b>	4.04	5.53	11.16
<b>C3=</b>	6.49	6.90	8.23
<b>iC4</b>	2.25	2.72	7.38
<b>nC4</b>	1.08	1.32	3.32
<b>LPG</b>	19.92	22.75	36.66
<b>C4=</b>	6.05	6.28	6.57
<b>C2= - C4=</b>	15.20	15.84	18.65
<b>Gasoline</b>	26.87	25.93	39.65
<b>LCO</b>	10.54	10.02	8.05
<b>HCO</b>	37.59	35.48	8.42
<b>Coke</b>	0.29	0.64	0.87

Table 18 Catalytic data of Ecat/ZSM-5(80) at different C/O ratios

<b>Ecat/ZSM-5(80)</b>			
<b>C/O</b>	<b>1</b>	<b>2</b>	<b>3</b>
<b>Conv%</b>	46.12	74.50	81.40
<b>Dry Gas</b>	4.67	5.30	6.93
<b>H2</b>	0.06	0.08	0.11
<b>C1</b>	0.87	0.78	1.06
<b>C2</b>	1.05	0.99	1.33
<b>C2=</b>	2.70	3.45	4.42
<b>C3</b>	1.95	4.27	5.75
<b>C3=</b>	8.15	11.07	11.74
<b>iC4</b>	1.67	5.39	6.37
<b>nC4</b>	0.70	1.89	2.29
<b>LPG</b>	20.20	33.40	36.33
<b>C4=</b>	7.72	10.78	10.20
<b>C2= - C4=</b>	18.58	25.30	26.36
<b>Gasoline</b>	20.76	34.87	36.60
<b>LCO</b>	10.40	11.15	9.37
<b>HCO</b>	43.48	14.35	9.23
<b>Coke</b>	0.49	0.93	1.54

Table 19 Catalytic data of Ecat/ZSM-5(280) at different C/O ratios

<b>Ecat/ZSM-5(280)</b>			
<b>C/O</b>	<b>1</b>	<b>2</b>	<b>3</b>
<b>Conv%</b>	37.84	66.47	76.95
<b>Dry Gas</b>	3.32	4.43	5.02
<b>H2</b>	0.04	0.06	0.08
<b>C1</b>	0.70	0.80	0.81
<b>C2</b>	0.82	0.94	0.95
<b>C2=</b>	1.77	2.64	3.18
<b>C3</b>	0.75	1.64	2.31
<b>C3=</b>	4.85	10.86	13.24
<b>iC4</b>	1.02	3.44	4.93
<b>nC4</b>	0.27	0.82	1.18
<b>LPG</b>	11.87	27.66	34.10
<b>C4=</b>	4.98	10.89	12.44
<b>C2= - C4=</b>	11.60	24.40	28.87
<b>Gasoline</b>	22.33	33.88	36.93
<b>LCO</b>	11.67	11.51	11.17
<b>HCO</b>	50.49	22.01	11.88



Table 20 Catalytic data of Ecat/D-ZSM-5(30) 1C(0.05) at different C/O ratios

<b>Ecat/D-ZSM-5(30) 1C(0.05)</b>			
<b>C/O</b>	<b>1</b>	<b>2</b>	<b>3</b>
<b>Conv%</b>	32.57	55.72	82.42
<b>Dry Gas</b>	3.42	5.46	7.67
<b>H2</b>	0.05	0.11	0.18
<b>C1</b>	0.68	1.03	1.25
<b>C2</b>	0.81	1.17	1.43
<b>C2=</b>	1.88	3.15	4.81
<b>C3</b>	1.46	3.38	6.73
<b>C3=</b>	4.53	8.67	11.22
<b>iC4</b>	0.96	2.54	6.77
<b>nC4</b>	0.42	1.10	2.54
<b>LPG</b>	11.40	23.48	36.08
<b>C4=</b>	4.04	7.78	8.83
<b>C2= - C4=</b>	10.44	19.60	24.86
<b>Gasoline</b>	17.43	26.07	37.77
<b>LCO</b>	11.54	10.69	10.01
<b>HCO</b>	55.90	33.59	7.56
<b>Coke</b>	0.32	0.72	0.90

Table 21 Catalytic data of Ecat/D-ZSM-5(80) 1C(0.05) at different C/O ratios

<b>Ecat/D-ZSM-5(80) 1C(0.05)</b>			
<b>C/O</b>	<b>1</b>	<b>2</b>	<b>3</b>
<b>Conv%</b>	40.48	73.24	80.44
<b>Dry Gas</b>	3.70	5.50	6.77
<b>H2</b>	0.05	0.08	0.12
<b>C1</b>	0.68	0.86	0.97
<b>C2</b>	0.82	1.01	1.13
<b>C2=</b>	2.15	3.55	4.55
<b>C3</b>	1.21	2.68	3.97
<b>C3=</b>	6.54	12.36	13.51
<b>iC4</b>	1.34	4.27	5.86
<b>nC4</b>	0.47	1.33	1.84
<b>LPG</b>	15.69	32.77	36.70
<b>C4=</b>	6.12	12.13	11.53
<b>C2= - C4=</b>	14.82	28.04	29.59
<b>Gasoline</b>	20.72	34.29	36.01
<b>LCO</b>	11.69	11.51	9.85
<b>HCO</b>	47.84	15.25	9.71
<b>Coke</b>	0.37	0.68	0.96

Table 22 Catalytic data of Ecat/D-ZSM-5(280) 1C(0.05) at different C/O ratios

<b>Ecat/D-ZSM-5(280) 1C (0.05)</b>			
<b>C/O</b>	<b>1</b>	<b>2</b>	<b>3</b>
<b>Conv%</b>	53.07	70.84	78.28
<b>Dry Gas</b>	3.42	4.20	5.39
<b>H2</b>	0.04	0.06	0.08
<b>C1</b>	0.64	0.70	0.85
<b>C2</b>	0.78	0.84	0.99
<b>C2=</b>	1.96	2.61	3.47
<b>C3</b>	1.00	1.73	2.43
<b>C3=</b>	8.50	12.32	14.16
<b>iC4</b>	1.70	3.70	4.87
<b>nC4</b>	0.48	0.94	1.25
<b>LPG</b>	20.69	31.33	35.88
<b>C4=</b>	9.00	12.63	13.16
<b>C2= - C4=</b>	19.46	27.56	30.79
<b>Gasoline</b>	28.75	34.79	36.17
<b>LCO</b>	12.69	12.35	10.85
<b>HCO</b>	34.24	16.81	10.88
<b>Coke</b>	0.21	0.52	0.84

Table 23 Catalytic data of Ecat/2wt.% Mn ZSM-5(30) at different C/O ratios

<b>Ecat/2 wt.%Mn ZSM-5(30)</b>			
<b>C/O</b>	<b>1</b>	<b>2</b>	<b>3</b>
<b>Conv%</b>	56.33	74.85	77.78
<b>Dry Gas</b>	4.32	5.95	7.07
<b>H2</b>	0.06	0.09	0.14
<b>C1</b>	0.75	0.88	1.04
<b>C2</b>	0.91	1.06	1.22
<b>C2=</b>	2.61	3.93	4.66
<b>C3</b>	1.87	3.37	4.49
<b>C3=</b>	10.29	13.06	13.22
<b>iC4</b>	2.46	4.93	5.83
<b>nC4</b>	0.89	1.62	1.99
<b>LPG</b>	26.50	35.38	37.00
<b>C4=</b>	10.98	12.39	11.48
<b>C2= - C4=</b>	23.88	29.38	29.36
<b>Gasoline</b>	25.15	32.83	32.62
<b>LCO</b>	10.99	10.48	10.11
<b>HCO</b>	32.68	14.67	12.11
<b>Coke</b>	0.36	0.68	1.10

Table 24 Catalytic data of Ecat/4wt.% Mn ZSM-5(30) at different C/O ratios

<b>Ecat/4 wt.%Mn ZSM-5(30)</b>			
<b>C/O</b>	<b>1</b>	<b>2</b>	<b>3</b>
<b>Conv%</b>	59.81	72.07	78.65
<b>Dry Gas</b>	3.95	4.90	5.66
<b>H2</b>	0.05	0.09	0.11
<b>C1</b>	0.75	0.86	0.87
<b>C2</b>	0.88	0.96	0.98
<b>C2=</b>	2.27	3.00	3.70
<b>C3</b>	1.29	1.82	2.93
<b>C3=</b>	10.76	13.59	14.08
<b>iC4</b>	2.15	3.51	5.58
<b>nC4</b>	0.65	0.95	1.54
<b>LPG</b>	26.76	33.56	37.25
<b>C4=</b>	11.92	13.69	13.13
<b>C2= - C4=</b>	24.94	30.28	30.91
<b>Gasoline</b>	28.79	32.97	34.62
<b>LCO</b>	12.78	11.16	10.19
<b>HCO</b>	27.41	16.76	11.16
<b>Coke</b>	0.31	0.63	1.12

Table 25 Catalytic data of Ecat/2wt.% Mn ZSM-5(80) at different C/O ratios

<b>Ecat/2 wt.%Mn ZSM-5(80)</b>			
<b>C/O</b>	<b>1</b>	<b>2</b>	<b>3</b>
<b>Conv%</b>	61.55	67.31	79.65
<b>Dry Gas</b>	4.26	4.98	6.00
<b>H2</b>	0.06	0.08	0.12
<b>C1</b>	0.77	0.84	0.92
<b>C2</b>	0.91	0.97	1.04
<b>C2=</b>	2.52	3.09	3.93
<b>C3</b>	1.43	2.08	3.10
<b>C3=</b>	11.72	12.63	14.75
<b>iC4</b>	2.26	3.67	5.69
<b>nC4</b>	0.71	1.01	1.55
<b>LPG</b>	28.60	31.81	37.92
<b>C4=</b>	12.48	12.42	13.41
<b>C2= - C4=</b>	26.72	28.13	32.09
<b>Gasoline</b>	28.36	29.82	33.97
<b>LCO</b>	10.88	11.06	9.77
<b>HCO</b>	27.57	21.64	10.58
<b>Coke</b>	0.34	0.69	1.18

Table 26 Catalytic data of Ecat/4wt.% Mn ZSM-5(80) at different C/O ratios

<b>Ecat/4 wt.%Mn ZSM-5(80)</b>			
<b>C/O</b>	<b>1</b>	<b>2</b>	<b>3</b>
<b>Conv%</b>	39.11	70.29	80.13
<b>Dry Gas</b>	3.30	4.39	5.28
<b>H2</b>	0.05	0.08	0.12
<b>C1</b>	0.68	0.81	0.91
<b>C2</b>	0.80	0.93	1.00
<b>C2=</b>	1.77	2.57	3.24
<b>C3</b>	0.75	1.63	2.27
<b>C3=</b>	5.49	11.40	14.14
<b>iC4</b>	1.16	3.41	5.03
<b>nC4</b>	0.30	0.84	1.21
<b>LPG</b>	13.29	29.22	36.15
<b>C4=</b>	5.59	11.94	13.51
<b>C2= - C4=</b>	12.84	25.90	30.89
<b>Gasoline</b>	22.13	36.02	37.59
<b>LCO</b>	11.53	11.31	10.48
<b>HCO</b>	49.36	18.41	9.39
<b>Coke</b>	0.39	0.66	1.11

Table 27 Catalytic data of Ecat/2wt.% Mn ZSM-5(280) at different C/O ratios

<b>Ecat/2 wt.%Mn ZSM-5(280)</b>			
<b>C/O</b>	<b>1</b>	<b>2</b>	<b>3</b>
<b>Conv%</b>	34.70	70.23	80.37
<b>Dry Gas</b>	3.15	4.04	4.50
<b>H2</b>	0.04	0.06	0.08
<b>C1</b>	0.69	0.79	0.84
<b>C2</b>	0.81	0.91	0.95
<b>C2=</b>	1.62	2.29	2.63
<b>C3</b>	0.62	1.37	1.83
<b>C3=</b>	4.88	12.57	14.13
<b>iC4</b>	1.02	3.31	4.89
<b>nC4</b>	0.23	0.72	1.00
<b>LPG</b>	11.66	31.07	35.87
<b>C4=</b>	4.92	13.11	14.02
<b>C2= - C4=</b>	11.42	27.96	30.79
<b>Gasoline</b>	19.57	34.56	39.03
<b>LCO</b>	10.70	11.37	9.53
<b>HCO</b>	54.60	18.40	10.10
<b>Coke</b>	0.31	0.55	0.98

**Table 28 Catalytic data of Ecat/4wt.% Mn ZSM-5(280) at different C/O ratios**

<b>Ecat/4 wt.%Mn ZSM-5(280)</b>			
<b>C/O</b>	<b>1</b>	<b>2</b>	<b>3</b>
<b>Conv%</b>	51.52	71.37	76.96
<b>Dry Gas</b>	3.61	3.72	4.67
<b>H2</b>	0.05	0.06	0.08
<b>C1</b>	0.78	0.72	0.91
<b>C2</b>	0.89	0.83	1.02
<b>C2=</b>	1.89	2.11	2.65
<b>C3</b>	0.73	1.26	1.61
<b>C3=</b>	7.39	11.93	13.11
<b>iC4</b>	1.40	3.23	4.18
<b>nC4</b>	0.33	0.69	0.85
<b>LPG</b>	17.92	29.62	32.66
<b>C4=</b>	8.07	12.51	12.91
<b>C2= - C4=</b>	17.35	26.55	28.66
<b>Gasoline</b>	29.72	37.46	38.68
<b>LCO</b>	12.99	11.93	11.12
<b>HCO</b>	35.49	16.70	11.93
<b>Coke</b>	0.27	0.58	0.95

## References

- [1] P. K. Niccum, G. F. Maureen , T. J. Michael and S. R. Chris , "Future Refinery : FCC's Role In Refinery and Petrochemical Integration," Texas, USA, 2001.
- [2] A. Aitani, "Propylene Production," in *Encyclopedia of chemical processing*, New York, Taylor & Francis, 2006, p. 2461.
- [3] M. A. Bari Siddiqui, A. M. Aitani, M. R. Saeed and S. Al-Khattaf, "Enhancing the Production of Light Olefins by Catalytic Cracking," *Springer Science+Business Media*, 2010.
- [4] P. Giordano, "Global Polypropylene Market," Davison Catalagram, White Plains, NY, 2004.
- [5] Nexant, "Nexant, Propylene Technology-The Next Generation," New York, 2009.
- [6] S. J. Zinger, "The Critical Role of the Refinery in the Propylene Market," in *World Petrochemical Conference*, Houston, Texas, March,2000.
- [7] S. Sahebdehfar and F. Tahriri Zangeneh, "Dehydrogenation of Propane to Propylene Over Pt-Sn/Al<sub>2</sub>O<sub>3</sub>," *Iranian Journal of Chemical Engineering*, vol. 7, no. 2, 2010.
- [8] J. Mol and P. Leeuwen, "Metathesis of alkenes," in *Handbook of Heterogeneous catalyst*, 2008.
- [9] J. .. Plotkin, "Propylene: olefin of the future?," in *21st Annual Petrochemical World Trade Conference, Chemical Week and Chemo-systems*, Houston, 2003.
- [10] S. .. M atar and L. .. Hatch, *Chemistry of Petrochemical Processes*, vol. 2nd Ed., Boston: Gulf Professional Publishing, 2001.
- [11] N. Rahimi and R. Karimzadeh, "Catalytic Cracking of Hydrocarbons Over Modified ZSM-5 to Produce Light Olefins: A Review," *Applied Catalysis A: General*, vol. 398, pp. 1-17, 2011.
- [12] P.O'Conner, "Catalytic Cracking: the future of an evolving process," *Stud.Surf.Sci.Catal*, vol. 166, pp. 227-251, 2007.
- [13] R. H. Harding, A. W. Peters and J. D. Nee, "New developments in FCC catalyst

- technology," *Appl.Catal*, vol. A, pp. 389-396, 2001.
- [14] G. M. Bollas , I. A. Vasalos, A. A. Lappas, D. K. Iatridis and G. K. Tsioni, "Bulk molecular characterization approach for the simulation of FCC feedstocks," *Ind.Eng.Chem.Res.*, pp. 43,3270, 2004.
- [15] W. Letzsch, "The role of the FCC in the refinery of the future," in *How to Meet Environmental Targets*, Paris, 2002.
- [16] "CMAI News," 12 Nov 2001.
- [17] "( to Socony Mobil)". US 3 Patent 140 249, 7 July 1964.
- [18] "(to Socony Mobil)". US 3 Patent 140 251 , 7 July 1964.
- [19] "( to W R Gracy )". US 3 Patent 595 611, 27 July 1971.
- [20] " (to W R Gracy)". US 3 Patent 595 623, 18 May 1976.
- [21] "(to Texaco)". US 5 Patent 549 813, 27 August 1996.
- [22] J. S. Buchanan and Adewuyi, *Applied Catalysis A:General*, no. 134, pp. 247-262, 1996.
- [23] F. Thomas and J. Degnan, "Applications of zeolites in petroleum refining," *Topics in Catalysis* , no. 13, p. 349–356, (2000).
- [24] S. Wang, T. Don, Y. Zhang, X. Li and Z. Yan , "Catal Commun," 2000.
- [25] J. Jung , J. Park and G. Seo , *Appl Catal A*, p. 288:149, 2005.
- [26] X. Yang , Y. Feng , G. Tian , Y. Du , X. Ge , Y. Di and Y. Zhang , *Angew Chem Int*, no. 44, p. 2563, 2005.
- [27] M. Hartmann , *Angew Chem Int Ed*, no. 43, p. 5880.
- [28] C. Christensen, K. Johannsen, . I. Schmidt, C. Christensen and J. Am., *Chem. Soc.*, no. 125, p. 13370, 2003.
- [29] Y. Tao, . H. Kanoh and . K. Kaneko, *Langmuir* , no. 21 , p. 504, 2005.
- [30] M. Kustova, P. Hasselriis and . C. Christensen, *Catal. Lett*, no. 96, p. 256, 2004.

- [31] Y. Tao, H. Kanoh and K. Kaneko, *J. Phys.Chem. B*, no. 107, p. 10974, 2003.
- [32] K. Egeblad, M. Kustova, S. Klitgaard, , K. Zhu and C. Christensen, *Micropor. Mesopor. Mater*, no. 101, p. 214, 2007.
- [33] R. Bezman, *Chem. Commun.*, p. 1562, 1987.
- [34] R. Dessau, E. Valyocsik and N. Goeke, *Zeolites* , no. 12 , p. 776, 1992.
- [35] M. Ogura, . S. Shinomiya, J. Tateno, . Y. Nara, . E. Kikuchi and M. Matsukata, *Chem. Lett.* , p. 882, 2000.
- [36] I. Melia´n-Cabrera, S. Espinoza, . J. Groen, B. Linden, F. Kapteijn and J. Moulijn, *J. Catal.* , no. 238, p. 250, 2006.
- [37] J. Groen, J. Jansen, J. Moulijn and J. Pe´rez-R, *J. Phys.Chem. B*, no. 108 , p. 13062, 2004.
- [38] X. Wei and . P. Smirniotis, *Micropor. Mesopor. Mater.*, p. 97, 2006.
- [39] M. Siddiqui, A. Aitani, . M. Saeed, N. Al-Yassir and S. Al-Khattaf, "Enhancing propylene production from catalytic cracking of Arabian Light VGO over novel zeolites as FCC catalyst additives," *Elsevier*, no. 90, pp. 459-466, 2011.
- [40] T. Degnan, G. Chitnis and . P. Schipper, "History of ZSM-5 fluid catalytic cracking additive development at Mobil," *Microporous and Mesoporous Materials*, vol. 35–36, p. 245–252, 2000.
- [41] H. S. Cerqueira, R. Rawet and J. C. Pinto, "The influence of experimental errors during laboratory evaluation of FCC catalysts and hydrogen transfer properties evaluation," *Catal.Rev.-Sci.Eng.*, pp. 36,3,405, 1994.
- [42] "Impact of Zeolites on the Petroleum and Petrochemical Industry," *Top Catal*, no. 52, p. 1131–1161, 2009.
- [43] i. P.Leprince, *Conversion Processes*, Paris: Editions Technip, 1998, pp. 169-223.
- [44] N. Al-Yassir, *Multifunctional Catalysts Used in The Therm-Catalytic Cracking of Hydrocarbon Feedstocks For The Production Of Light Olefins*, Montreal, 2007.
- [45] S. Tung and E. McIninch, *J.Catal.*, vol. 10, p. 166, 1968.



- [46] D. Nace, *Ind. Eng. Chem. Prod. Res. Dev.*, vol. 8, p. 31, 1969.
- [47] A. Borodzinski, A. Corma and B. Wojciechowski, *Canad. J. Chem. Eng.*, vol. 58, p. 219, 1980.
- [48] B. Greensfelder, H. Voge and G. Good, *Ind. Eng. Chem.*, vol. 16, p. 742, 1957.
- [49] P. Janardhan and R. Rajeswari, *Ind. Eng. Chem. Prod. Res. Res. Dev.*, vol. 16, p. 1, 1977.
- [50] J. Planelles, F. Sanchez-Martin, F. Tomas and A. Corma, *J. Mol. Catal.*, vol. 32, p. 365, 1985.
- [51] J. Abbot and I. Head, *J. Catal*, vol. 125, p. 187, 1990.
- [52] S. Raseev, *Thermal and Catalytic Processes in Petroleum Refining*, New York: Marcel Dekker, Inc., 2003, pp. 275-421.
- [53] R. Dessau and W. Haag, "Proc. 8th Int. Congr. Catal.," Berlin, 1984.
- [54] Y. Adewuyi and J. Buchanan, *Appl. Catal A , Gen.*, vol. 131, pp. 121-133, 1995.
- [55] B. Lippens and J. de Boer, *J. Catal.*, vol. 4, pp. 319-323, 1968.
- [56] E. Barret, L. Joyner and P. Halend, *J. Am. Chem. Soc.*, vol. 73, pp. 373-380, 1973.
- [57] J. Groen, J. Moulijn and J. Perez-Ramirez, *J. Mater. Chem.*, vol. 16, pp. 2121-2131, 2006.
- [58] J. Groen, L. Peffer, J. Moulijn and J. Perez-Ramirez, *Chem. Eur. J.*, vol. 11, pp. 4983-4994, 2005.
- [59] D. Verboekend and J. Perez-Ramirez, *Chem. eur. J.*, vol. 17, pp. 1137-1147, 2011.
- [60] F. Kapteijn, L. Singoredjo, A. Andreini and J. Moulijn, *Appl. Catal. B.*, vol. 3, pp. 173-189, 1994.
- [61] O. Wimmers, P. Arnoldy and J. Moulijn, *J.Phys.Chem.*, vol. 90, pp. 1331-1337, 1986.
- [62] E.-M. El Malki, R. Van Santen and W. Sachtler , *J.Phys. Chem. B. ,* vol. 103, pp. 4611-4622, 1999.

- [63] A. Avidan and R. Shinnar, *Ind. Eng. Chem. Res.*, vol. 29, p. 931-942, 1990.
- [64] Xionghou Gao, Zhicheng Tang, Haitao Zhang, Dong Ji, Gongxuan Lu, Zhifeng Wang and Zhengguo Tan, "Influence of particle size of ZSM-5 on the yield of propylene in fluid catalytic cracking reaction," *Journal of Molecular Catalysis A: Chemical*, vol. 325, no. 1-2, p. 36-39, 2010.
- [65] D. Wallenstein, M. Seese and X. Zhao, "A novel selectivity test for the evaluation of FCC catalysts," *Appl.Catal.A:Gen.*231, pp. 227-242, 2002.
- [66] Siau H. Ng, Yuxia Zhu, Sdrian Humphries, Nobumasa Nakajima, Thomas Y.R. Tsai, Fuchen Ding, Hao Ling and Sok Yui, "Key observations from a comprehensive FCC study on Canadian heavy gas oils from various origins:1. Yield profiles in batch reactors," *Fuel Processing Technology*, no. 87, pp. 475-485, 2006.
- [67] Roberta C. Vieira, Jose´ Carlos Pinto, Evaristo C. Biscaia, Jr., Claudia M. L. A. Baptista and Henrique S. Cerqueira, "Simulation of Catalytic Cracking in a Fixed-Fluidized-Bed Unit," *Ind. Eng. Chem. Res.* , no. 43, pp. 6027-6034, 2004.
- [68] E. L. Moorehead, J. B. McLean and W. A. Cronkright, "Microactivity evaluation of FCC development catalysts in the laboratory:principles,approaches and applications," *Stud.Surf.Sci.Catal.*76, pp. 223-255, 1993.
- [69] J. Groen, J. Jansen, J. Moulijn and J. Perez-Ramirez, *J.Phys. Chem. B.*, vol. 108, pp. 13062-13065, 2004.

## **Vitae**

Name : **OMAR Ratib M. AWAYSSA**

Nationality : **PALESTINIAN**

Date of Birth : **8/11/1986**

Email : **umar\_a993@hotmail.com**

Address : **HEBRON, PALESTINE**

Academic Background : **CHEMICAL ENINGEERING**